



INTERACTION OF EMBEDDED RAIL WITH BRIDGES

Author: Md. Mohasin Howlader

Supervisor: Doc. Ing. Pavel Ryjáček, Ph.D.

University: Czech Technical University in Prague



Czech Technical University in Prague
Date: 19.12.2014



CZECH TECHNICAL UNIVERSITY IN PRAGUE
Faculty of Civil Engineering
Thákurova 7, 166 29 Prague 6, Czech Republic

MASTER'S THESIS PROPOSAL

study programme: CIVIL ENGINEERING
study branch: SUSCOS
academic year: 2014/15

Student's name and surname: MD. MOHASIN HOWLADER
Department: Fakulta stavební ČVUT v Praze
Thesis supervisor: Doc. Ing. Pavel Ryjáček, Ph.D.
Thesis title: The interaction of the embedded rail with bridges
Thesis title in English: The interaction of the embedded rail with bridges

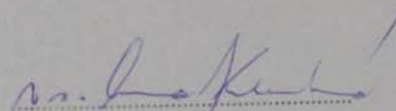
Framework content: Combined response of the bridges with direct fastening systems under different vertical loads, connected with small size experiment in the lab.
Numerical FEM model of the sample, analysis of the behavior, evaluation of the coupling functions, analysis of the different real load situation and their impact on the bridge structure

Assignment date: 30.9.2014 Submission date: 19.12.2014

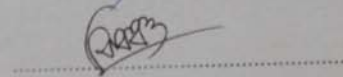
If the student fails to submit the Master's thesis on time, they are obliged to justify this fact in advance in writing. If this request (submitted through the Student Registrar) is granted by the Dean, the Dean will assign the student a substitute date for holding the final graduation examination (2 attempts for FGE remain). If this fact is not appropriately excused or if the request is not granted by the Dean, the Dean will assign the student a date for retaking the final graduation examination, FGE can be retaken only once. (Study and Examination Code, Art 22, Par 3, 4.)

The student takes notice of the obligation of working out the Master's thesis on their own, without any outside help, except for consultation. The list of references, other sources and names of consultants must be included in the Master's thesis.


.....
Master's thesis supervisor


.....
Head of department

Date of Master's thesis proposal take over: 30.9.2014


.....
Student

This form must be completed in 3 copies – 1x department, 1x student, 1x Student Registrar (sent by department)

No later than by the end of the 2nd week of instruction in the semester, the department shall send one copy of BT Proposal to the Student Registrar and enter data into the faculty information system KOS. (Dean's Instruction for Implementation of Study Programmes and FGE at FCE CTU Art. 5, Par. 7)

DECLARATION

I hereby declare that, all the analyses works and information published in this submitted Thesis has been produced and furnished by me. I also confirm that plagiarism and all other ethical issues has been rightly understood and obeyed from this end.

Prague, 19 December, 2014

.....

Md. Mohasin Howlader

To my one and only Elder Brother.....

His sacrifice and support has paved my way until this far.

ACKNOWLEDGEMENT

I would like to convey my heartfelt thanks and gratitude to my thesis supervisor, Ing. Pavel Ryjáček, Ph.D for providing me with the opportunity to work on such a novel and interesting topic on bridge structures. His continual support and mentorship has highly enriched my scope of knowledge in the field of railway bridges and acquainted me with innovative technologies of Railway Engineering. Without his support, patience and confidence on me, the thesis would not have come to fruition with new and attractive findings.

I am really thankful to Ing. Jan Vidensky Ph.D. who has appreciated my works in continuous basis and has given me ample time out of his busy schedule to work and learn about the software (ANSYS) used in the thesis. Without his support in ANSYS installation and giving me the opportunity to use the high configuration computer processors of CVUT, it would have been impossible to get the results within the timeframe for the thesis.

I would also like to extend my gratitude to Ing. Miroslav Vokac Ph.D. and his assistants, who have responded timely and have given kind effort to arrange and execute the laboratory test in Klokner Institute, Czech Technical University of Prague. The appreciation and explanation from Ing. Miroslav Vokac Ph.D. has enabled me to quickly understand the whole test procedure.

Special thanks goes to Edilon)(SedraTM for supplying with the ERS sample, necessary material and fabrication data, that has eventually made the way to study on this specific topic.

I would like to thank my all my SUSCOS mates in Prague who have endlessly supported and encouraged me; not only with the study but also to have a wonderful presence in this city.

Gratitude also goes to Erasmus Mundus Scholarship Program, other than this; I might not have got the opportunity come to this end.

Finally, my deepest appreciation goes to my beloved wife, Begum Moriom Zamila, my son Raiyan Sadik and my daughter Radiyah Sehrish and my Parents who have kept their patience and sacrificed a lot until the finish of this Master Program. Their endless support, unwavering love, endurance and motivations throughout will make this period of severance unforgettable for the rest of my life.

ABSTRACT

The primary purpose of this study is to investigate the response of the bridges with Embedded Rail System (ERS) under different combinations of vertical and longitudinal load. With a view to find the response, at first a small scale test has been conducted on a sample of ERS in laboratory. The data for the thesis has been taken from the test and subsequently a Finite Element Model (FEM) has been developed to simulate the test. The specific objectives of the simulation were to find out the longitudinal resistance of the ERS and to investigate its influences on a bridge system. Therefore, the Finite Element Model has been verified and validated (V&V) prior to determine the effects of ERS. The Finite Element Analysis (FEA) results for the unloaded track condition has been found fairly close to the experimental results and the results for loaded track conditions has also been found of similar nature but varying gradually with the increment of vertical load. Effect of debonding of physical parts in the ERS sample has also been considered during the study and infinitesimal effect has been observed. Stress softening characteristics of the embedding material under short term repetitive load has been identified as the principle reason behind the variation. Further development on the study and refinement of the result has been suggested through incorporating extensive static and dynamic material test data and automatic property assignment on bimodular elements (while transforming from tension to compression and vice versa) in the simulated model.

Keywords: *Direct Fastening System, Longitudinal Track Resistance, CWR, ERS, FEA, FEM, Stress Softening, Bimodular Materials.*

Table of Contents

SI No.	Description	Page No
	<i>Thesis Proposal</i>	
	<i>Declaration</i>	
	<i>Acknowledgement</i>	
	<i>Abstract</i>	
1	Introduction	01-02
2	State of Art	03-30
2.1	CWR Direct Fixation Track	03
2.2	Rail Tracks	04
2.3	Categorization of Fastening System	06
2.4	The Embedded Rail System (ERS)	09
2.4.1	Components of ERS	10
2.4.2	Important Features of ERS	12
2.4.3	Examples of ERS	12
2.5	Rail-Bridge Interaction	14
2.5.1	Principles of Stress generation	14
2.5.2	Parameters affecting the Track-Bridge Interaction	17
2.5.3	Actions to be considered	19
2.5.4	General principle governing the Track behavior	20
2.6	Identification of track behavior for Embedded Rail System	21
2.6.1	Linear Function	21
2.6.2	Bilinear Function	22
2.6.3	General Function	22
2.7	Longitudinal and Transversal Load Distribution on Track	23
2.8	Longitudinal and Vertical Load input Parameters	25
2.9	Load Distribution on Track for ERS	27
2.10	Literature Review	27
3	Objectives	31
4	The Test	32-53
4.1	Description of the laboratory sample	32
4.1.1	The Girder	32
4.1.2	The Embedded Rail System (ERS)	34

4.1.3	The Connection between Girder and ERS	40
4.1.4	Arrangement for Loading	41
4.1.5	The Final Assembly	44
4.2	The Test	45
4.2.1	The Static Scheme	45
4.2.2	Load Combinations	46
4.2.3	Test Output Arrangement	46
4.3	Analysis of Test Output Data	48
4.3.1	Analysis for Resistance of ERS	48
4.3.2	Additional Data for FEM Validation	51
5	Development of the Simulation Model	54-76
5.1	Modeling tool	54
5.2	Modeling Principles	54
5.2.1	Basic principles to choose elements	54
5.2.2	Physical parts for simulation	55
5.2.3	Choice of Elements	55
5.2.4	Description of the Elements	56
5.3	Model Generation Approach	59
5.4	Selection of Modeling Approach	60
5.5	Geometric Modeling	60
5.6	Defining Elements and Material Properties	67
5.7	Assigning Attributes and Meshing	70
5.8	Assigning Loads and Constraints	73
5.9	Final Model	75
5.10	Analysis Option	75
6	Verification of the Model	77-86
6.1	Verification of the software	77
6.2	Verification of the solution accuracy	77
6.2.1	Proper use of Element Characteristics	78
6.2.2	Mesh quality	81
6.2.2.1	Mesh Type	82
6.2.2.2	Mesh Density	84
6.2.2.3	Mesh Quality Parameters	84
6.2.3	Check for unloaded model in ANSYS	85

7	Validation of the Model	87-106
7.1	Validating dimensions and locations of result points	87
7.2	Validating FEA results with Experimental results	87
7.2.1	Loading case-1 and 2 (Zero Vertical Load)	90
7.2.2	Validation for static scheme	96
7.2.3	Comparison of FEA and Experimental data for the Higher Vertical load cases	97
7.3	Reason behind the deviation of FEA results from Experimental	104
8	Parametric Study	107-112
8.1	Effect of Poisson's Ratio of embedding material	107
8.2	Effect of eccentricity of vertical load	110
9	Findings	112-122
9.1	Coupling relationship of the rail ERS rail track	112
9.2	Design stress for Bridge Deck with ERS	117
9.3	Effect of ERS in Stress development in Rail and Girder	121
9.4	The FEM and areas of possible refinement	122
10	Future Study	123
11	Summary and Conclusion	124-126
	References	
	Appendices	
	<i>Appendix-I: Material data provided by Edilon)(SedraTM</i>	(Attached CD)
	<i>Appendix-II: Design details for support channels for longitudinal load</i>	
	<i>Appendix-III: Test Results</i>	
	<i>Appendix-IV: Final Report of test from Klokner Institute</i>	

List of Tables

Table No.	Table Name	Page No
Table 4.1	Maximum Loads and Displacements on test specimen	46
Table 4.2	Locations of strain gauges and displacement transducers on rail & girder.	47
Table 4.3	Longitudinal Resistance under incremental vertical load at different displacement level	50
Table 5.4	Compressive stress-strain data and Modulus of elasticity of embedding material in compression	70
Table 7.5	Bonding conditions	88
Table 7.6	FEA Results for fully bonded case with zero vertical load (Bonding case-1)	90
Table 7.7	FEA Results for partially debonded case with zero vertical load (Bonding case-2)	91
Table- 7.8	Comparison of FEA and Experimental Data for V=0 kN load case	92
Table-7.9	Reaction solution from FEA for V=0 kN load case	96
Table- 7.10	Result comparison for V=40kN load case (Bonding case-3)	97
Table- 7.11	Result comparison for V=80kN load case (Bonding case-4)	100
Table-7.12	Result comparison for V=125kN load case (Bonding case-5)	102
Table- 8.13	Result comparison for different poisson's ratio for (V=0 kN load case)	108
Table- 8.14	Result comparison for different poisson's ratio for (V=40 kN load case)	109
Table- 8.15	Result comparison for eccentricity of vertical loading (V=125 kN load case)	111
Table-9.16	Comparison of resistance k value of track (UIC vs FEA & Experimental result)	115
Table-9.17	Effective width calculation of vertical pressure distribution in transverse direction	118
Table-9.18	Improvement of girder stress due to use of ERS	122

List of Figures

Figure No.	Figure Name	Page No
Figure 2.1	<i>Branches of Rail Track System</i>	5
Figure 2.2	<i>Direct Fastening</i>	7
Figure 2.3	<i>Indirect Fastening</i>	8
Figure 2.4	<i>Cross-section of Typical Embedded Rail-1</i>	10
Figure 2.5	<i>Cross-section of Typical Embedded Rail-2</i>	10
Figure 2.6	<i>Embedded rail construction INFUNDO</i>	12
Figure-2.7	<i>BBERS MkII system details</i>	13
Figure 2.8	<i>Artist impression of the Deck-Track design</i>	13
Figure 2.9	<i>Behavior of CWR under effect of temperature changes</i>	14
Figure 2.10	<i>Additional stress generation in rails placed over aerial structure</i>	16
Figure 2.11	<i>Example of the determination of equivalent longitudinal stiffness at</i>	18
Figure 2.12	<i>Longitudinal resistance of a track as a function of longitudinal displacement (Bilinear Function)</i>	20
Figure 2.13	<i>Linear function of longitudinal resistance for ERS</i>	21
Figure 2.14	<i>Bilinear function of longitudinal resistance for non-ballasted tracks</i>	22
Figure 2.15	<i>Longitudinal distribution of a point force or wheel load by the rail</i>	23
Figure 2.16	<i>Longitudinal distribution of load by a sleeper and ballast</i>	24
Figure 2.17	<i>Transverse distribution of actions by the sleepers and ballast, track without cant</i>	25
Figure 2.18	<i>Load Model 71(EN 1991-2:2003)</i>	26
Figure 2.19	<i>Lateral Displacement of Rail During Fatigue Test in Case of Different Flexible Fastening Types and Embedded Rail Systems</i>	29
Figure 2.20	<i>Longitudinal Displacement of Rail in Case of Different Embedded Rail Systems and a Flexible Fastening Type</i>	30
Figure 4.21	<i>I girder Cross Section</i>	33
Figure 4.22	<i>Long section of girder</i>	33
Figure 4.23	<i>Top view of girder</i>	34
Figure 4.24	<i>The Edilon)(Sedra Embedded Rail System</i>	35
Figure 4.25	<i>Static Compressive stress-strain curve</i>	36
Figure 4.26	<i>Static Compressive stress-strain curve of Resilient Base Strip</i>	38
Figure 4.27	<i>Bolt Grid for Connection between Girder and ERS</i>	40
Figure 4.28	<i>Connection between ERS and the Girder</i>	41

Figure No.	Figure Name	Page No
Figure 4.29	<i>The vertical Load Cell</i>	41
Figure 4.30	<i>The longitudinal Load Cell</i>	42
Figure 4.31	<i>Top View of End Connection</i>	43
Figure 4.32	<i>Elevation of the End Connection</i>	43
Figure 4.33	<i>The Final Assembly of Test Specimen</i>	44
Figure 4.34	<i>Static Scheme of the Test</i>	45
Figure 4.35	<i>Load Model 71(EN 1991-2:2003)</i>	48
Figure 4.36	<i>Longitudinal Resistance vs Longitudinal Displacement of ERS</i>	49
Figure 4.37	<i>Functions representing Longitudinal Resistance vs Longitudinal Displacement of ERS</i>	50
Figure 4.38	<i>Trend of Longitudinal Resistance of ERS under incremental Vertical load</i>	51
Figure 4.39	<i>Vertical Displacement of Rail along the length for different level of Vertical Load</i>	52
Figure 4.40	<i>Longitudinal Stress on Rail along the length for different level of Vertical Load</i>	53
Figure 5.41	<i>Basic area and volume types available in the ANSYS program</i>	54
Figure 5.42	<i>SOLID185 3-D 8-Node Structural Solid element geometry</i>	57
Figure 5.43	<i>SOLID185 Stress Output</i>	57
Figure 5.44	<i>SOLID186 3-D 20-Node Structural Solid element geometry</i>	58
Figure 5.45	<i>SOLID185 Stress Output</i>	59
Figure 5.46	<i>ANSYS Classical Interface: Main Menu for model generation</i>	61
Figure 5.47	<i>Creating Keypoints.</i>	62
Figure 5.48	<i>Creating Areas</i>	62
Figure 5.49	<i>Creating and modifying Volumes</i>	63
Figure 5.50	<i>Separation of PVC pipe from embedding (Front and rear end)</i>	65
Figure 5.51	<i>Separation of Elastomer Strip from Steel Girder (Rear end)</i>	65
Figure 5.52	<i>Simulation for Separation of PVC Pipes</i>	66
Figure 5.53	<i>Simulation for Separation of Elastomer</i>	66
Figure 5.54	<i>Arruda Boyce model parameter</i>	68
Figure 5.55	<i>Arruda Boyce curve vs. curve from Experimental data.</i>	69
Figure 5.56	<i>Assigning attributes for element generation</i>	71
Figure 5.57	<i>Volume Sweeping options for Mesh Generation</i>	72

Figure No.	Figure Name	Page No
Figure 5.58	<i>Meshed Volume</i>	73
Figure 5.59	<i>Longitudinal surface Load from load cell and concentrated counter load</i>	74
Figure 5.60	<i>The Final Model</i>	75
Figure 5.61	<i>Analysis options</i>	76
Figure 6.62	<i>ANSYS current technology element recommendations</i>	78
Figure 6.63	<i>Use of flexible element control options</i>	79
Figure 6.64	<i>Topologies of Solid Elements</i>	82
Figure 6.65	<i>Skewness Measurement of Quadrilaterals</i>	85
Figure 6.66	<i>Shape error check in ANSYS</i>	86
Figure 7.67	<i>Segmentation of embedding below rail foot for assigning different tension and compression properties.</i>	89
Figure 7.68	<i>Segmentation of elastomer strip for assigning different tension and compression properties</i>	90
Figure 7.69	<i>Comparison of FEA and Experimental results for longitudinal stress in rail (V=0 kN).</i>	93
Figure 7.70	<i>Comparison of FEA and Experimental results for vertical displacement of rail (V=0 kN).</i>	95
Figure 7.71	<i>Comparison of FEA and Experimental results for longitudinal stress in rail (V=40 kN)</i>	98
Figure 7.72	<i>Comparison of FEA and Experimental results for vertical displacement of rail (V=40 kN).</i>	99
Figure 7.73	<i>Comparison of FEA and Experimental results for longitudinal stress in rail (V=80 kN)</i>	101
Figure 7.74	<i>Comparison of FEA and Experimental results for vertical displacement of rail (V=80 kN).</i>	101
Figure 7.75	<i>Comparison of FEA and Experimental results for longitudinal stress in rail (V=125 kN)</i>	103
Figure 7.76	<i>Comparison of FEA and Experimental results for vertical displacement of rail (V=125 kN).</i>	103
Figure 7.77	<i>Compression element generation at the end section of embedding material besides rail web</i>	105
Figure 8.78	<i>Effect of Poisson's ratio on longitudinal stress on rail</i>	110

Figure No.	Figure Name	Page No
Figure 8.79	<i>Effect of eccentric vertical loading on longitudinal stress on rail</i>	111
Figure 9.80	<i>Comparison of longitudinal resistance found from FEA and Experiment (for 2.19m ERS on single rail)</i>	112
Figure 9.81	<i>Longitudinal resistance as a function of longitudinal displacement of 1 m ERS track (unloaded)</i>	113
Figure 9.82	<i>Short & long term response of ERS (unloaded track).</i>	114
Figure 9.83	<i>Comparison of longitudinal resistance found from FEA and Experiment (for 2.19m ERS on single rail)</i>	115
Figure 9.84	<i>Longitudinal resistance as a function of longitudinal displacement of 1 m ERS track (loaded)</i>	116
Figure 9.85	<i>Vertical Stress distribution along the central line of base plate top (below elastomer)elastomer)</i>	117
Figure 9.86	<i>Vertical Stress distribution along the length of ERS (generalized pressure distribution on effective width)</i>	118
Figure 9.87	<i>Vertical Stress distribution along transverse direction (Z=1800mm)</i>	119
Figure 9.88	<i>Vertical Stress distribution along transverse direction (Z=800mm)assembly)</i>	119
Figure 9.89	<i>Vertical Stress distribution along transverse direction (Z=1300mm)assembly)</i>	120
Figure 9.90	<i>Idealized vertical pressure distribution in transverse direction</i>	120
Figure 9.91	<i>Stress comparison for top fiber stress of girder (With & without ERS assembly)</i>	121
Figure 9.92	<i>comparison for bottom fiber stress of girder (With & without ERS assembly)</i>	121

1. Introduction

For any industry, change is inevitable for existence. Railway industry is no exception to that. The change in this industry can better be achieved through satisfying the demand in terms of reduced travel time, punctuality, sustainability and comfort. The particular need for higher speed of communication as well as the increased density of traffic has tremendously brought the change with low maintenance and cost effective solution of track than that of the traditional ballasted tracks. Traditionally, for approximately 130 years, railway track has consisted of rails laid on timber or concrete sleepers, supported by a ballast bed. The main drawback of this traditional track is its requirement for frequent inspection and maintenance which with the higher speed can manifold the associated cost. The higher the speed, the higher is the need for accuracy in positioning the rails. Due to churning up of ballast particles at high speeds, serious damage of wheels and rails as well as associated extra stress interaction can occur and moreover, the behavior is irreversible. That is why in modern applications, a railway track design tends more and more towards railway structures without ballast [1]. In addition, for bridges or tunnels, these requirements have been more craved due to the lower height and weight properties of ballasted track. Now, as the new practice of ballastless or directly fastened track is growing its demand, the requirement for improvement of the fastening technology developing its priority with time. However, the absence of a ballast bed does mean that elasticity has to be created by other means. For the years, numerous methods of direct fastening has been developed compensating for few advantageous behavior of the ballasts. The main difference among those can be established as whether the rail is fastened at discrete points with the track/sleepers or supported continuously. The latter one which is also known as Embedded Rail System (ERS) has been first in use since 1976 in Netherlands in small scale. Since the beginning of the fastening system in railways, probably this ERS is one of the most spectacular one of the developments. The development has become more rapid, especially in the last decade due to its competitive advantages from others with respect to higher speed, cost effectiveness, environmental sustainability and others. But with the increasing demand, the demand for detail characteristics behavior of this type of fastening has to be met. Since the inception of direct fastening system, numerous analysis and

experiments has been made to establish the behavior of those different types of fastening systems. And, there exist established codes of practice for the ballasted track like Union Internationale des Chemins de fer/ International Union of Railways (UIC), Eurocode 1991-2 or national codes DIN Fb-101 in Germany. But still there is lack of specific interaction model, especially when it comes to bridges with ERS system. Mechanical properties of a track without ballast can better be determined and therefore the track behavior can be more accurately described and analyzed using numerical methods.

With a view to establish the typical behavior pattern of ERS, this thesis paper is dedicated to find out the interaction of a specific Embedded Rail System with bridges. Edilon)(Sedra Embedded Rail System with EDILON Corkelast embedding compound as a high-performance and maintenance-free rail fastening system with special elastic characteristics will be tested in laboratory at small scale under different vertical load in combination with the longitudinal load and a Finite Element Model (FEM) will be validated and analyzed with the help of globally recognized ANSYS to find out the Rail-Track coupling function, influence of combined load and afterwards, the subsequent behavioral impact on bridge structures.

2. State of Art

2.1. CWR Direct Fixation Track

Interaction is a particular way of influencing one another in which the idea of two way effect is an essential. Similarly, Interaction of rail track with bridges is a consequence of the behavior of one, on the behavior of the other because of their obvious interlink by the nature of construction. This interlinks may be established through various methods; where the major classification depends on whether it is a ballasted track and non-ballasted or directly fastened track. As of modern practices, the latter one has been more in use in contrary to the former one due to some disadvantages inherited by it like, greater depth of required deck, higher cost of maintenance and material (ballast), frequent development of rail break due to horizontal, vertical and angular displacements etc. Direct fixation deck construction has now become the most expected standard practice for many transit purposes. It has been credited with huge amount of savings on transit projects by eliminating the need for crossties and ballast. Though the ballasted track is considered useful in some cases (especially for medium spans) with its less interaction characteristics with the track, directly fastened track has got the upper hand because of the following novel benefits-

- Noise and vibration reduction due to the use of elastic fasteners with vertical flexibility.
- Aesthetic improvement by using shallower and less massive structure.
- Low dead load.
- Providing electric isolation and adjusting the line and grade of the track.
- Involves less maintenance.
- Retains much longer geometry than ballasted track
- Better riding quality and so on.

The majority of the early transit systems used track work comprised of jointed rail structures. Rather than the classical jointed rail with bolted connections, now-a- days the track work is normally constructed with continuous welded rail (CWR). Though The bolted connections used with jointed rail allow sufficient longitudinal expansion and contraction to reduce the accumulation of thermal stresses along the rails, it has been found obsolete

due to various reasons like noise and vibration generation, producing derailment problems, dynamic impacts on aerial structures, low riding quality and others. Over the last three decades, CWR has been established as the most common track configuration overcoming all those limitations. Specially it reduces the maintenance requirements, provides a smooth and quiet ride and also from structural point of view, reduces the fatigue and dynamic effects on the structures associated with the joints.

Therefore, the CWR direct fixation track has become the most commonly used practices of modern aerial structures. But with all the benefits, CWR Direct fixation track has introduced new difficulties and intuitive structural complexities to be discovered by the Engineers. Railway bridges or aerial structures which were introduced as ballasted structures had little structural interaction between the rails and the structures. On the other hand, CWR Direct fixation track can have significant interaction with the underlying structures, as it is directly attached to the superstructure and does not have any cushion in between. Here, the rails are basically stationary because of their continuity throughout the length of the bridge and because they are anchored off the bridge. Thus it inherits complexity in coupling between the rail and the superstructure, induced due to different forces like longitudinal forces from differential temperature change of rail and superstructures, traction and braking force, derailment force, vertical impact and transversal horizontal impact from vehicle load, centrifugal forces on curves or others.

2.2. Rail Tracks

Since the deployment of rail as supporting and guiding element in sixteenth century, the rail industry has gone through rapid expansion and the system of rail track has become an ever changing phenomena. The classical or conventional track in use from the past is the ballasted tracks for which the variety was due to the variety of materials used for ballast (crushed stone, gravel, crushed gravel), rail profiles (flat-bottom rail, groove rail, block rail, crane rail etc) or in sleepers (concrete, wood sometimes steel) retaining the basic formation. As discussed earlier, though ballasted track is still in use, the recent applications are more towards the non-ballasted or slab tracks. The Embedded Rail System is a modern concept lying within the slab track category. The position of ERS in the detail classification can be shown as below [17],

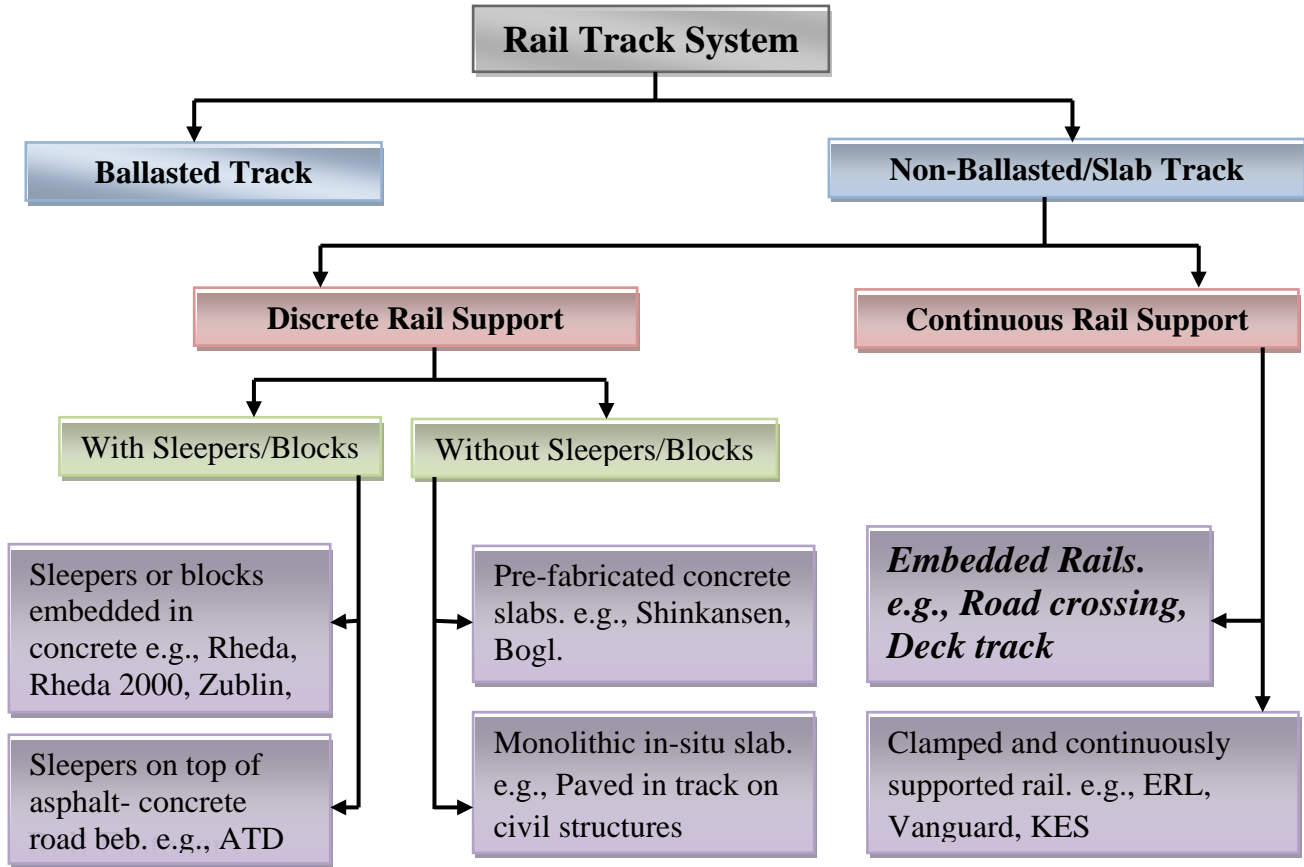


Figure-2.1: Branches of Rail Track System [17]

The term "fastening systems" or in short "fastenings" are the devices that provide flexible and strong connection between the rail and the supporting structure that can be sleeper or slab. It is the fundamental component of a railway system to secure the position of the rail providing necessary structural stability for safe movement of the locomotives over the rail. In addition to the main function, fastening system has to fulfill some other functions which can better describe the definition of a railway fastener.

Functions [2]

Rail Stability Aspects

- To have sufficient resistance to the vertical and lateral wheel forces transferred by rail.
- To be able to accept the longitudinal loads and thus avoid rail creep and ensure the utilization of ballast resistance in case of continuously welded track



- To allow sufficient frame rigidity by having large rotation resistance and thus avoid buckling of track.
- To behave elastically against the vertical and horizontal forces thus the damages caused by dynamic forces can be reduced.

Construction and maintenance aspects

- To be suitable to be built in any section of track - in straight and curved, on bridges and tunnels, in open tracks, in station tracks and in turnouts.
- To ensure the electric isolation of the rails.
- Its construction and maintenance to be simple, fast and mechanized. Individual parts of fastening should be simply and fast replaceable as well as the rails and sleepers.
- Not to cause too large wear, damage on the rail and the sleeper due to traffic.

Economic aspects

- To contain only few parts.
- Its price should correspond to its quality and lifespan.
- To need little maintenance.

2.3. Categorization of Fastening System

Fastenings can be classified in following two major classes,

Direct Fastening: Here, the rail and, if necessary, the base plate are fixed to the sleeper using the same fasteners. Direct fastenings also include the fastening of track on structures without ballast bed and sleepers [16].

Indirect (Separated) Fastening: Here, the rail is connected to an intermediate component, such as the base plate, by other fasteners than those used to fix the intermediate component to the sleeper. The advantages of indirect fastenings are that the rail can be removed without having to undo the fastening to the sleeper and the intermediate component can be placed on the sleeper in advance fastening [16].

And both can be,

-Rigid or,

-Flexible; depending on the elements used in the system.

Followings are some examples of direct/indirect, rigid/flexible fasteners as per Ludvig².

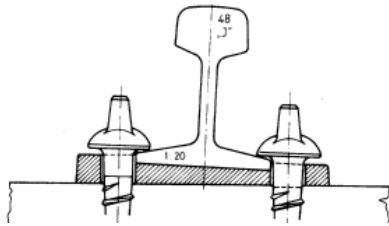


Figure: Direct, Rigid Fastening with Coach Screw on Wooden sleeper

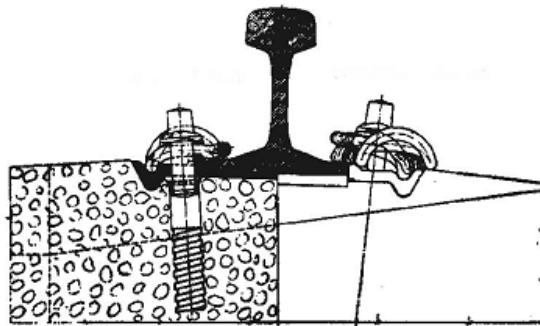


Figure: Flexible Fastening System, type w14 with Skl Clamp on Concrete sleeper



Figure: Vossloh System DFF 300 with tension clamp Skl 15

Figure-2.2: Direct Fastening²

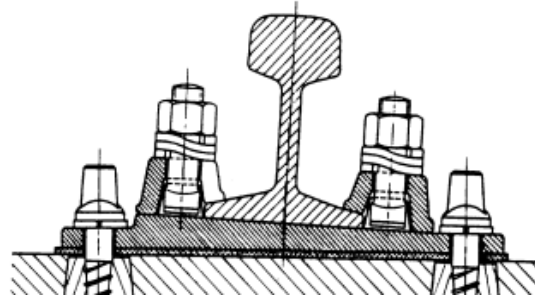


Figure: GEO Rigid Fastening System on Concrete Sleeper

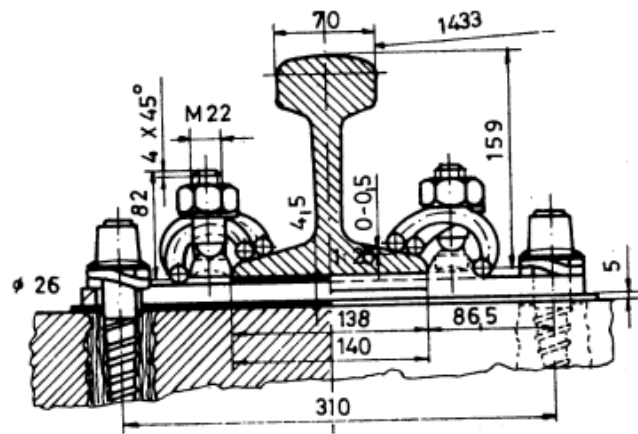


Figure: GEO Flexible System with Skl Clamp on Concrete sleeper

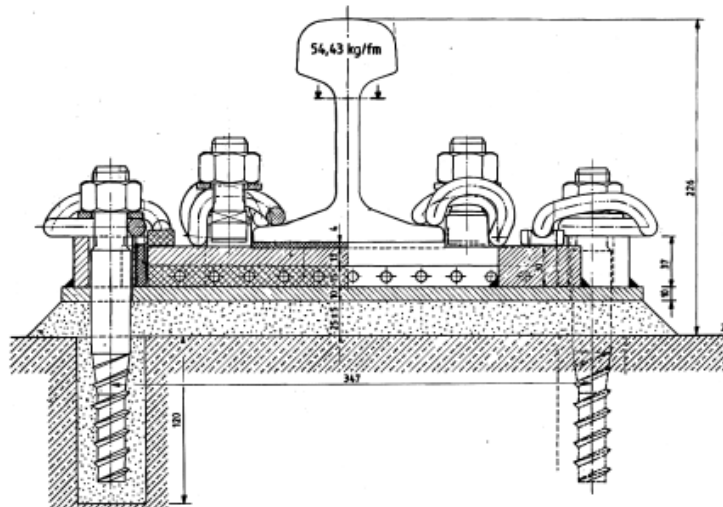


Figure: Flexible Fastening System with Skl 12 and Skl ET Clamps on Concrete Slab

Figure-2.3: Indirect Fastening²

According to Ludvigh², due to the new plastic industrial technologies a new fastening category named Embedded Rail System has been formed that can satisfy the increasing demands as stated earlier. Hence, the fastening system can be further categorized to

- Discrete or point fasteners and
- Embedded fasteners

These elastic embedded rail systems that can be further categorized as follows,

- A. The rail is continuously embedded without using clamping, anchoring element.
- B. The rail is discontinuously embedded without using any clamping, anchoring element.
- C. The rail is fixed down traditionally with a flexible fastening system and rail is embedded afterwards.

2.4. The Embedded Rail System (ERS)

The ERS rail fastening system is characterized by continuous support of the rails, as well as by the elimination of small hardware components. This also means avoidance of the support-point frequencies of traditional, discrete rail fastening systems.

The ERS rail fastening system was first developed in the early 1970s, in collaboration with Netherlands Railways (NS). Many pilot tracks of ERS has been used throughout Europe since then for different purposes like, bridges (since 1973), level railway crossings (since 1976), and for ballastless railway track (since 1976). The concept of ERS can cover the full range from light rail to high-speed tracks.

The fields of application for ERS rail fastening systems in the heavy-rail (HR) version today include the following: high-speed rail traffic (with axle loads of 18 to 20 metric tonnes and $v_{\max} \geq 300$ km/h), classic standard- gauge railways (with axle loads from 16 to 25 metric tonnes and $v_{\max} \geq 200$ km/h), and the heaviest of industrial rail traffic with axle loads up to 35 or 45 metric tonnes.[3]

2.4.1. Components of ERS

According to Ludvig², the general cross section of a ERS system can be shown as figure below,

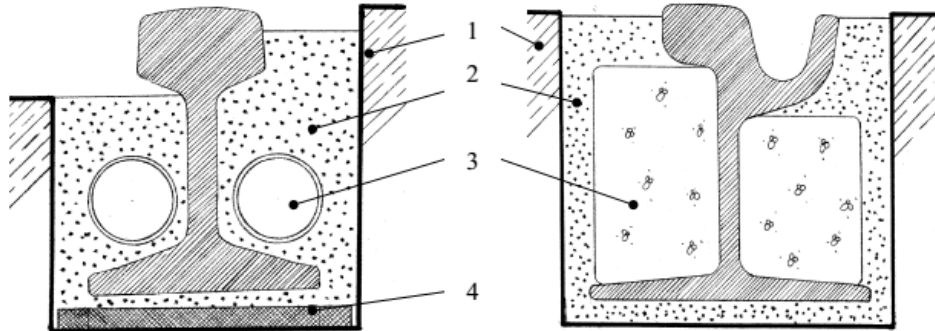


Figure-2.4: Cross-section of Typical Embedded Rail-1

Where, the main components suggested are,

1. Longitudinal recess created in the base structure,
2. Elastic embedding material,
3. Space filling elements,
4. Elastic base strip.

The above generalization suggests that the rail is laid in a longitudinal recess created in the base structure. But, it can also be built upon the deck/bed with the help of bounding frame either made of steel channels or by concrete as shown in the following figure,

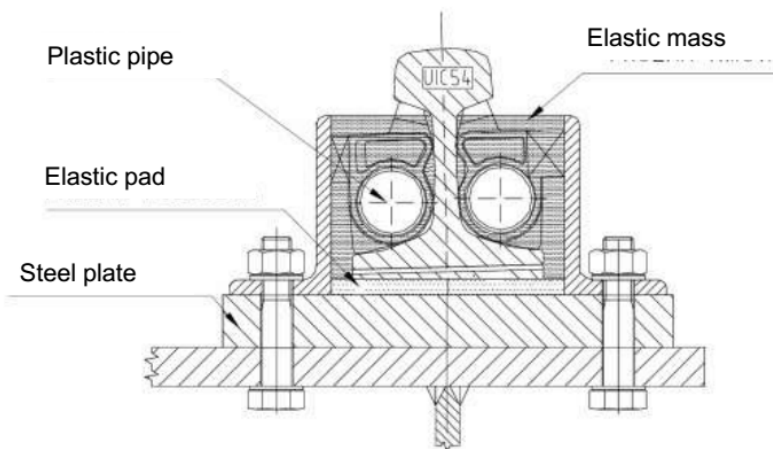


Figure-2.5: Cross-section of Typical Embedded Rail-2

Hence, the general cross-sectional arrangement of ERS consists of the following major elements-

1. Bounding frame for longitudinal recess,
2. An elastic embedding mass,
3. Elastic base strip,
4. Space filling element and
5. The Rail.

The longitudinal recess enclosing the embedding element can be made in different ways, either by concrete or steel, above or below the track bed depending on the track structure. The longitudinal recess surface created above the base structure may be set upon the deck and later connected to the deck or base.

The main product in the ERS rail fastening system is the embedding compound bounded within the longitudinal recess. Fixing the rail is ensured by contact of the embedding material with the rail and the longitudinal recess surface. The composition of the material varies in different uses. In most of the cases, it is a two-component elastomer, polyurethane occasionally added with cork.

A Resilient Strip is used under the rail for obtaining greater vertical elasticity to dampen noise and vibration and also longitudinal elasticity to accommodate rail/structure interaction movements and distribution of the wheel loads longitudinally along the rail. It controls the rail deflection under the prevailing loads, provides isolation of the high wheel/rail impact forces from the deck and also the electric isolation. Such strip mats are available with various thickness and hardness characteristics, according to requirements for system stiffness.

For reducing the amount of embedding material, space filling elements are placed with in the embedding material which can be either PVC pipe, cement-based brick or other suitable materials. Empty tubes employed for this purpose can also be used for the passage of cables of signals and other functions.

2.4.2. Important Features of ERS

The most important features of these systems are:

- The track becomes laterally stable that ensures the permanence of the gauge with less or no influence of dynamic forces.,
- Facilitate low structural height,
- Vibration damping and less noise emission,
- Low track maintenance,
- Aesthetic appearance.

2.4.3. Examples of ESR

According to Esveld¹⁶, different systems of adopting ERS are,

- INFUNDO-EDILON system

The INFUNDO and EDILON designs are the same type sharing the same construction characteristics and principles. This system was first developed in Netherlands in 1970's and its development continues until today. A continuous rail is continuously supported by elastic compounds in a groove. A concrete supportive layer is laid by a slip form paver. This layer is 40 cm thick and 2.4 m wide. The horizontal and vertical forces are compensated by the cork underpad and the elastic two-component mass surrounding the rail. The INFUNDO-EDILON design is intended mainly for urban passenger rails (subways, tramways).

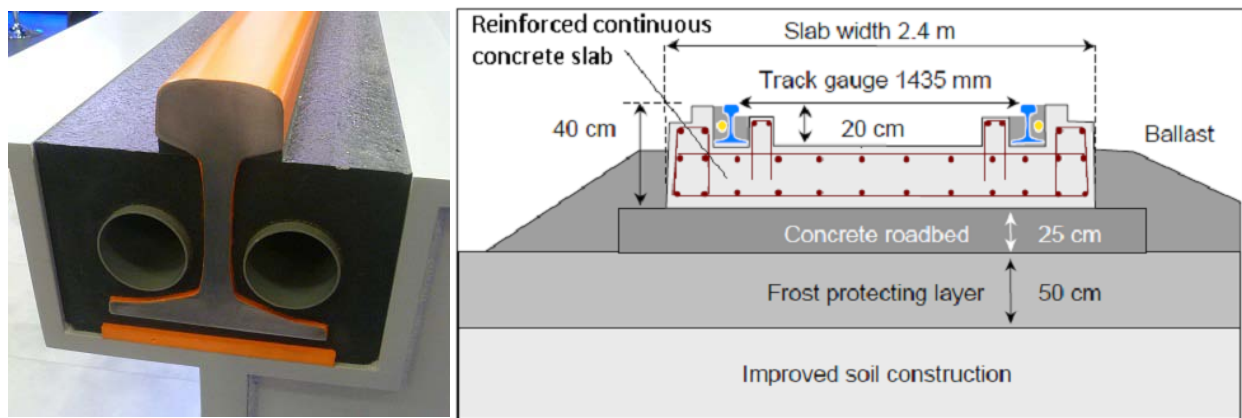


Figure-2.6: Embedded rail construction EDILON)(SEDRA and INFUNDO

- BBERS design

This system shares exactly the same construction principles as INFUNDO. The difference is the smaller rectangular rail (BB14072) which has resulted to a much smaller groove and the different rail elastic support elements. The BBERS uses, a U shaped continuous pulltruded glass reinforced plastic shell, a U-shaped pad (micro cellular polyurethane) to fit both the shell and the rectangular rail (139.7 ×69.85 mm, advance track design) with a standard rail head profile (removable rail, 74 kg/m) as show in figure.

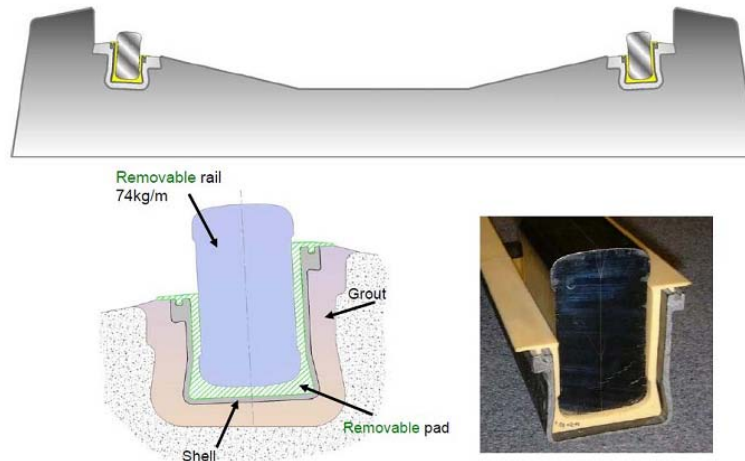


Figure-2.7: BBERS MkII system details

- Deck-Track design

Deck-Track is a system of high flexural stiffness which can be applied in soft soils. It consists of a continuous in-situ or prefabricated concrete bearer (concrete frame structure) laid into the ground as shown in figure. The rails can either be embedded or directly fixed on the concrete surface.

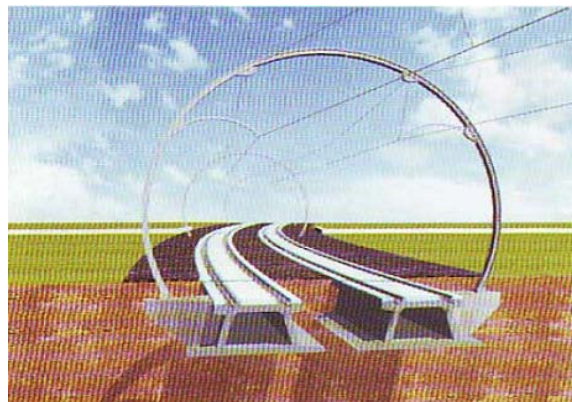


Figure-2.8: Artist impression of the Deck-Track design

2.5. Rail-Bridge Interaction

The basic principles for understanding the rail-bridge interaction has been described in UIC Code 774-3R. The interaction effects have been described here in terms of support reaction, additional stress in the rail and relative/ absolute displacement of track and deck. It has described the track behavior for the ballasted track mainly , actions to be considered for interaction analysis, consequences of the bridge and the track under those actions, permissible values for additional stresses, deformations and also methods to find out the combined effect of the actions.

2.5.1. Principles of Stress generation

Traditionally in a ballasted track, the rails are fastened to the sleeper with elastic fastening in which the clamping force is normally such that all the longitudinal movements are transmitted to the sleepers. The resistance to rail/sleeper sliding is greater than the resistance to longitudinal movement offered by the ballast. As the free movement of the rail is opposed by the ballast under the thermal and traffic load, the rails are subjected to longitudinal force. In a Continuously Welded Rail (CWR), which contains a Central Zone restricting expansion and contraction and breathing Zone at the ends with allowing expansion and contraction, the force in the rail can be shown as following,

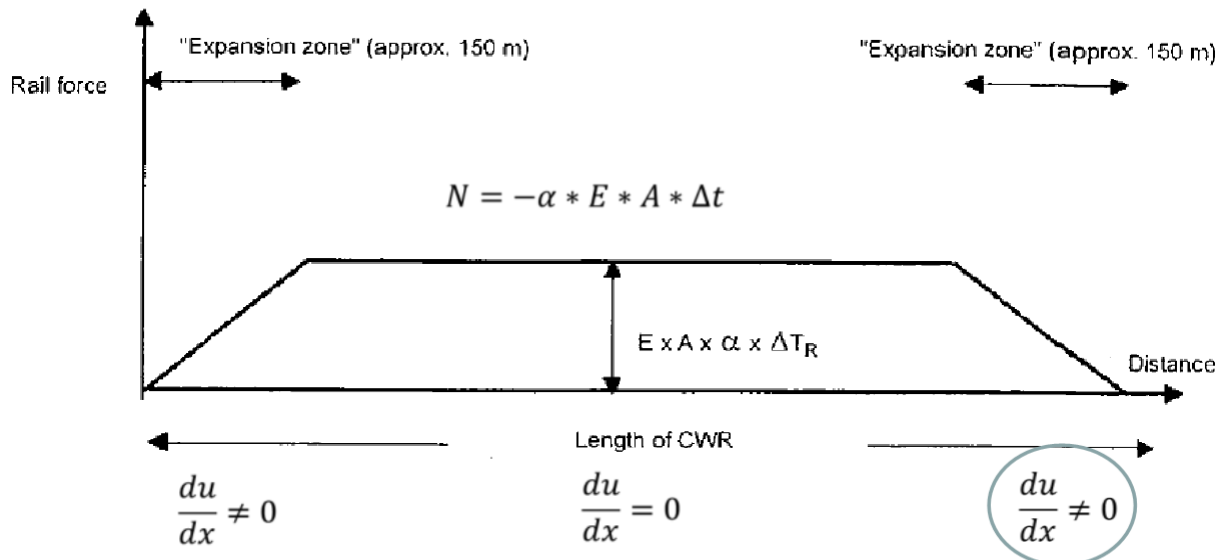


Figure-2.9: Behavior of CWR under effect of temperature changes



Where,

α = Co-efficient of thermal expansion

ΔT_R = Change in rail temperature relative to reference of laying temperature

E = Young's modulus for Steel

A = Combined cross-sectional area of rails

Now, for the breathing end where $du/dx \neq 0$ (u being the displacement of the rail), the equilibrium equation of force with external load (traction/braking force) can be written as,

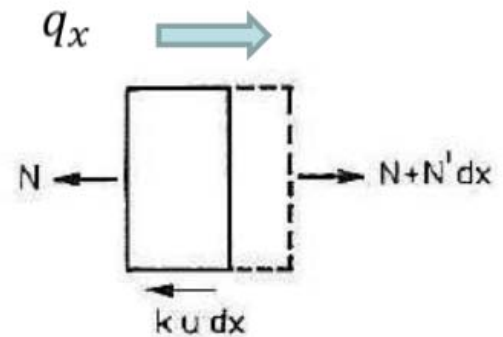
$$-dN/dx + k.u = q_x$$

Where, $N = EA.du/dx$

Hence, the equation becomes,

$$-EA.d^2u/dx^2 + k.u = q_x$$

k =ballast stiffness between rail and ground.



Now, if there exist a bridge under the CWR track, it means that the track is resting on a movable and deformable surface which in turns causes displacement of the track. Given that both track and bridge are able to move, any force or displacements that act on one of them will induce forces in the other. Interaction therefore takes place between the track and the bridge as follows:

i) Forces applied to a CWR track induce additional forces into the track and/or into the bearings supporting the deck and movements of the track and of the deck.

ii) Any movement of the deck induces a movement of the track and an additional force in the track and, indirectly, in the bridge bearings [4]



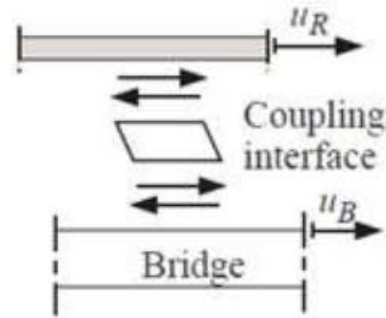
Hence, it is easily understandable that, for the coupling interface between the rail and the deck $du/dx \neq 0$.

Therefore, the equilibrium equation of force becomes,

$$-EA \cdot d^2u/dx^2 + k \cdot (u_B - u_R) = q_x$$

Where, u_B = Rail displacement

u_R = Deck displacement



This suggests that, it causes additional stresses in the rail. For a Simply supported deck with fixed bearing at one end it can be shown as [5],

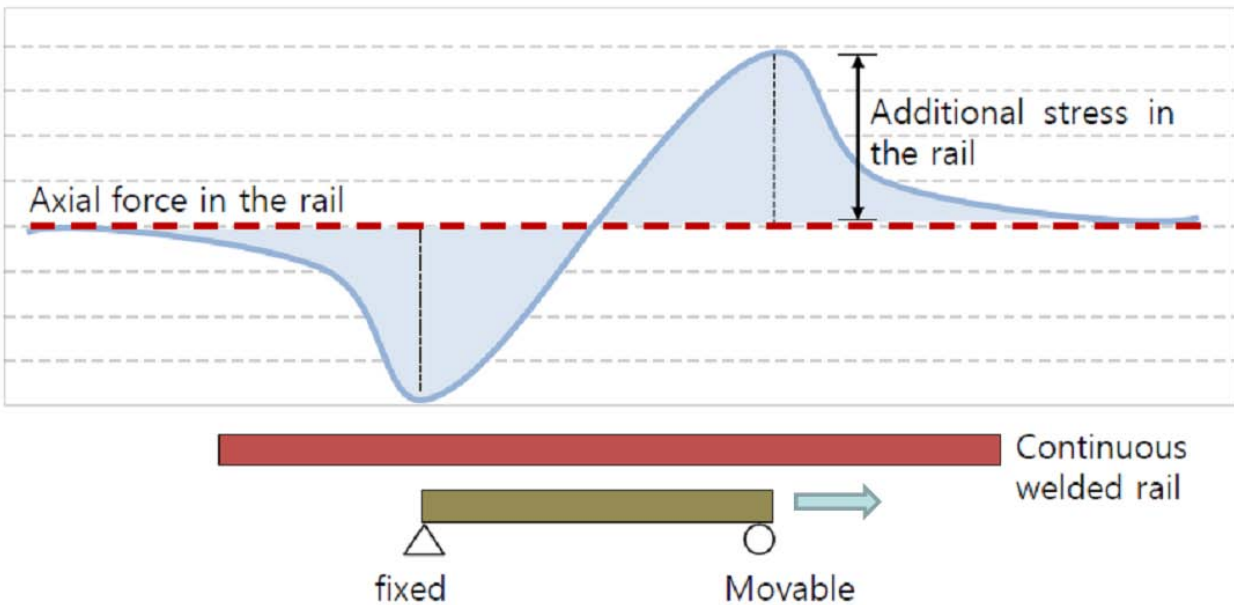


Figure-2.10: Additional stress generation in rails placed over aerial structure.

Though the UIC report 774-3R has made some recommendations for unballasted track, it has been made useful for ballasted deck mainly. But it has described the main principles and paved the way for future design and construction of the new types of bridges. Therefore, it may

be adopted for unballasted decks also by evaluating the values of track stiffness (k) according to the type and arrangement of fastening and subsequently, making the necessary assumptions and substitution in place of ballast stiffness.

2.5.2. Parameters affecting the Track-Bridge Interaction

The governing forces that generated due to track-bridge interaction depends on number of factors. As per UIC 774-3R the factors can be stated as,

Bridge parameters

- Configuration of the structure/Static arrangement of the bridge

The static arrangement of the bridge can be defined by support scheme, the number of decks, number of supports per deck, the position of fixed and movable supports, the number of span and span length, position of thermal fixed point, the expansion length L_T between the thermal fixed point and the end of the deck etc.

- Support stiffness

Support stiffness is defined as the resistance of the deck to the horizontal displacement. This parameter is calculated by composing stiffness of all the supports present termed as total stiffness. And the individual support stiffness is calculated from the stiffness of the bearing, pier, base, foundation and soil.

For example the total longitudinal stiffness of a single pier is given by,

$$K = \frac{F_l}{\delta_p + \delta_\phi + \delta_h}$$

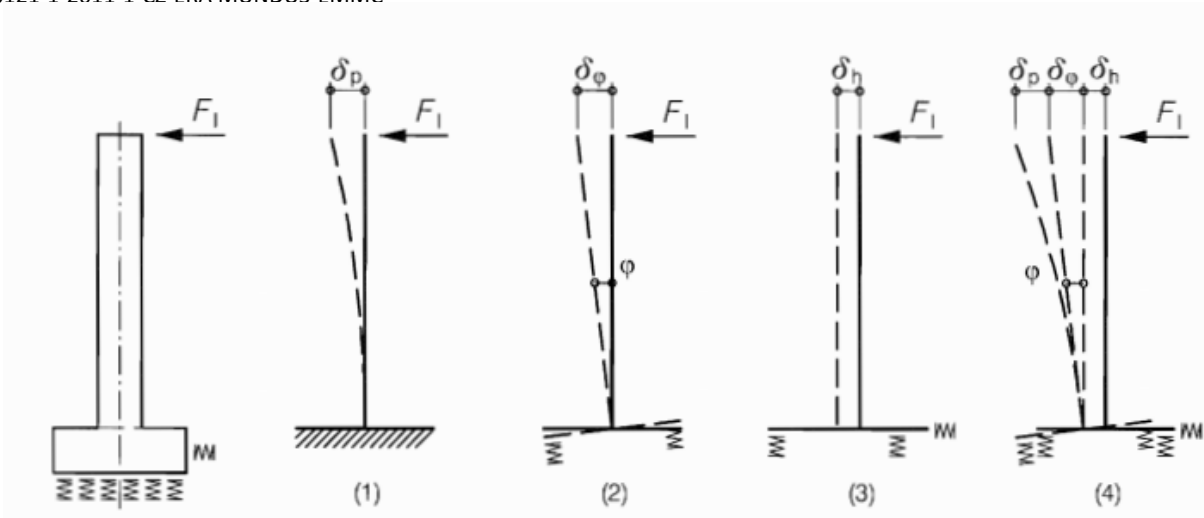


Figure-2.11: Example of the determination of equivalent longitudinal stiffness at bearings.

Where,

- (1) Bending of the pier
- (2) Rotation of the foundation
- (3) Displacement of the foundation
- (4) Total displacement of the pier head

- Bending stiffness of the Deck

Deck bending causes horizontal displacement of the upper edge of the deck and this deformation causes interaction forces.

- Height of the Deck

The distance of upper surface of the deck slab to the neutral axis of the deck and the distance from neutral axis to the center of rotation of the bearing are the important values to control the bending of the deck and the associated interaction forces.

Track parameters

- Cross sectional area of the Rail/Axial stiffness of the rail

The cross sectional area of rail is directly associated in the calculation of the rail expansion or relative moments.



- Configuration of the track

Configuration of the track depends on whether it is a ballasted track or non-ballasted track system, the vertical distance between the upper surface of the deck and the neutral axis of the rails and the location of rail expansion devices.

- Track resistance

Probably, the most important and widely ranged parameter is the track resistance. It is the resistance of the track per unit length to longitudinal displacement. The parameter depends on large number of factors like, whether it is loaded or unloaded, ballasted or non-ballasted, type of fasteners used in non-ballasted track, standard of maintenance etc [4, 8].

2.5.3. Actions to be considered

Actions that can lead to the interaction effects are those that can cause relative displacement between track and deck. According to EN 1991-2 or UIC, actions that are to be considered for railway bridges are for evaluating combined response of structure and track to variable actions are,

- Thermal effects in the combined structure and track system.
- Traction and braking forces
- Classified vertical traffic loads (LM71, SW/O, SW/2, and HSLM. Model for unloaded train), associated dynamic effects may be neglected.
- Other actions such as creep, shrinkage, temperature gradient etc. shall be taken into account for the determination of rotation and associated longitudinal displacement of the end of the decks where relevant [4,8].

2.5.4. General principle governing the Track behavior

The resistance of the track to longitudinal displacement is a function of the displacement of the rail relative to its supporting structure. The behavior of the ballast track is more or less known from the professional literature [4]. An approximation made in the calculations of the behavior has always been in common practice. Actually the longitudinal resistance of the ballast track develops gradually. Following a displacement of some millimeters the longitudinal resistance reaches its maximum and that value does not change any more during further displacement. Aiming to facilitate practical calculations, the initial section with changing resistance is traditionally neglected, i.e. only a constant value is taken into account. However, UIC recommends that the same principle can be used for identifying the behavior of unballasted tracks also.

Referring to UIC-774-3R, the resistance increases rapidly while the displacement is too low, but remains virtually constant as the displacement reaches a certain magnitude. In order to simplify the curves, a bilinear shape can be replaced or approximated for the original curve. Hence, a bilinear relationship between the track resistance (k) and the longitudinal displacement (u) of the track relative to the supporting structure as has been proposed in UIC-774-3R as shown in the following figure.

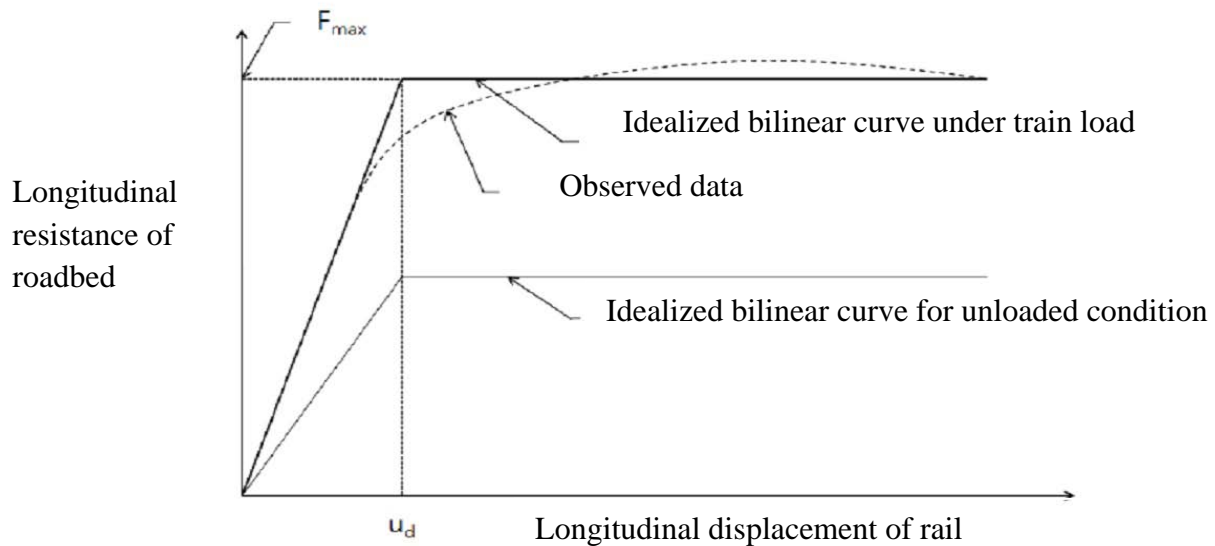


Figure-2.12: Longitudinal resistance of a track as a function of longitudinal displacement (Bilinear Function).

2.6. Identification of track behavior for Embedded Rail System (ERS)

Function describing the relationship between longitudinal resistances of the track against longitudinal deformation can be established in different ways. UIC-774-3R has defined a special case linear relationship for embedded rails. It also recommended bilinear function as stated in the previous section for the ballastless track system. Apart from those recommendations, with the development of modern Finite Element Modeling software, it is now more realistic to handle each case differently. General cases approximate the common behavior of a system. But with the innovations like Embedded Rail System and new materials the general relationship may vary in large scale. FEM analysis can provide accurate results and establish the more exact relationship related to those new innovations.

2.6.1. Linear Function

Theoretically, elastic materials are characterized by linear behavior. Basically, this is the initial part of the bilinear curve before the plastic zone has been reached. As stated in UIC-774-3R, the special case of rail embedded in resin may be dealt with by adopting a linear relation without a plastic zone, with the following resistance (k) values [4],

Unloaded Track: $k=13\text{kN/mm}$ per linear meter track for a maximum displacement of, $u_0 = 7\text{mm}$

Loaded Track: $k=19\text{kN/mm}$ per linear meter track for a maximum displacement of, $u_0 = 7\text{mm}$

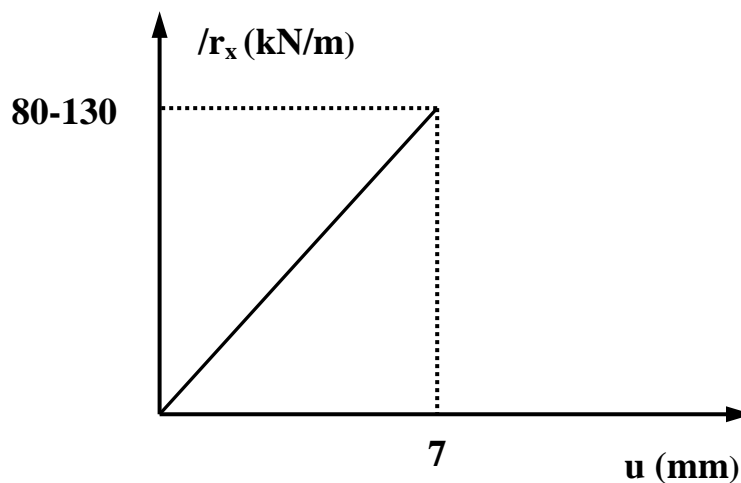


Figure-2.13: Linear function of longitudinal resistance for ERS

2.6.2. Bilinear Function

By far this is the most commonly used function of behavior for all types of fastening systems. As UIC recommends, the bilinear function applies for the rails fastened with direct fastenings. It has recommend the specific values of displacement and stiffness for loaded and unloaded track also as shown in figure below,

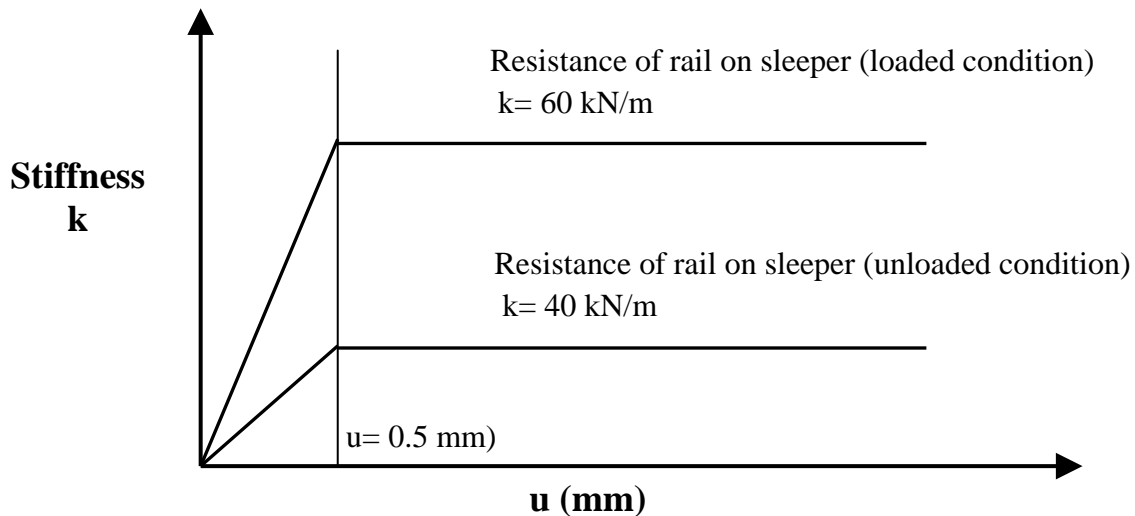


Figure-2.14: Bilinear function of longitudinal resistance for non-ballasted tracks

But, it is obvious that when determining the longitudinal strains of an elastically embedded rail; different from methodology applied for ballast track, only the elastic domain of the embedding material's displacement or inelastic domain if exists could be taken into account.

2.6.3. General Function

The longitudinal resistance features of an elastic bedding material can be determined in theory, but the width of the bedding material placed between the rail's cross section and the space filling elements (put in to reduce the volume of the bedding material) is varying, therefore the internal spatial displacements of the elastic bedding material are extremely different from each other. There are more complex factors. Since under the impact of the dilatation force, the

displacement of each cross section on the moving section reaches that of the rail's end gradually, it is commonplace that the embedding material's longitudinal resistance is also changing gradually, proportionally with the displacement. Taking into consideration, that neither the distribution of the internal forces, nor the displacements of the moving section are known previously, determining the longitudinal behavior of a rail embedded in an elastic material is much more complicated than that laid on ballast track.

A general function for embedded rail system is the one that will describe the true behavior under real load situation taking into consideration all the major variables that can significantly change the behavior. Hence, it is much realistic to use modern software along with laboratory/in field testing to establish the general function of the relationship. Specially, using the FEM tools will give rise to most accurate relationships and help make optimal design.

2.7. Longitudinal and Transversal Load Distribution on Track

EN 1991-2, Section 6 (Rail traffic actions and other actions specifically for railway bridges), describes about the vertical load models and their distribution in both longitudinal and transverse directions. But those distributions are established for the tracks on sleepers and ballasted tracks only. Longitudinal load distribution of vertical load has been shown in two parts,

1) Longitudinal distribution of a point force or wheel load by the rail

A point force in Load Model 71 (or classified vertical load in EN 1991-2) or wheel load may be distributed over three rail support points as shown in Figure below:

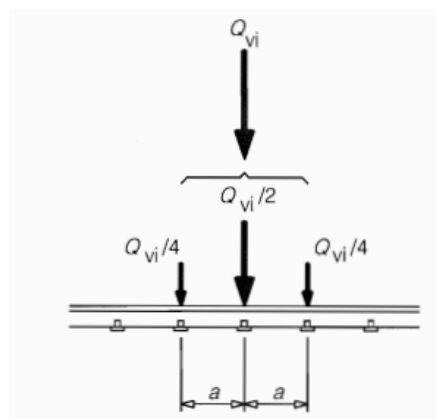


Figure-2.15: Longitudinal distribution of a point force or wheel load by the rail

Where,

Q_{vi} = The point force on each rail due to Load Model 71 (or classified vertical load in EN 1991-2) or a wheel load of a Real Train.

a = The distance between rail support points

2) Longitudinal distribution of load by sleepers and ballast

Generally the point loads of Load Model 71 or an axle load may be distributed uniformly in the longitudinal direction (except where local load effects are significant). The longitudinal distribution beneath sleepers as shown in Figure below should be taken into account, where the reference plane is defined as the upper surface of the deck.

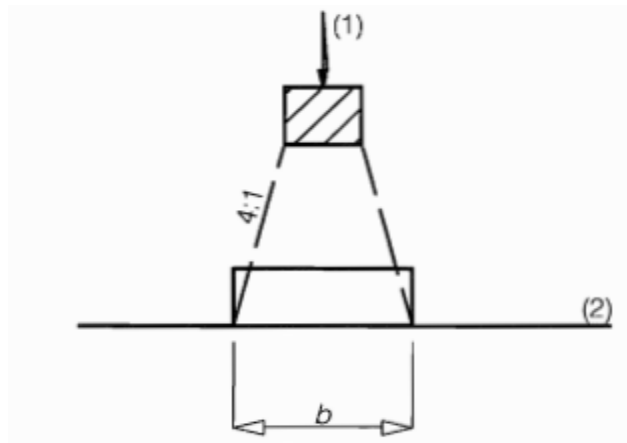


Figure-2.16: Longitudinal distribution of load by a sleeper and ballast

Where,

(1) Load on sleeper

(2) Reference plane

3) Transversal load distribution

On bridges with ballasted track without cant, the actions should be distributed transversely as shown in Figure below,

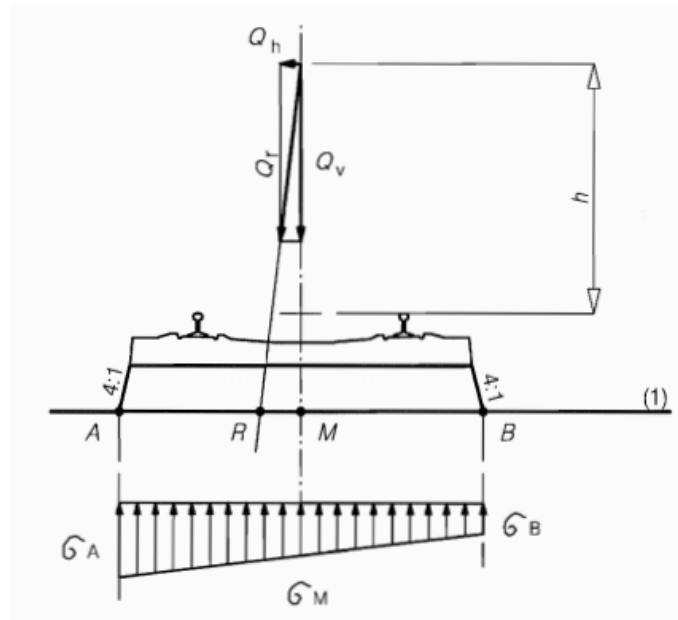


Figure-2.17: Transverse distribution of actions by the sleepers and ballast, track without cant

2.8. Longitudinal and Vertical Load input Parameters

Longitudinal Load

Maximum longitudinal load has not been directly mentioned in EN 1991-2:2003. It is suggested that the load has to be considered uniformly distributed along the influence length. However, the worst case can be considered when the effect of temperature, traction/braking and deformation of the bridge deck combines together. Considering the worst case (**as per EN 1991-2:2003: 6.5.4.6**),

Action due to Braking: 20 kN/m for Load model 71 or Load model SW/0

35kN/m for Load Model SW/2

Action due to Traction: 33kN/m

Action due to Temperature variation: $0.6k = 0.6 \cdot 60 = 36 \text{ kN/m}$; k being the plastic shear resistance for loaded track. (For bridges with continuous welded rails at both deck ends and fixed bearings at one end of the deck)

Action due Bridge deck deformation: 20 kN/m . (For bridges with continuous welded rails at both deck ends and fixed bearings on one end of the deck and with rail expansion devices at the free end of the deck)

Summing up for worst case the maximum longitudinal force can be obtained as, $35 + 36 + 20 = 91 \text{ kN/m}$

In another reference, maximum longitudinal restoring force in rail for loaded track has been recommended as 130 kN/m in Dutch Code,

Vertical Load

EN 1991-2:2003 describes 5 load models for vertical actions on track due to rail traffic. Load model 71 and Load Model SW/0 for continuous bridges describe vertical action in response to represent normal rail traffic on mainline railways. Load Model SW/2 represents the static effect of vertical loading due to heavy rail traffic. Other models are Load model for unloaded train and HSLM Load model for trains at speeds exceeding 200 km/h . HSLM model is

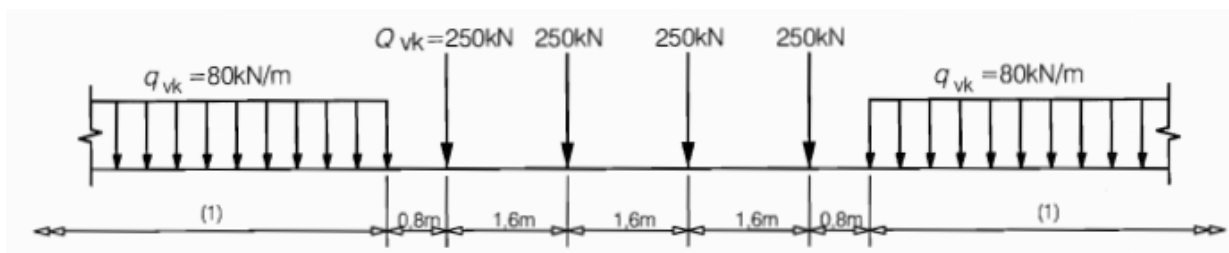


Figure-2.18: Load Model 71(EN 1991-2:2003)

out of the scope of this study as it is considered for dynamic testing of rail over bridges. SW/0 and SW/2 considers uniformly distributed load only. Hence the maximum vertical point load has been considered according to Load model 71, which suggests 250 kN of point axle load on railway track.

2.9. Load Distribution on Track for ERS

Embedded Rail Systems (ERS) are inherently built on the non ballasted tracks. There has been limited study on the load distribution characteristics of ERS after its innovation. And by nature of construction, ERS are differently connected to the deck (continuously built/attached on the decks) other than the point or discrete fasteners. Now depending on the elastic material, filler material or any other major elements used and their arrangement with the deck, the behavior of load distribution would be definitely different as that of ballasted tracks described in EN 1991-2 and also from the non-ballasted point fastened tracks. Moreover, with each type of its class (continuous fastening) the behavior may vary. A finite element model that has been intended to make for identification of track resistance behavior can also be used for this purpose. The FEM of the track with the deck and its analysis under the classified vertical loads defined by EN1991-2 will be a useful method of finding out the pattern or the distribution of wheel load both in longitudinal and transversal direction for Edilon)(Sedra Embedded Rail System selected under this thesis.

2.10. Literature Review

The investigation of longitudinal stress in the rail due to temperature variation, braking/acceleration force in combination with vertical bending in CWR on bridge decks has been discussed intensively in the last decades. Initiated by UIC-Recommendation 774-3R [4] in 1995, the European Committee for Standardization (CEN) released Eurocode 1(EC-1) [8] in 2003 that provides information on actions on bridges and design methods for present practice.

The interaction between track and bridge has been described in UIC774-3R [5] by introducing a bridge under a CWR track. The considering aspect is that the bridge provides displacements and movements causing displacements of the track. It has described the methods of calculations also. But the interaction methodologies are predominantly oriented with ballasted tracks, single track and for limited support conditions.

Other works that deal with the practical design aspects concerning the track bridge interaction are discussed in [14, 15, 16, 17, and 18]. The longitudinal coupling between track and bridge plays an important role in the track-bridge interaction. Here, the coupling element is presented by rail pad and ballast if they exist or by the presence of a fastener system. Researchers completed several investigations on the stiffness of the coupling interface and its components especially for the ballasted system [9, 13].

So far there has been no standard test carried out for finding the response of the embedded rail system under combined load (Vertical, longitudinal and lateral). There has been a study along with small size laboratory test for ballasted track with three dimensional load by Zand et, el. [14] which showed the response of the track in individual directions in combination with others. Their analytical result found from the study showed more or less expected behavior and concluded that *there is a good linear relationship between the peak and minimum resistance force and between the peak resistance force and vertical load. This applies for the lateral as well as for the longitudinal resistance. The separate test series to determine the longitudinal resistance of the rail on a fixed sleeper also showed a bilinear behavior. But concluded with a remark that, for higher vertical load levels, the peak longitudinal resistance may be determined by the fastening system rather than the track panel in ballast system.*

Optimum design of ERS has been explained by V. L. Markine et, el.¹². Here the optimality criteria has been chosen based on cost reduction, design efficiency, low noise emission and minimum wear of rails and wheels. The design variables were the material and geometry properties of ERS e.g., elastic properties and volume of compound, shape of rails and size of troughs etc. The study included the finite element modeling of ERS for both dynamic and static analysis.

Embedding of a rail laid in an elastic material poured into a concrete or steel recess gives to it continuous flexible support and lateral fixing. The longitudinal and lateral behavior of the rail under this system is expected to have significant difference than that of the ballasted tracks. So far, there has been a lot of study regarding the longitudinal behavior of ballasted tracks [9, 14, 16, 18]. There are also standard tests for elastic materials like push/ pull tests but too little information has been found regarding the behavior of rail embedded in elastic materials.

KORMOS, GY⁷ in an attempt has studied the longitudinal resistance of the elastic bedding material in embedded rail system, dilatational behavior of a rail embedded in a flexible material and concluded that, *the behavior of a rail embedded into elastic material is practically identical to that of a welded track.*

Eszter Ludvigh², studied the elastic behavior of continuously embedded rail system and evaluated different important co-efficients like vertical bedding co-efficient, longitudinal bedding factor with the help of mechanical testing. He also compared the lateral and longitudinal resistance of the embedded fastening systems with other flexible ones. He concluded that, *continuously embedded fastening systems suffer less lateral displacement as an effect of repeated load than flexible spring fastenings. It is also an experimental observation that these materials have delayed elasticity, which means that after load removal the residual deformation was always less than 1.5 mm.*

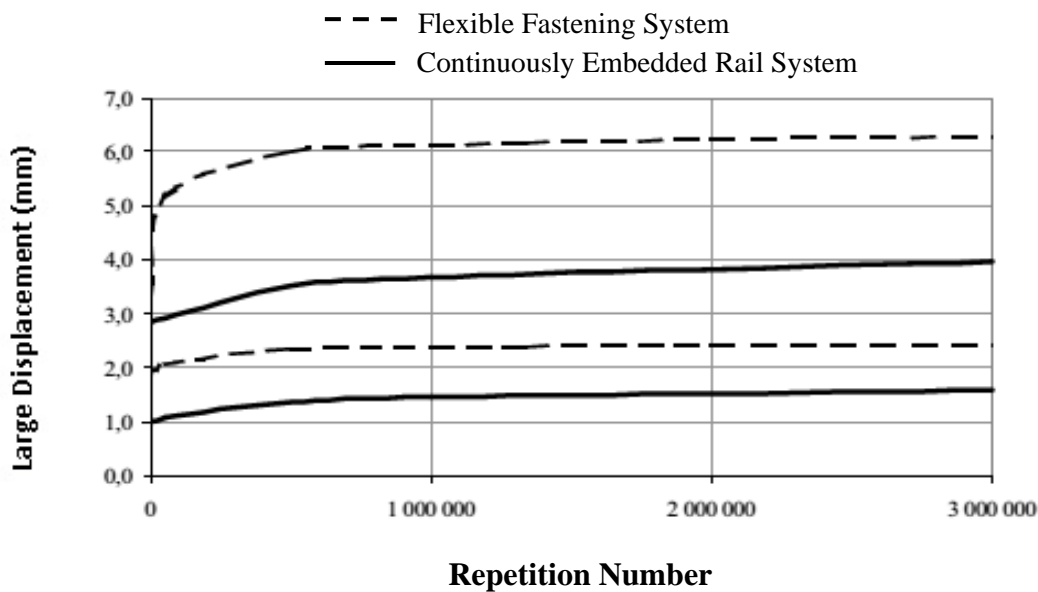


Figure-2.19: Lateral Displacement of Rail during Fatigue Test in Case of Different Flexible Fastening Types and Embedded Rail Systems.

The study also concluded that, *continuously embedded rail systems can bear much more longitudinal force without destruction and have smaller residual deformation than the traditional, flexible fastenings.*

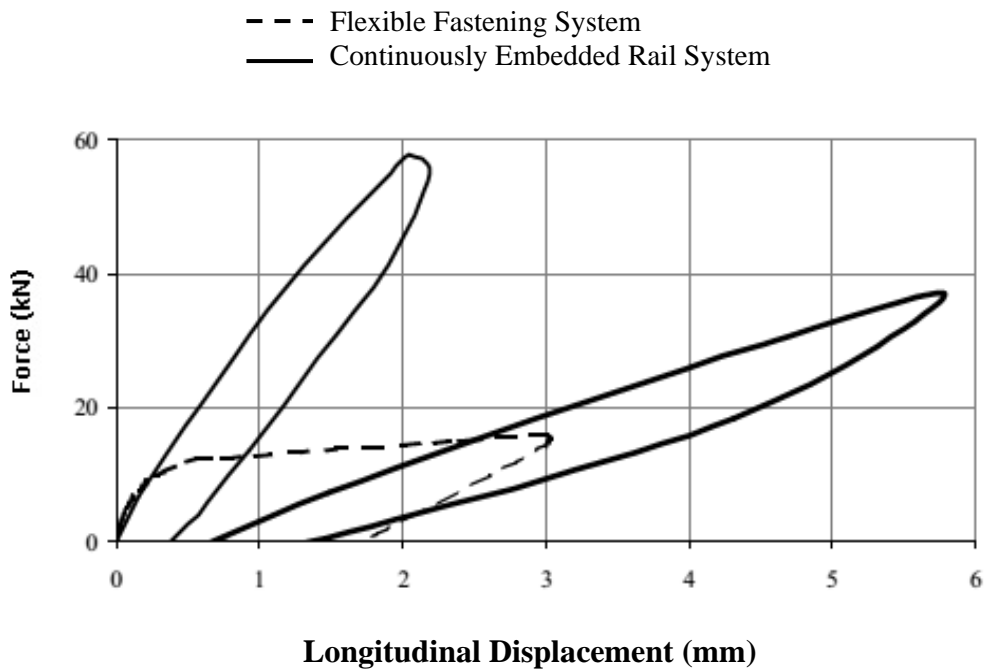


Figure-2.20: Longitudinal Displacement of Rail in Case of Different Embedded Rail Systems and a Flexible Fastening Type

3. Objectives

The Primary objective of the thesis is:

- To find out the response of the bridges with Direct Fastening System ERS under different combinations of load (Vertical and Longitudinal).

To achieve the primary objective the followings have been the particular objectives of the study:

- To carry out small size lab experiment of ERS combined with Steel I Girder and simulate the laboratory test specimen by Finite Element Modeling (FEM) tools.
- To validate the FEM under combined (vertical & longitudinal) load as executed in the laboratory.
- To find out the coupling relationship between longitudinal displacement and longitudinal resistance of ERS;
- To find out the distribution of vertical load from track to deck due to ERS.
- To analyze the possible influences of ERS on bridge structure.

4. The Test

4.1 Description of the laboratory sample

The laboratory test sample is an assembly of a continuously embedded rail system fabricated by Edilon)(SedraTM mounted over an asymmetric I girder of 2650mm length. Edilon)(SedraTM is an international supplier of rail fastening systems which are commonly applicable on on ballastless and embedded rail track. The company has an experience of 130 years in rail infrastructure manufacturing and supply. Being supplied, the ERS has been directly fastened to predesigned steel I girder in Klokner Institute (KI), Czech Technical University of Prague. The assembly has been done under the direct supervision of Ing. Miroslav Vokac, the main researcher in KI. The technical requirements for the assembly has been done following the “Certified Guidelines” furnished in project called **Centre for Effective and Sustainable Transport Infrastructure (CESTI)** that deals with road and railway transport network including bridges and tunnels in Czech Republic. The project is supported by Competence Centers program of Technology Agency of the Czech Republic (TA CR) (Project no. TE01020168).

The Detail of the sample is furnished below,

4.1.1. The Girder

The girder is an asymmetric steel cross section with a height of 300 mm. The top flange is of the cross-section of 15x500 mm, bottom flange of the cross-section of 15x150 mm. The web is a cross-section of 270x15 mm. Upper flange stiffeners are of 15X100 mm cross section. Beam length is 2650 mm and the span of the beam for testing purpose is 2500 mm. The transverse stiffeners are placed 75 mm offset of the beam ends to aid the cantilever ends. Stiffeners dimension is 470x270x15 mm.

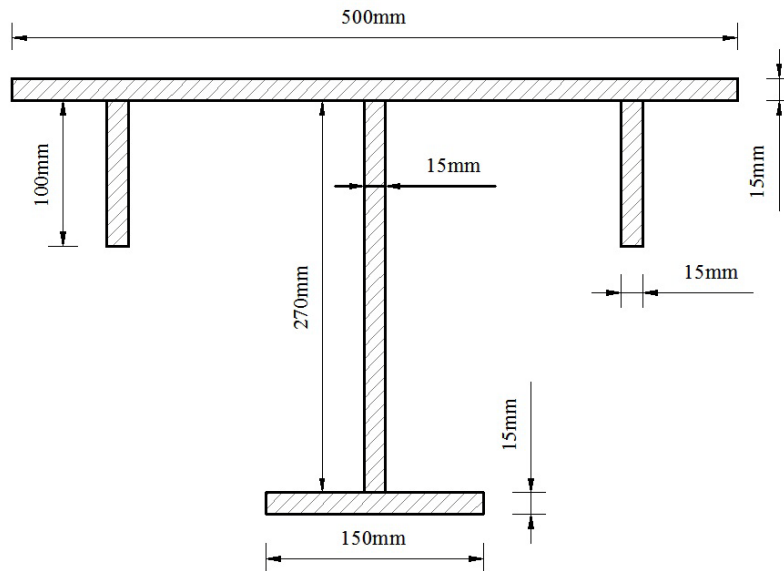


Figure-4.21: I girder Cross Section

Material Properties:

S355 has been used for the girder assembly. Hence,

Tensile strength of steel, $f_y = 355 \text{ MPa}$

Density, $\rho = 7850 \text{ kg/m}^3$

Poisson's ratio, $\nu = 0.3$

Modulus of Elasticity, $E = 200000 \text{ GPa}$

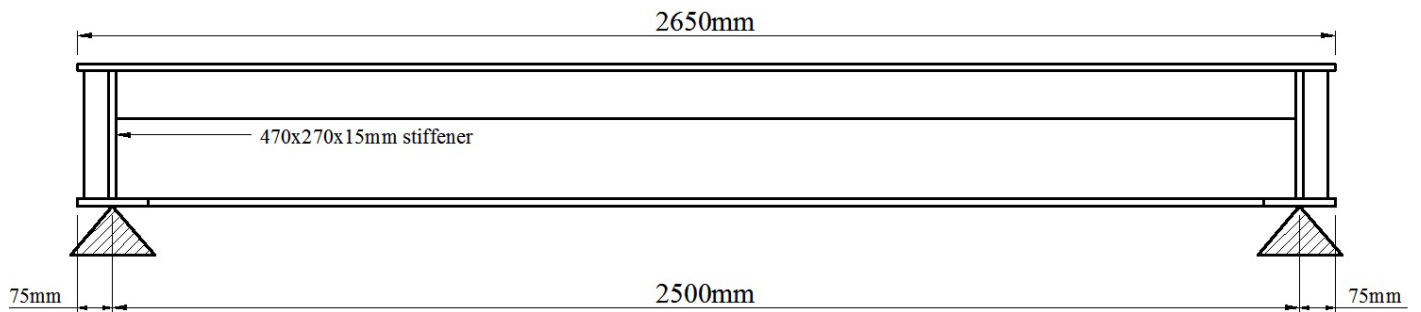


Figure-4.22: Long section of girder

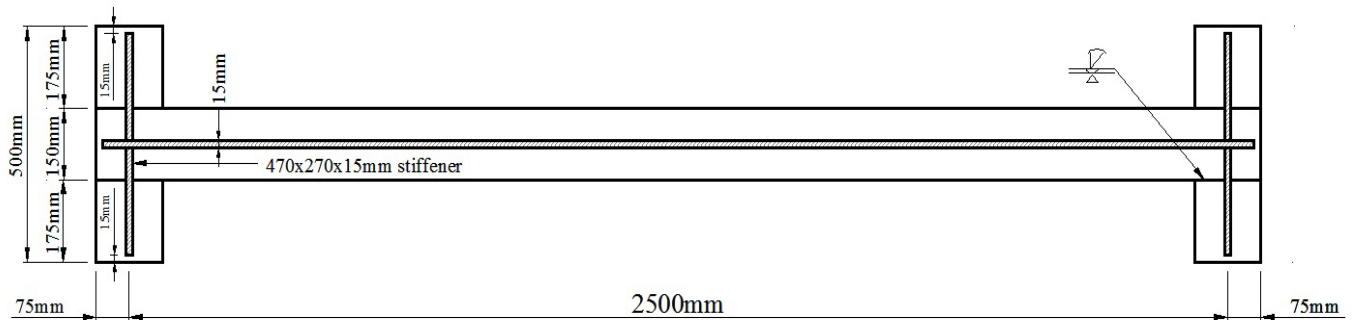
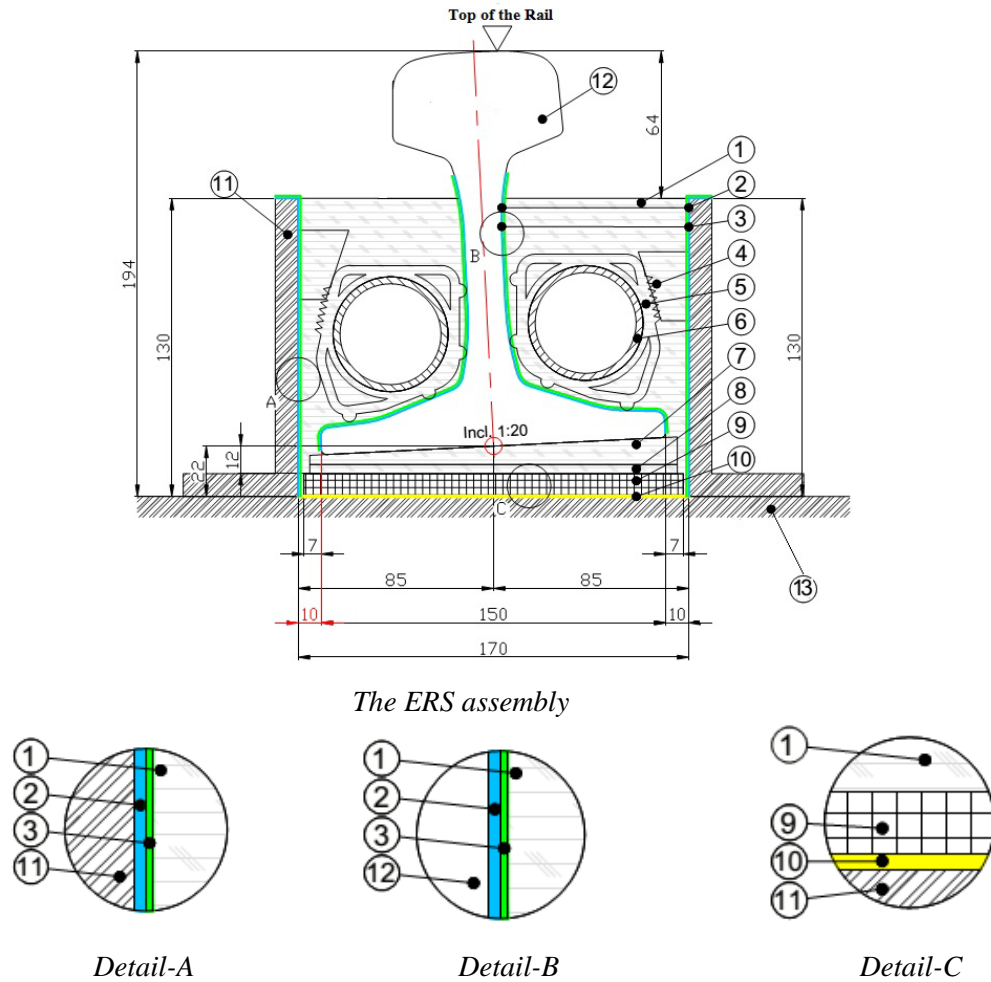


Figure-4.23: Top view of girder

4.1.2. The Embedded Rail System (ERS)

The test has been performed on an embedded rail system manufactured and provided by Edilon)(Sedra™. All the components used to prepare the ERS sample for the test (ref. figure-4.24) are [All the information and material data has been collected from Edilon)(Sedra right reserved report and data and annexed in Appendix-I];

1. Elastic embedding material: **Edilon)(Sedra Corkelast VA-60**
2. Pre-treatment primer applied on surface of channel & rail:
Edilon)(Sedra Primer U90WB
3. Bonding primer applied on Primer U90WB:
Edilon)(Sedra Primer 21 2K
4. Rail alignment (horizontal) fixation component:
Edilon)(Sedra ERS Cork Wedge T (every 1.5 - 2 mtr)
5. PVC tube fixation component: **Edilon)(Sedra ERS Spacer (50 mm)** (every 1.5 - 2 m)
6. 50 mm diameter PVC tube: **Edilon)(Sedra ERS PVC Tube**
7. Rail alignment (Vertical) fixation component:
Edilon)(Sedra ERS Polymer Inclination Shim (every 1.5 - 2 mtr.)
8. Rail alignment (Vertical) fixation component:
Edilon)(Sedra ERS Polymer Shims (every 1.5 - 2 mtr.)
9. Resilient Base Strip: **165 x 10 mm Edilon)(Sedra Trackelast RS/RPU/3000**
10. Adhesive for bonding strip at bottom channel: **Edilon)(Sedra Dex-G type 20**
11. Steel channel: **L 130x75x10mm**
12. Rail: **UIC 60/60E1**
13. Base Plate: **2650x330x15mm steel plate**



*Figure-4.24: The Edilon)(sedra Embedded Rail System
 (ref. edilon)(sedra drawings-1 (see Appendix-I)*

4.1.2.1. Embedding material: edilon)(sedra Corkelast VA-60

Edilon)(sedra Corkelast VA-60 is a solvent and plasticizer free, two component, self-leveling casting elastomer system based on state-of-the-art polyurethane resins with cork granulate and mineral fillers. It is an elastomer material for in-situ pouring applications in rail constructions.

Edilon)(sedra Corkelast VA-60 provides both elastic support and fixation of the rail. It accommodates insulation of electric currents in the rail. It is specially developed for use in rail fastening systems for heavy rail (freight and passenger trains, including high speed trains).

Material Properties:

Density = 1.05 ± 0.05 gm/cc

Modulus of Elasticity = 3.5 MPa

Static compressive modulus = 5.9 MPa (on a test sample size = $50 \times 50 \times 25$ mm)

Adhesive properties on primed steel > 0.8MPa (tested on Primer 21 and Primer U90WB)

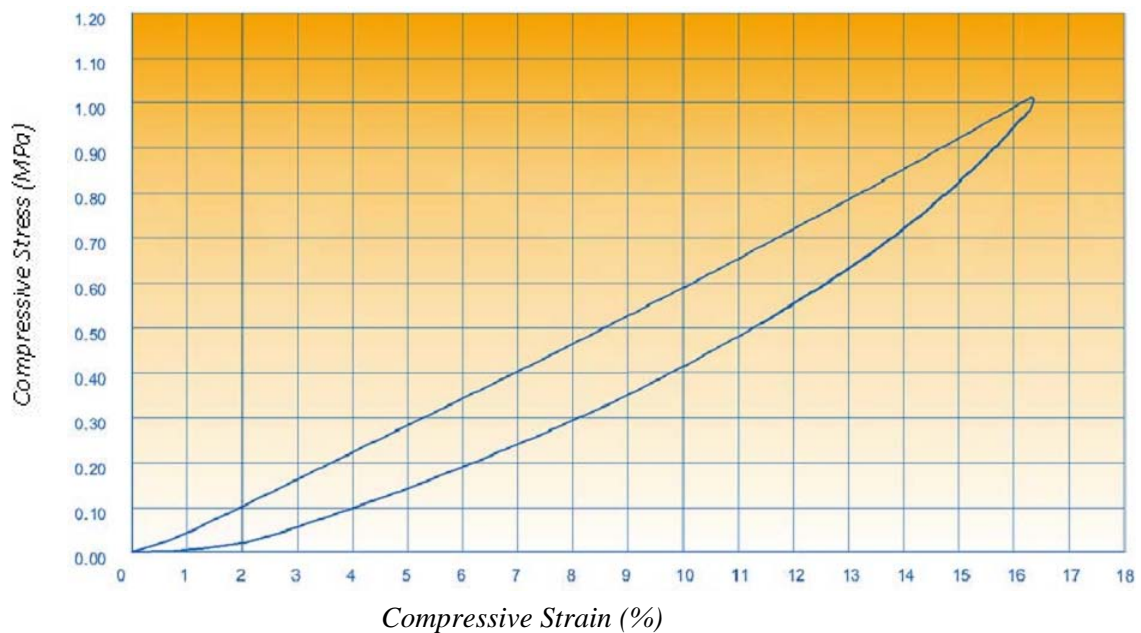


Figure-4.25: Static Compressive stress-strain curve

4.1.2.2. Pre-treatment primer : edilon)(sedra Primer U90WB

It is a two-component pre-treatment primer based on epoxy resins, which can be directly applied on pre-treated steel and concrete surfaces. It can be applied by means of a brush / roller or with airless spray equipment. The primer increases the adhesive strength of concrete and steel surfaces. It can be used on earlier applied and cured layers.

Material Properties:

Density = 1.4 ± 0.1 gm/cc

Adhesive strength on primed steel (1 layer Primer U90WB / 1 layer Primer 21) > 10MPa
(After 7 days + 20^0 C)

4.1.2.3. Bonding primer: edilon)(sedra Primer 21 2K

edilon)(sedra Primer 21 is a one-component, fast curing bonding primer specially formulated for use in combination with edilon)(sedra elastomer systems. edilon)(sedra Primer 21 is designed to ensure an optimal bonding between surfaces pre-treated with edilon)(sedra Primer U90WB and which will be covered with an edilon)(sedra elastomer.

Material Properties:

Density = 1.3 ± 0.1 gm/cc

Adhesive strength on primed steel (1 layer Primer U90WB / 1 layer Primer 21) > 10MPa
(After 7 days + 20⁰ C)

4.1.2.4. PVC tube: edilon)(sedra ERS PVC Tube

PVC (Poly Vinyl Chloride) is a thermoplastic polymer. Usually it comes in two basic forms; and flexible. The rigid form of PVC is used in construction for pipe and in profile applications. 50mm diameter PVC pipe has been used in the ERS assembly as space filling or utility passage component.

Material Properties: (www.professionalplastics.com)

Density = 1.3 ~ 1.45 gm/cc (ASTM D792)

Modulus of Elasticity = 420000 psi = 2896.6 MPa (ASTM D638)

Poisson's ratio, $\nu = 0.33$

4.1.2.5. Resilient Base Strip: edilon)(sedra Trackelast RS/RPU/3000

EDILON Resilient ERS Strip 3000 is an elastic strip based on a state-of-the-art elastomer material. The elastic properties of EDILON Resilient ERS Strip 3000 are designed for the absorption of short, intensive dynamic loads and vibrations. The elastomer maintains these properties even after large numbers of load repetitions under various climatic conditions. It also accommodates the insulation of electric currents in the rail. It is developed for use in rail fastening systems for heavy rail (track for freight and passenger trains, including high speed trains). It provides reduced support stiffness for improved damping of noise and vibration as well.

Material Properties:

Tensile Strength > 3 MPa

Modulus of Elasticity = 1.8 MPa

Static compressive modulus = 2.2~2.3 MPa

(on a test sample size = 136 mm diameter x 10 mm thickness)

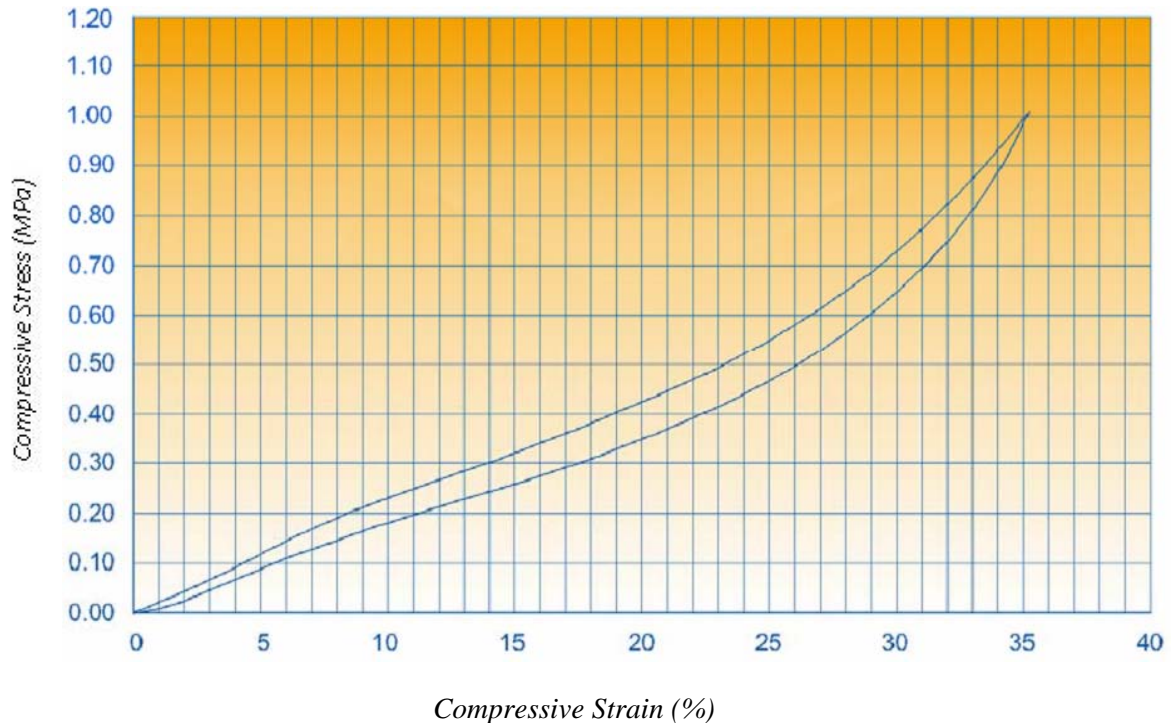


Figure-4.26: Static Compressive stress-strain curve of Resilient Base Strip

4.1.2.6. Adhesive for bottom channel: edilon)(sedra Dex-G type 20

Edilon)(Sedra Dex-G is a solvent free, self-leveling grout system (based on special epoxy resins and high quality mineral filler materials) for durably under grouting of machines and engineering structures under heavy, dynamic load conditions. Its good adherence to damp, humid or wet surfaces and its high initial compression strength make edilon)(sedra Dex-G exceptionally suitable for difficult applications where working time is limited.

Material Properties:

Density = 1.6 ± 0.05 gm/cc

Flexural-tensile strength = 56.7 MPa (Test samples dimensions: 40x40x160 mm)

Compression strength > 90 MPa (Test samples dimensions: 100x100x40 mm)

Modulus of elasticity > 4500 MPa

Flexural strength > 39 MPa

Adhesive strength on steel (S235) > 35MPa

4.1.2.7. Steel channel, Rail and Base plate

Two steel channels L130x75x10mm, 170mm apart has been used along the length of the assembly to create the recess/bounding frame for pouring the embedding material.

UIC 60/60E1 type rail has been used.

All the ERS assembly has been done upon a 330x20mm steel base plate

Material Properties:

S355 has been used for the girder assembly. Hence,

Tensile strength of steel, $f_y = 355$ MPa

Density, $\rho = 7850$ kg/m³

Modulus of Elasticity, $E = 200000$ GPa

Poisson's ratio, $\nu = 0.3$

4.1.2.8. Rail alignment fixation components

There are mainly two types of alignment fixation components have been used in the Edilon)(Sedra ERS assembly.

a. Horizontal fixation:

Edilon)(Sedra ERS Cork Wedge and edilon)(sedra ERS Spacer are the horizontal fixation components of the ERS assembly as shown in figure-4.24 Cork wedge is used for precise horizontal alignment of the rail where, the pacer has been used for the fixation of the PVC pipe.

a. Vertical fixation:

Two types of polymer shims, ERS Polymer Inclination Shim and ERS Polymer plain Shims have been used for vertical positioning and alignment of the rail.

Fixation components have been used in at 1.5~2.0m spacing along the length of the assembly. They have no influence on the vertical support stiffness of the assembly.

4.1.3. The Connection between Girder and ERS

The top flange, base plate and the steel angles were drilled in a grid (Figure-4.27) for the fixing the ERS. The top flange of the beam has been directly bolted to the base plate and the steel channels of the ERS assembly (Figure-4.28). 11mm diameter bolts at 150mm spacing has been used. The end spacing has been kept 50mm.

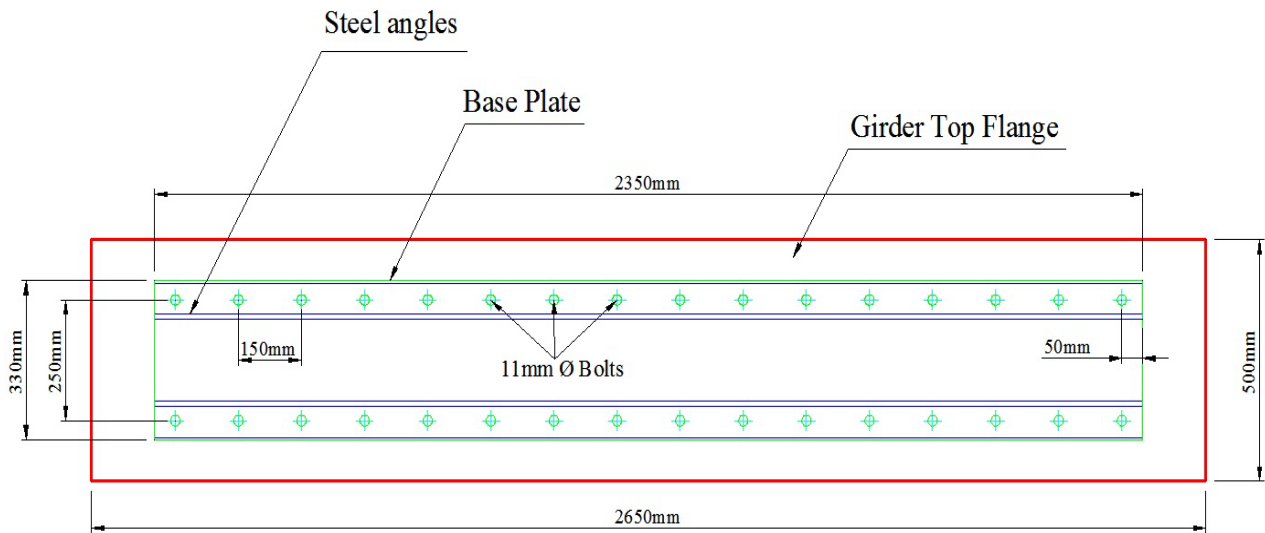


Figure-4.27: Bolt Grid for Connection between Girder and ERS

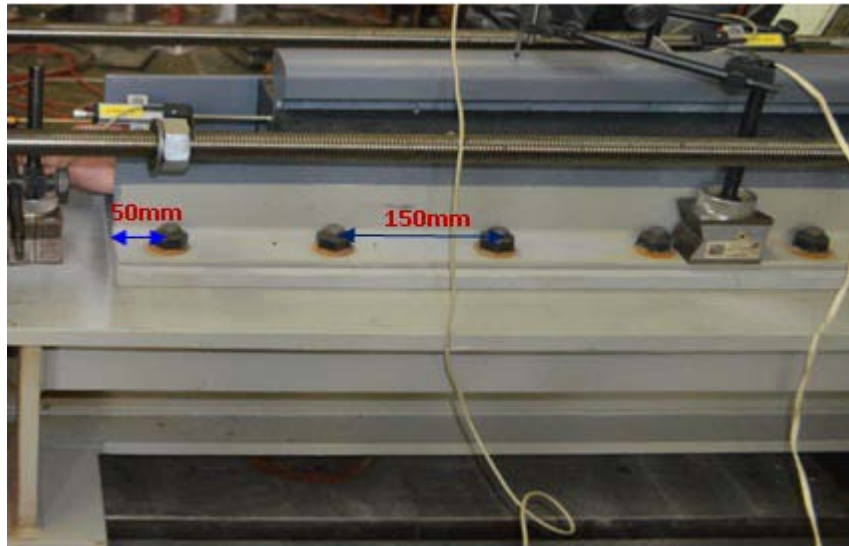


Figure-4.28: Connection between ERS and the Girder

4.1.4. Arrangement for Loading

The test specimen has been arranged for undergoing several stages of vertical and horizontal loading. The vertical load cell was positioned above the center of the girder to impose vertical load at the top of the rail and was supported by steel beam and column. (Figure-4.29)

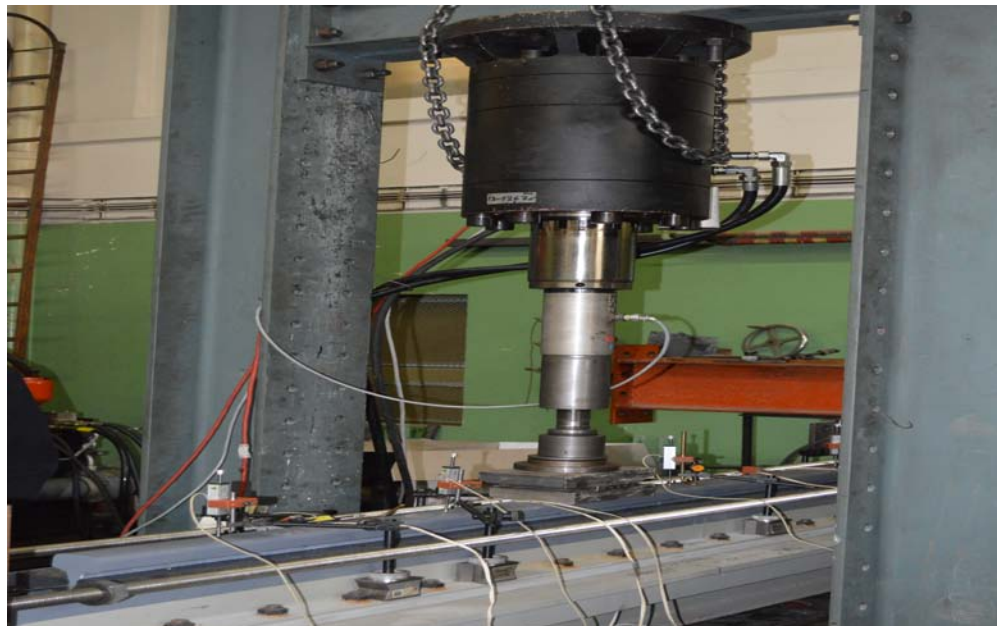


Figure-4.29: The vertical Load Cell

For the longitudinal load cell the vertical support was provided by a steel cross beam at the rear end of the specimen (figure- 4.30). The horizontal support of the load cell was ensured by steel sections welded at the front end of the Girder cross section.



Figure-4.30: The longitudinal Load Cell

For the anticipated maximum Longitudinal design load of 373.75 kN 4- UPN140 sections has been used. Design check for the UPN140 and associated connections has been annexed in Appendix-II. Two M30 steel bars have been used to support the horizontal load cell running on both sides of the rail. As such, to connect the UPN channels with the horizontal load cell, 10mm steel plates were welded to each two UPN channels to connect the M30 bars and similar plates were used to connect the bars with the horizontal load cell. The positions and arrangement for the end connections of UPN140 and M30 bars are shown in detail in figure-4.31 and 4.32.

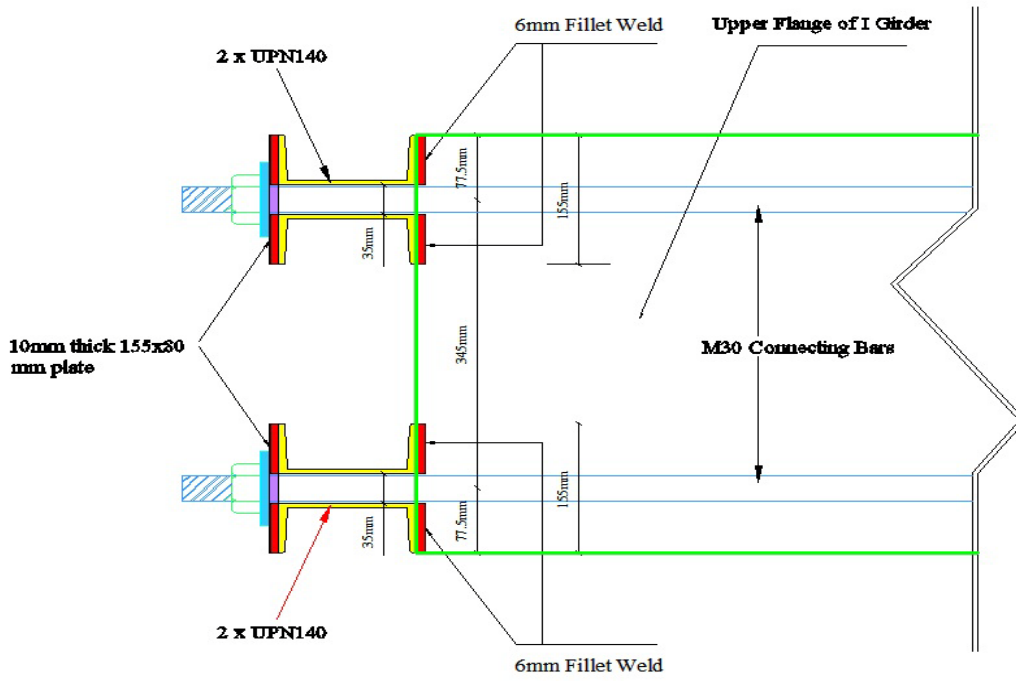


Figure-4.31: Top View of End Connection

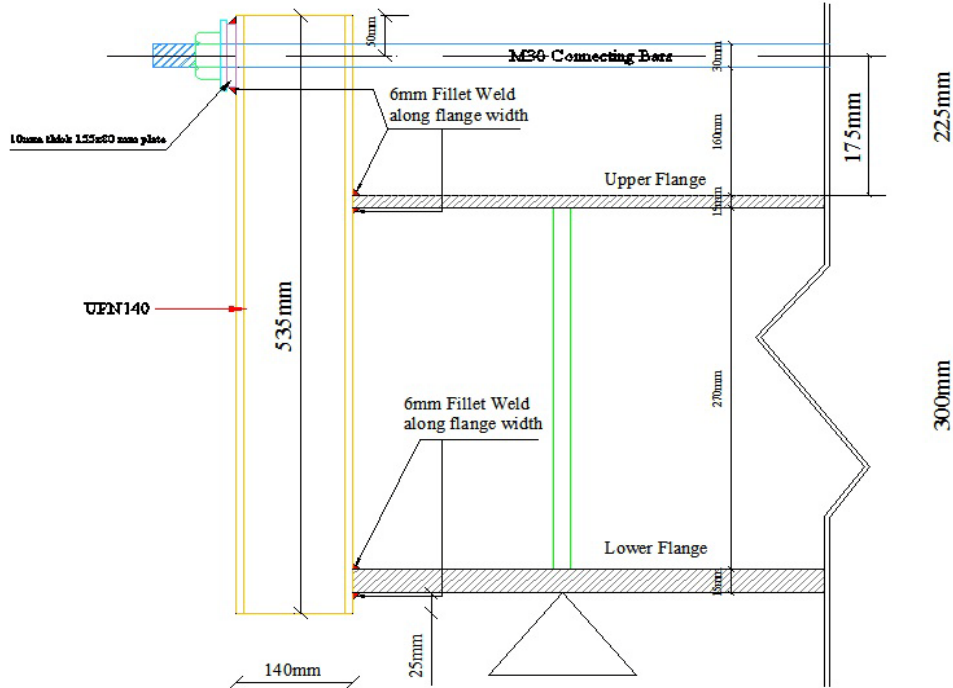


Figure-4.32: Elevation of the End Connection

4.1.5. The Final Assembly

The final assembly comprises steel base plate and angles creating the bounding frame for the embedding material running from 150mm to 2500mm in longitudinal direction above the Girder top flange (considering the end with UPN140 as the front face). Hence, the length of Steel base plate and angles are $(2500-150=)$ 2350mm. Steel girder length is 2650mm as stated above. The rail section is of 2640mm length and starts at 310mm of the girder along with the embedding material and the elastic strip, ends 300mm beyond the steel girder edge. But the embedding and elastic strip ends with in the bounding frame created by the steel base plate and angles at 2500mm. Hence the length of embedding and elastic strip is $((2650-310-150=)$ 2190mm. The Final assembly can be depicted as figure-4.33.

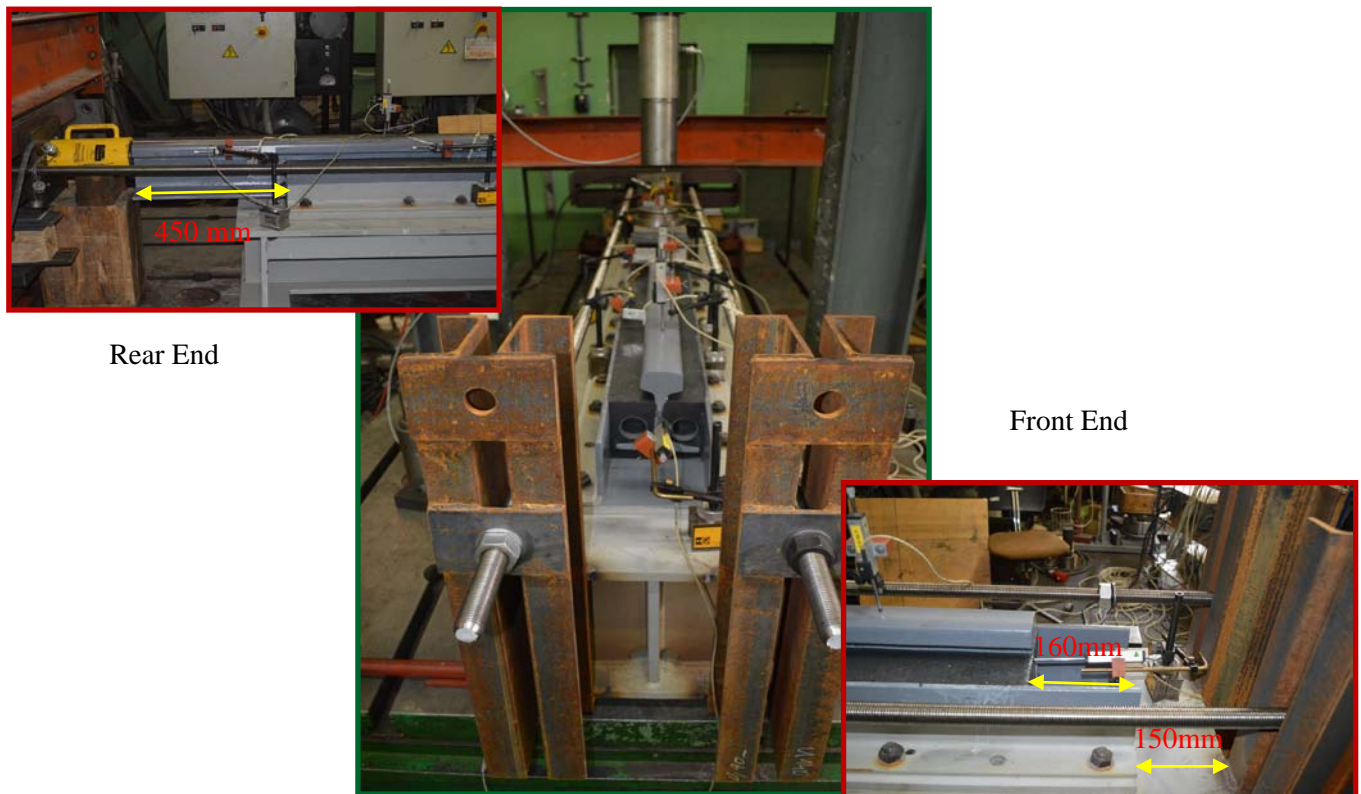


Figure-4.33: The Final Assembly of Test Specimen

4.2. The Test

4.2.1. The Static Scheme

The static scheme of the whole assembly can be shown as figure below,

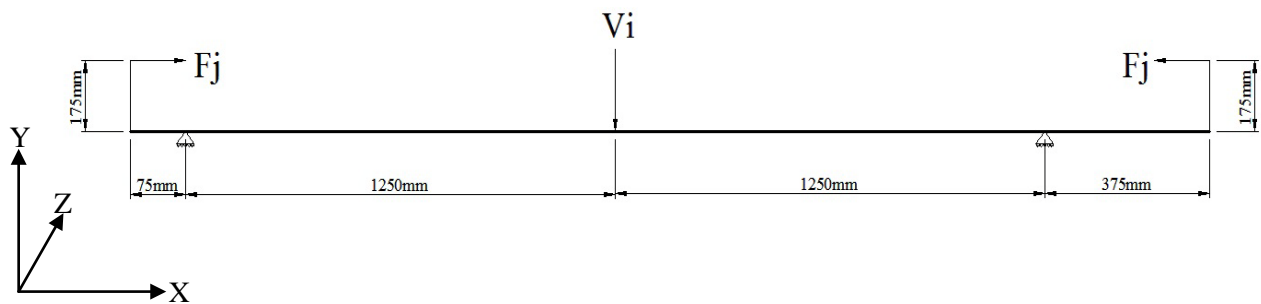


Figure-4.34: Static Scheme of the Test

The idea was to impose longitudinal load on the rail only and to represent the ideal length of the rail i.e., the continuous rail on the bridge deck. Hence, the arrangement was made as described above in 4.1.4 which represents, support welded to girder for the imposed longitudinal load cell at the opposite end. Because of the ERS system occupying some height over the girder a moment arm of 175mm had to consider while making such support arrangement. This would give rise to some extra moment compared to the ideal case; however, the amount of imposed extra moment will not affect the intended objective of the analysis to a great extent. There would be some moment imbalance due to eccentricity of self weight-center from the center of girder; which again would be of smaller scale to affect the analyses objective significantly.

Hence, the static scheme supports vertical restraints only as shown in the figure and also satisfies all the equilibrium equations of force ($\Sigma F_x = 0$, $\Sigma F_y = 0$, $\Sigma M_z = 0$). Due to the requirement of rail shift, the rail remains tilted inward in the track and the same has been simulated in the test. Therefore, there will be a small eccentricity of mass along Z axis and as the longitudinal load will be applied on the rail cross section only, small amount of loading eccentricity along x axis is also expected which will be also simulated in the FEM.

4.2.2. Load Combinations

Referring to 2.8, four stages of vertical point load have been considered up to maximum. And as the test has been conducted on a single rail only, these are 0, 40, 80 and 125 kN respectively.

According to UIC-774R, the maximum longitudinal displacement for embedded rail is recommended as maximum 6mm for unloaded and 7mm for loaded track. Eurocode has no recommendation on embedded rail. Hence, the maximum longitudinal load applied during the test has been monitored according to the longitudinal displacement of the rail (not to exceed too much beyond 7mm) and it has never exceeded the maximum design longitudinal force value.

Therefore, depending on the longitudinal displacement, the following four combination of load has been applied on the laboratory test specimen.

Table-4.1: Maximum Loads and Displacement on test specimen

Combinations	Max ^m Vertical Load (kN)	Max ^m Longitudinal Displacement(mm)	Max ^m Longitudinal Load (kN)
1	0	7.06	258.075
2	40	5.895	209.21
3	80	5.2	182.806
4	125	7.447	241.3

4.2.3. Test Output Arrangement

The test has been conducted on the final assembly as described in 3.1.5 with 5 horizontal displacement transducers, 4 vertical displacement transducers and 4 strain gauges set on different locations of the rail. Additionally, 2 more strain gauges are set at the center of the girder; one at the bottom of the top flange and the other at the top of the bottom flange. The first test has been conducted with vertical load = 0kN and the subsequent tests with 40, 80 and 125kN respectively. In all the cases, vertical incremental load has been applied and fixed to the maximum limit of each load combination first and then the longitudinal incremental load has been applied. The positioning of the displacement transducers and the strain gauges has been set as table-4.2.

Table-4.2: Locations of strain gauges and displacement transducers on rail & girder.

Positions of Strain Gauges						
<i>Dial Gauge no</i>	20	21	22	23	24**	25**
<i>Longitudinal (mm)</i>	680	1310	1930	2610	1325	1325
<i>Vertical (mm)</i>	417				15	285
Positions of Vertical Displacement Transducers						
<i>Dial Gauge no</i>	216	217	218	219		
<i>Longitudinal (mm)</i>	535	985	1595	2210		
<i>Vertical (mm)</i>	Top of the rail (514.1)					
Positions of Longitudinal Displacement Transducers						
<i>Dial Gauge no</i>	210	211	212	213	214	
<i>Longitudinal (mm)</i>	310	710	1295	1945	2580	
<i>Vertical (mm)</i>	434	499				

** All dimensions have been calculated considering the origin at the bottom-center of girder edge. And the dial gauges no for vertical and longitudinal loads were 230 and 235 respectively.*

*** Strain gauges on Girder*

All the test data has been annexed to Appendix-III

4.3. Analysis of Test Output Data

4.3.1. Data for Resistance Analysis of ERS

The longitudinal resistance of the ERS in response to longitudinal displacement has been plotted for all the four load combinations. Slightly curvilinear response has been found which can be approximated as linear relationship. The relationships has been compared for the vertical and longitudinal load combinations and shown in figure- 4.35.

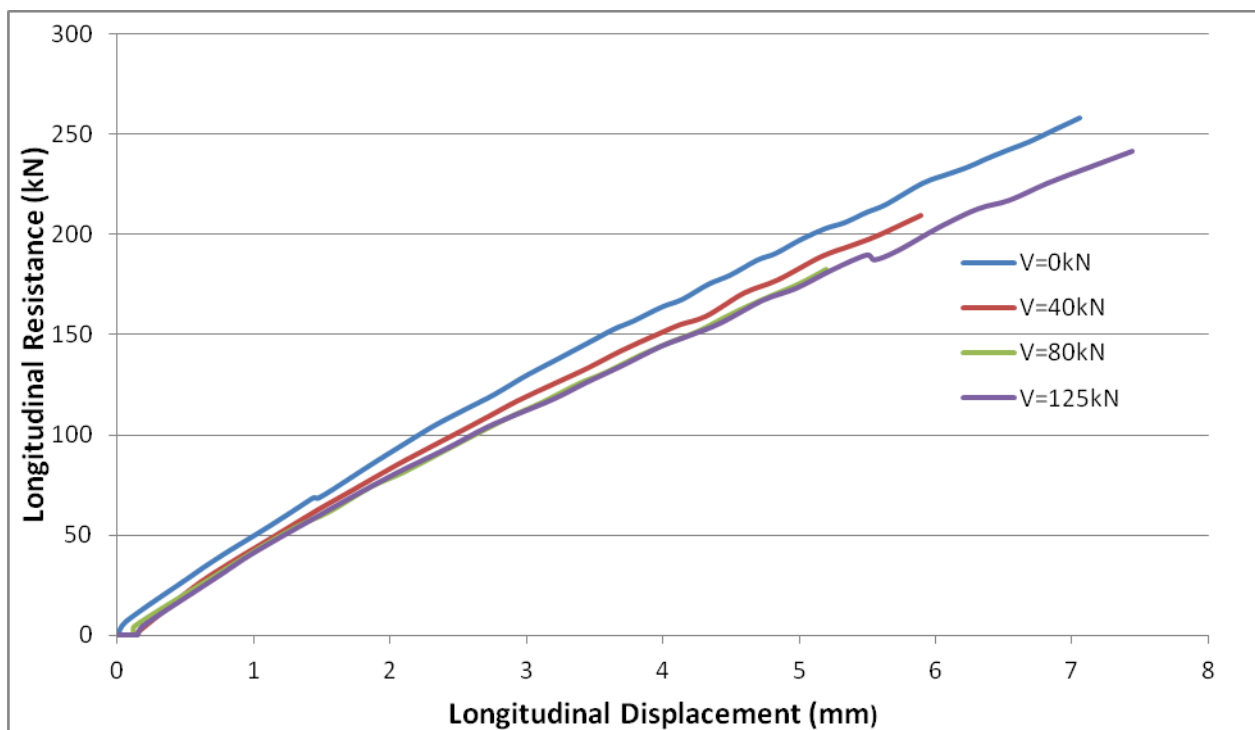


Figure-4.35: Longitudinal Resistance vs Longitudinal Displacement of ERS

Though, it can be approximated as liner response, Second order functions have been found with fairly good regression values ($r^2 > 0.99$) for all the curves and has been found as figure-4.36 below.

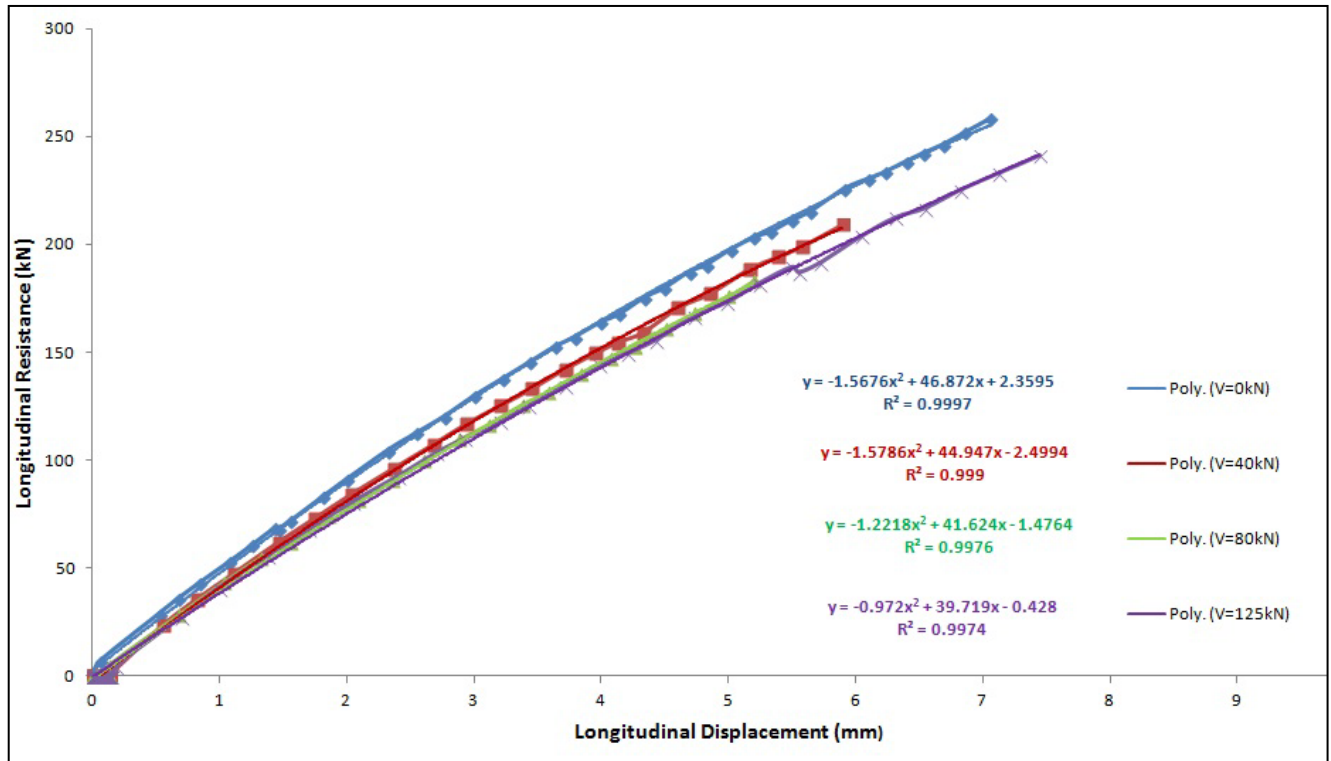


Figure-4.36: Functions representing Longitudinal Resistance vs Longitudinal Displacement of ERS

Though for a loaded track, higher longitudinal resistance of track has been obtained as compared to unloaded track in various studies of ballasted and non-ballasted track (UIC-774R & Euro Codes), the test data obtained from the testing of ERS has shown slight decrease of longitudinal resistance with the higher vertical load combinations. The Longitudinal resistance attenuation for the increment of vertical loads has been plotted from the test output data against the same level of displacements, which gives a better understanding on the level of decrement of the resistance. However, longitudinal resistance could not be found exactly at 1,2,3,4 or 5mm displacements and linear interpolation will lead to erroneous approximation. Hence, longitudinal resistance values have been taken here tentatively at or around those displacements. Moreover, no data were formed for 6mm or more displacements for 80 kN vertical load case. Therefore, the trends could have been shown only up to 7mm horizontal displacements with some missing data. The sorted data has been shown in Table-4.3.

Table-4.3 Longitudinal Resistance under incremental vertical load at different displacement level

0 kN		40 kN		80kN		125 kN	
Longitudinal Displacement (mm)	Longitudinal Resistance (kN)						
1.073	52.597	1.108	47.358	1.027	43.005	0.995	40.829
1.999	90.983	2.038	84.293	2.091	81.265	2.046	80.797
3.007	129.855	2.937	116.793	3.114	116.434	2.929	110.054
3.994	163.753	3.951	149.563	4.073	146.985	3.99	144.066
5.014	197.406	5.165	188.71	4.998	175.643	4.985	173.113
5.908	225.496	5.895	209.214			6.041	203.817
7.059	258.075					7.121	233.048

The trend lines has been plotted as figure- 4.37 below,

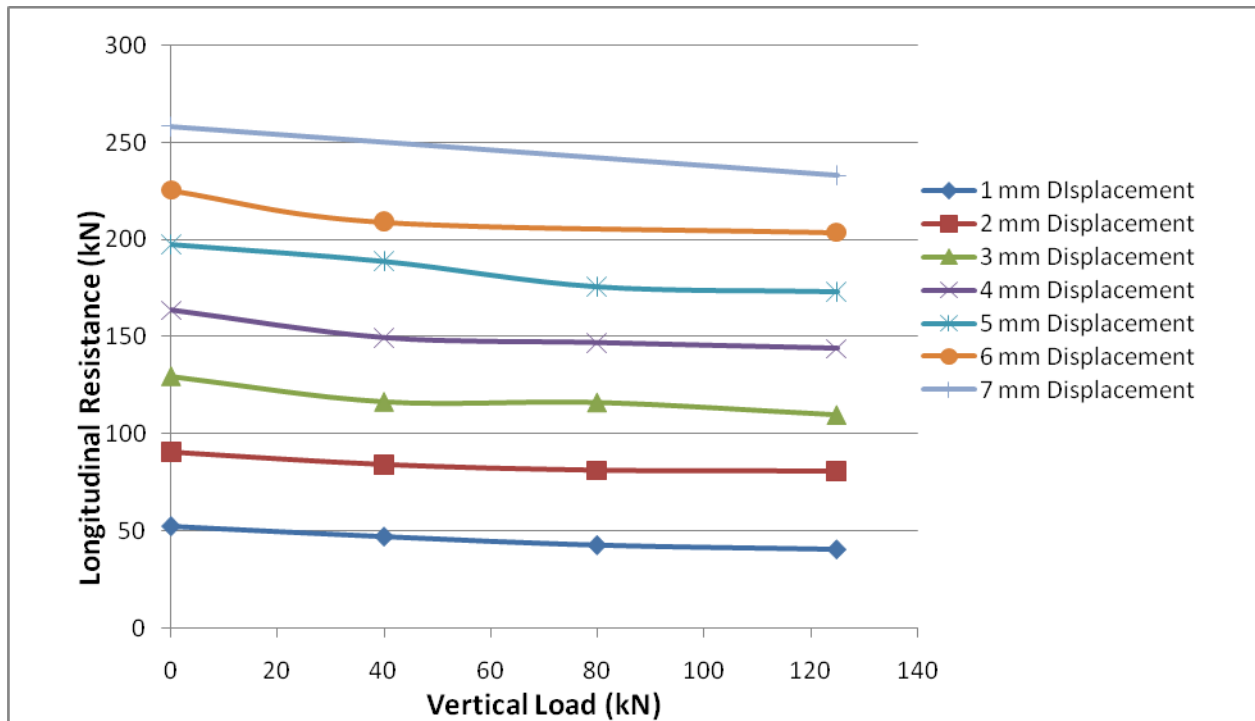


Figure-4.37: Trend of Longitudinal Resistance of ERS under incremental Vertical load

It is fairly observed that the attenuation of longitudinal resistance with incremental vertical loads is maintaining a similar trend at all level of displacements. The slight non-linear behavior for the upper curves is due to the deviation of displacement values from the assumed exact values of 3, 4 and 5mm displacements. Therefore, it can also be suggested that the rate of attenuation is also similar in all cases.

4.3.2. Additional Data for FEM Validation

Other than the longitudinal resistance and displacement data, data have been recorded for vertical displacements and horizontal stresses along the length of the rail. Also stresses at midspan of the girder have been recorded. These data will be used to validate the Finite Element Model of the test specimen on subsequent chapters.

However, the vertical displacement along the length of the rail for different vertical loads (at the maximum horizontal load of each combination) has been found as figure- .

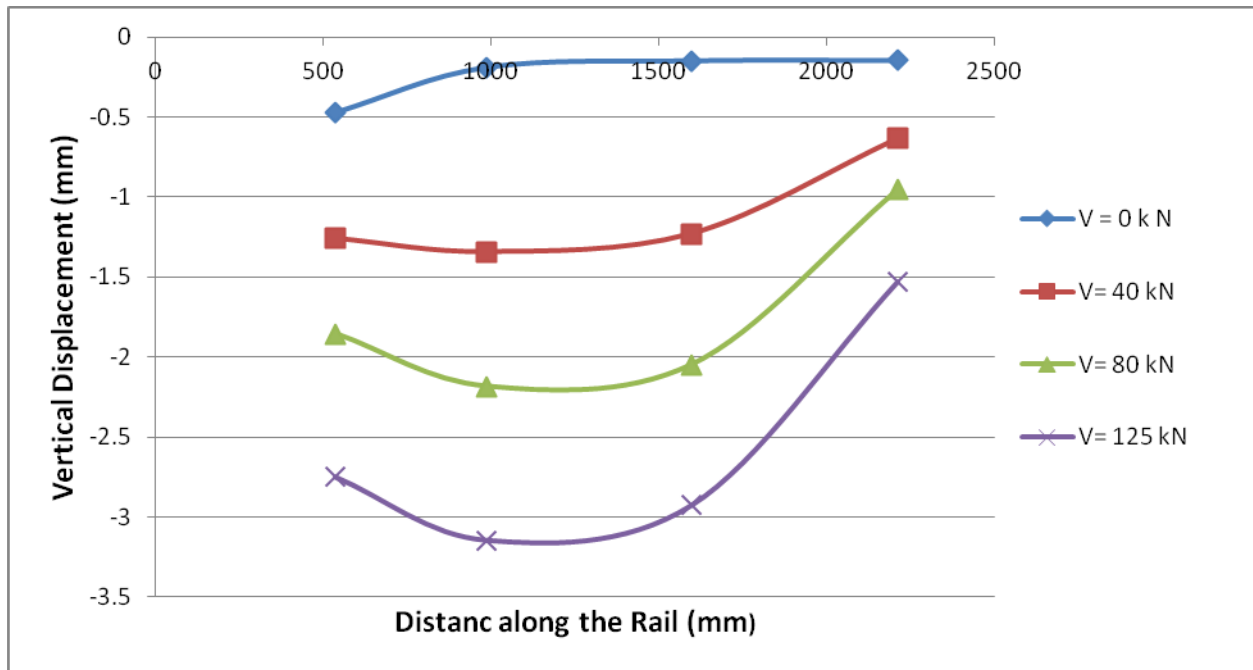


Figure-4.38: Vertical Displacement of Rail along the length for different level of Vertical Load

This behavior is understandable as it is simply depicting the downward deflection of the rail with incremental vertical load.

The longitudinal stress values along the length of the rail are simply understood to be decreasing from the load application area to the free end and it has been found the same for unloaded rail case. Then the behavior under vertical loads has been found and plotted along with the unloaded curve. Effect of vertical loads near the vertical load application area has been found which is decreasing the compression at that zone gradually and forcing towards tension at higher load cases.

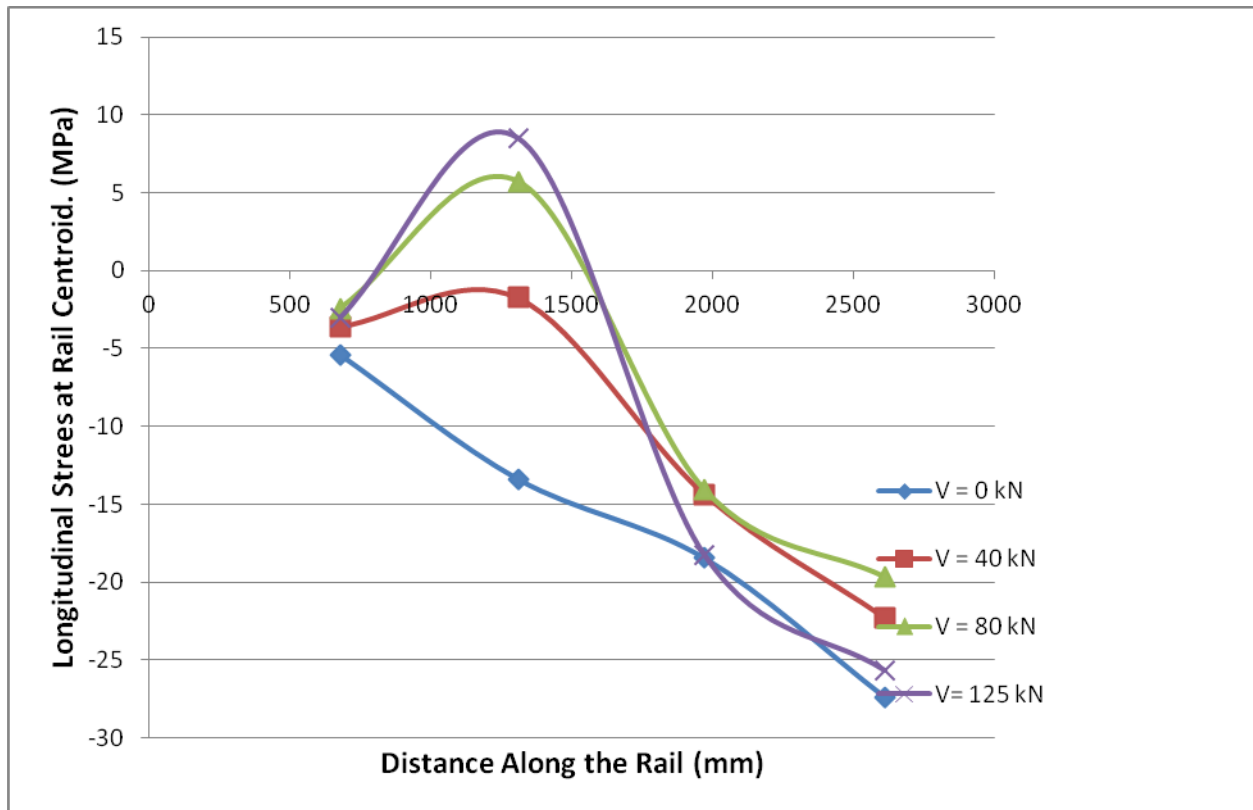


Figure-4.39: Longitudinal Stress on Rail along the length for different level of Vertical Load

Stress value has also been recorded at the midspan of the girder with two strain gauges at top and bottom flanges. The trend of stress change along with the increment of vertical load has been found as figure- 4.40.

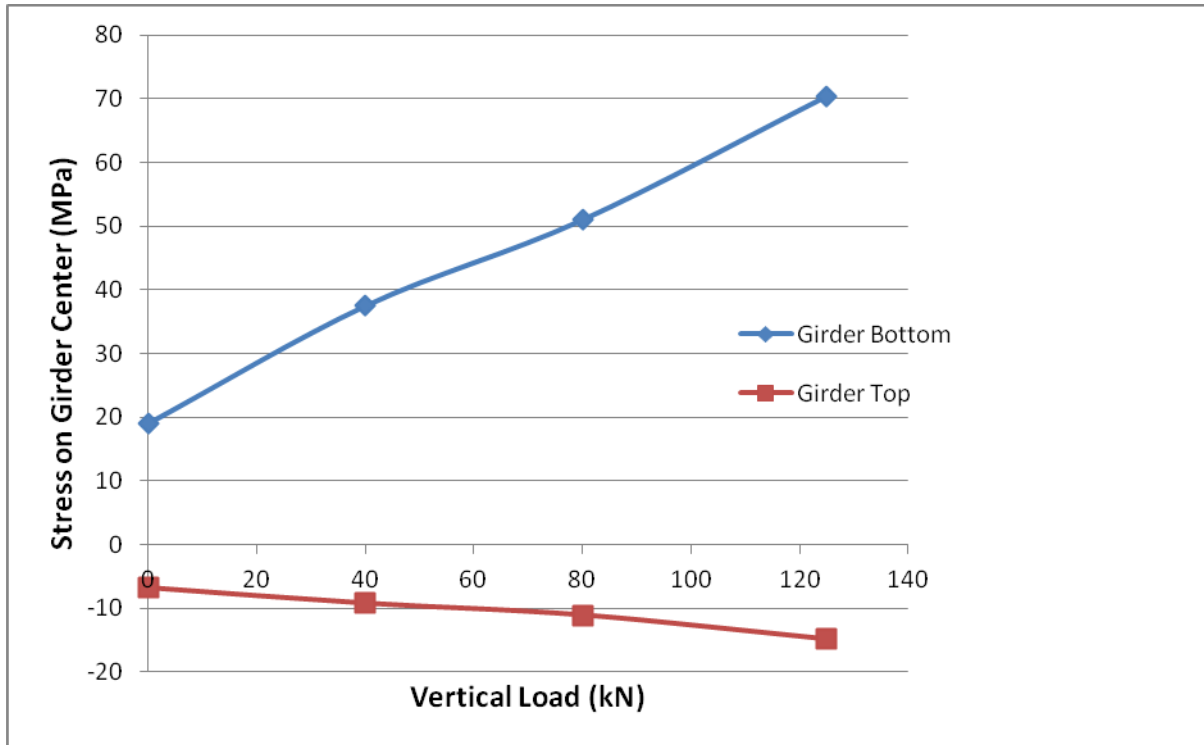


Figure-4.40: Stress on center of the girder for different level of Vertical Loads

This behavior of stress is also quite understandable as it is describing the simply supported beam stress phenomena, with increase in tension at bottom fiber and compression at the top fiber of the girder with the increment of vertical load.

5. Development of the Simulation Model

5.1. Modeling tool

The simulation model of the laboratory test specimen has been developed in ANSYS APLD version 14.0.

ni depoleved neeb sah nemiceps tset yrotarobal eht fo ledom noitalumis ehT

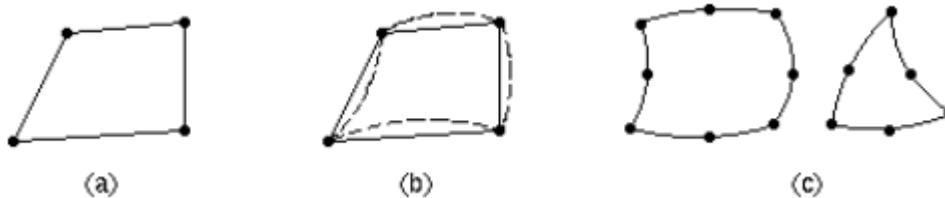
5.2. Modeling Principles

5.2.1. Basic principles to choose elements

The finite element model will be a 3 dimensional model composed of solid elements mainly. The inter-mix of different types of solid elements has been done following the basic principles. The following principles has been followed while choosing the elements and modeling purpose of the system,

- Using of elements with appropriate number of nodes (Linear or higher order) and Degrees of Freedoms (DoFs) and mesh density in an attempt to balance computational expense (CPU time, etc.) against precision of results,

- The ANSYS program's element library includes two basic types of volume elements; linear (with or without extra shapes), and quadratic (with extra shapes). **In nonlinear structural analyses**, usually it provides better accuracy at less expense for a model with fine mesh of linear elements rather than a comparable coarse mesh of quadratic elements. Elements with extra shapes are required to model curved surfaces or shapes, which can also be replaced by appropriate number of flat elements (without extra shapes),



- (a) Linear iso-parametric
- (b) Linear iso-parametric with extra shapes
- (c) Quadratic.

Figure-5.41: Basic area and volume types available in the ANSYS program

- Avoid using of the wedge or tetrahedral forms of 3-D linear elements in high results-gradient regions, or other regions of special interest,
- When mixing element types, connecting elements should have the same number of nodes along the common side. The corner node of an element should only be connected to the corner node, and not the mid-side node of an adjacent element,
- Hexahedral meshing,
- Use of isotropic material properties,
- To be consistent, two elements must have the same DOFs; for example, they must both have the same number and type of displacement DOFs and the same number and type of rotational DOFs. Furthermore, the DOFs must overlay (be tied to) each other; that is, they must be continuous across the element boundaries at the interface.

5.2.2. Physical parts for simulation

Different physical parts that has to be incorporated in the modeling are,

1. Bounding frame made of steel base plate and angles.
2. PVC Plastic pipes.
3. Elastomer/Resilient strip.
4. Edilon Corkelast filling element.
5. Rail.
7. Steel I Girder.

5.2.3. Choice of Elements

For simplicity and getting the results in reasonable time linear elements has been chosen for most of the physical part of the FEM model. And linear elements with extra shape functions always gives good results with time optimization and accuracy of solution than the use of

quadratic elements all over the model. But, it is of great concern in that case to avoid the degenerated forms of those elements in the critical regions. However, Quadratic elements has also been used at the region of high geometric complexity. Solid elements has been used all over the models and hexahedral meshing has been done to all the physical parts taking in concern a good ratio of the length to width of the elements formed. All theses effort was made to obtain a possible accurate result along with less amount of computational effort to incur by the analysis tool. The following elements have been used:

1. For all the parts of the arrangement like, the steel angles, girder, rail and edilon Corkelast **SOLID185** element will be used.
2. **SOLID186** with mid nodes will be used for the irregular rail part of the model
3. For PVC pipe **SOLID185** has been used with **finer meshing** to reduce the inaccuracy.
4. For the elastomer strip **SOLID185 with mixed u/p** has been used to justify the incompressibility of elastomer material.

5.2.4. Description of the Elements

ANSYS element library consists of hundreds of elements for structural, mechanical, fluid, thermal and other non-structural analysis. The study of the element has been carried out with the help of the vivid description written in that library. The elements chosen for the purpose of this thesis are described below following the description found in ANSYS element library¹⁹,

SOLID185

SOLID185 is used for 3-D modeling of solid structures in ansys. It is defined by eight nodes with three (3) degrees of freedom at each node that is translation in all 3 Cartesian axes /directions. The element has plasticity, hyperelasticity, stress stiffening, creep, large deflection and large strain capabilities. It has also the capability for simulating deformations of nearly incompressible elasto-plastic materials and fully incompressible hyperelastic materials. **SOLID185** is used for the three dimensional modeling of solid structures.

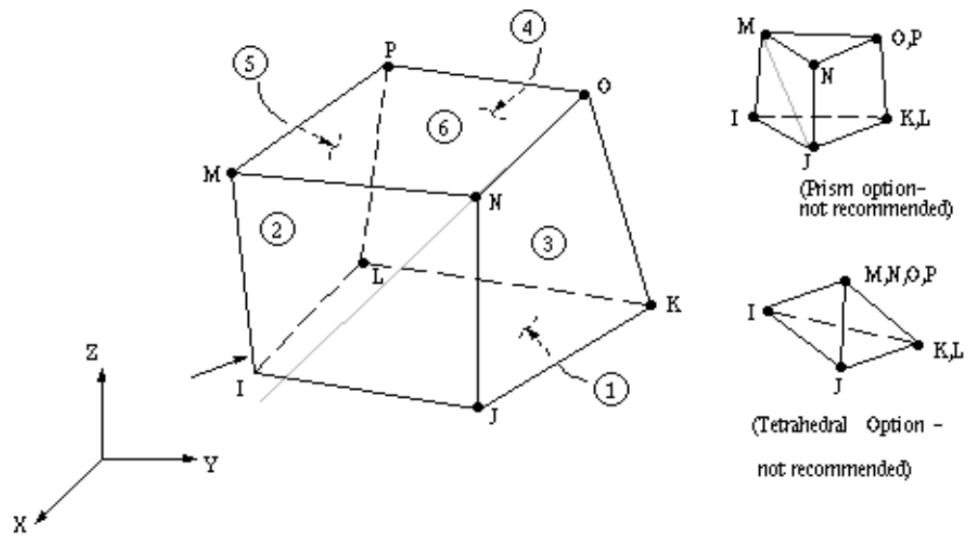


Figure-5.42: SOLID185 3-D 8-Node Structural Solid element geometry

The solution output associated with the element is in two forms:

- Nodal displacements included in the overall nodal solution
- Additional element output for stress, strain, temperature etc.

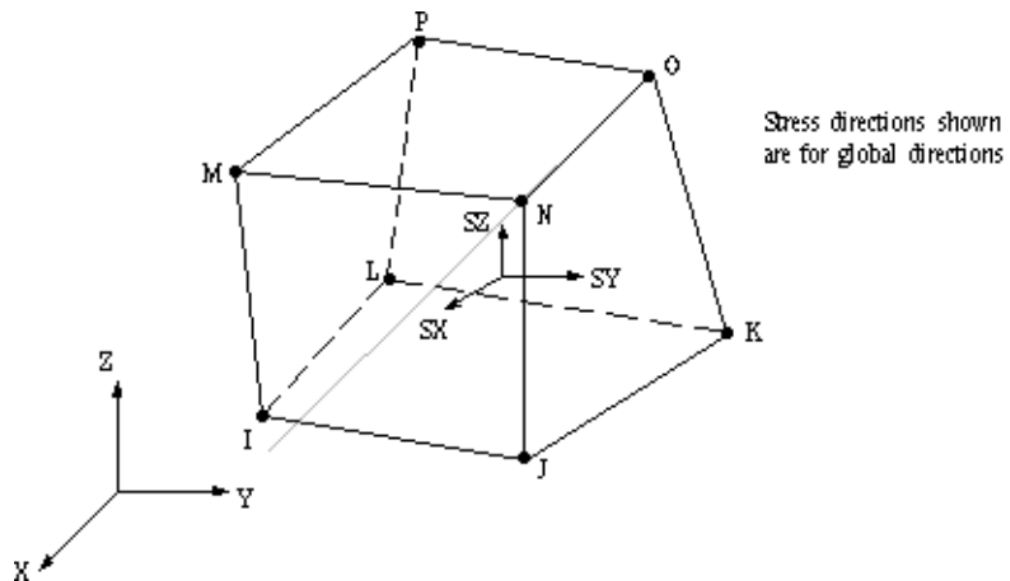


Figure-5.43: SOLID185 Stress Output

SOLID186

SOLID186 is a higher order 3-D 20-node solid element that exhibits quadratic displacement behavior. The element is defined by 20 nodes having three degrees of freedom per node: translations in the nodal x, y, and z directions. The element supports plasticity, hyperelasticity, creep, stress stiffening, large deflection, and large strain capabilities. It also has mixed formulation capability for simulating deformations of nearly incompressible elastoplastic materials and fully incompressible hyperelastic materials. SOLID186 Homogenous Structural Solid is well suited to modeling irregular meshing.

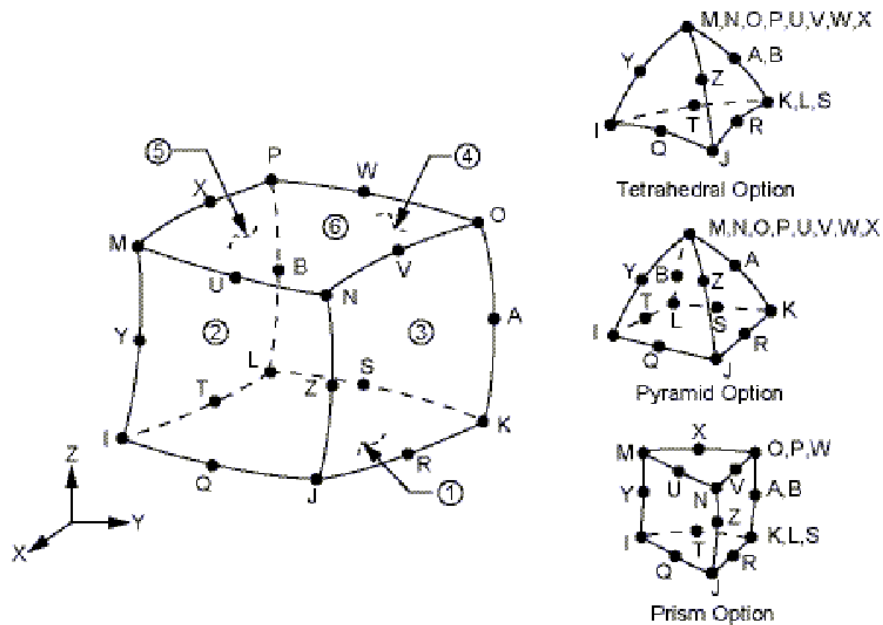


Figure-5.44: SOLID186 3-D 20-Node Structural Solid element geometry

The solution output associated with the element is in two forms:

- Nodal displacements included in the overall nodal solution
- Additional element output for stress, strain, temperature etc.

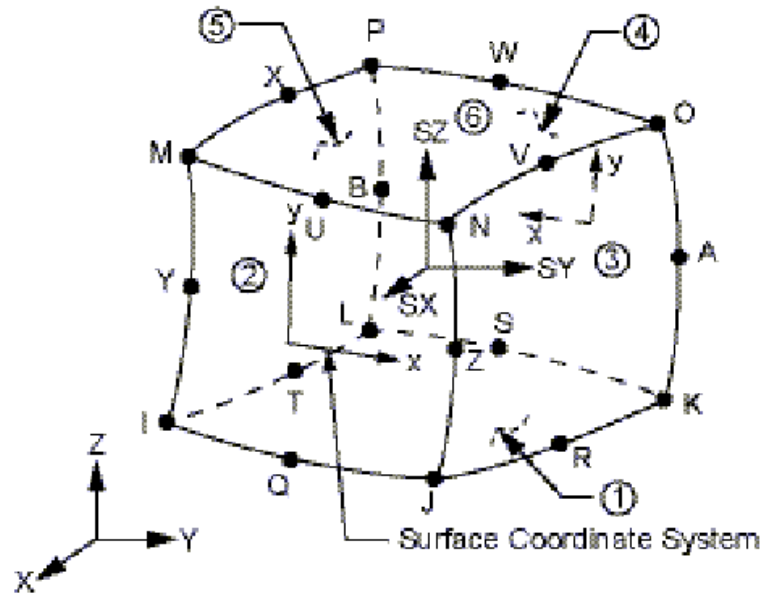


Figure-5.45: SOLID185 Stress Output

5.3. Model Generation Approach

In ANSYS, the nodes and elements are generated to define the spatial volume and connectivity of the whole system. Thus the model generation means the process of defining the geometric configuration of the model's nodes and elements. For achieving the right configuration different keypoints, lines, areas and volumes may be formed depending upon the approach of the generation. ANSYS provides different approaches to generate models, like,

- Solid modeling
- Direct generation
- Importing solid models created in CAD system etc.

- Direct generation

Direct generation deals with the approach where one will have to define the nodes and elements directly and have to track the record of each attributes which in turns become tedious job for large and complex models and contribute potential to modeling errors.

- Solid modeling

Solid modeling is more appropriate for 3D models of solid volumes. It allows to work with relatively low number of data items and different geometric operations and modifications. It also allows meshing even after the loading has been applied, i.e., it allows element redistribution and one is not bound to deal with one analysis model.

There are several approaches in Solid Modeling approach also. Like, Top-down and Bottom-up construction.

- Bottom-up construction

In this approach, the lowest order entities 'keypoints' are developed first then the higher order entities like, line, area and volumes are generated later based on the keypoints.

- Top-down construction

Ansys allows the use of Primitives which are fully defined lines, areas and volumes. program creates automatically the lower order attributes associated with it.

5.4. Selection of Modeling Approach

The laboratory test sample for the thesis is a complex one with irregular shapes like the rail and the embedding material. To follow the node numbers for this complex model will be a cumbersome job and there is lack of all primitives suitable for the total construction of the model also. Hence, the **Solid Modeling : Bottom-up construction method** has been selected for model generation in the thesis.

5.5. Geometric Modeling

ANSYS classical interface dedicates the preprocessor tab in its Main Menu for necessary model generation operation. In which the Modeling subtab is dedicated for the geometric development only (see figure-5.46)

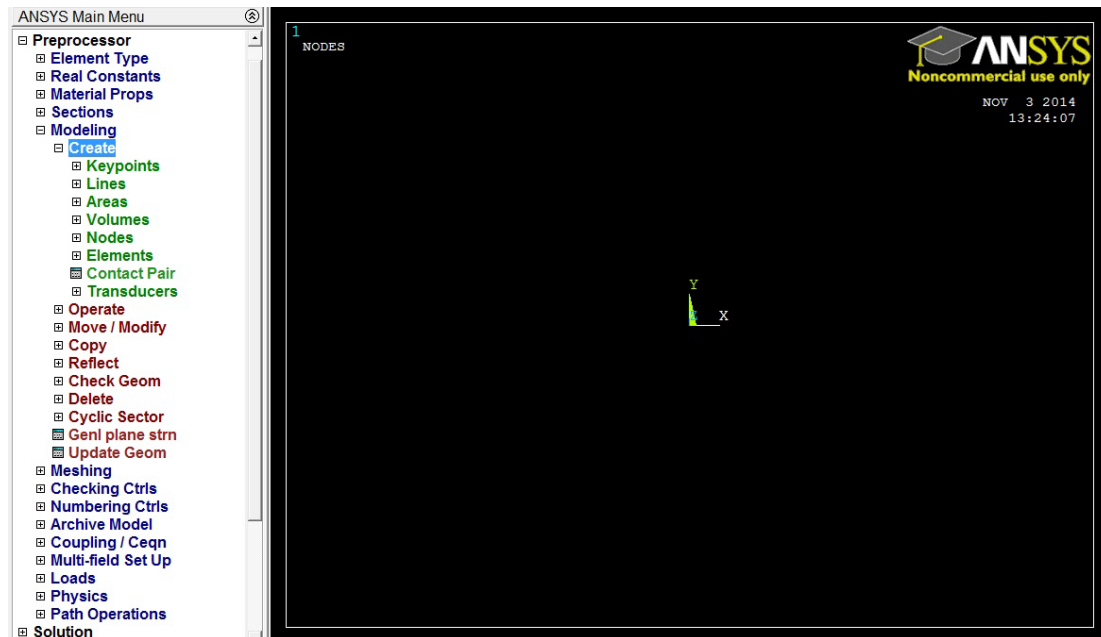


Figure-5.46: ANSYS Classical Interface: Main Menu for model generation

Steps in generating 3D Solid Volumes

- Selecting Co-ordinate system

ANSYS has different types of co-ordinate systems. Such as global and local co-ordinate system for locating geometry items, element co-ordinate system for showing orientation of material properties and element results, Nodal co-ordinate system for showing DoFs direction and orientation of nodal results data etc. For geometric modeling it has Global Cartesian, global cylindrical and global spherical systems. The global cartesian system has been chosen as the active co-ordinate system for model generation initially in the thesis.

Where, the axis perpendicular to the screen is the z axis. Later local cartesian co-ordinate systems have been created and aligned as the active co-ordinate system time to time whenever required for the ease of model construction.

- Creating Keypoints

Keypoints describe the geometric boundaries of the intended volume. Following figure shows the keypoints generated for the girder cross-section @ $z=0$.

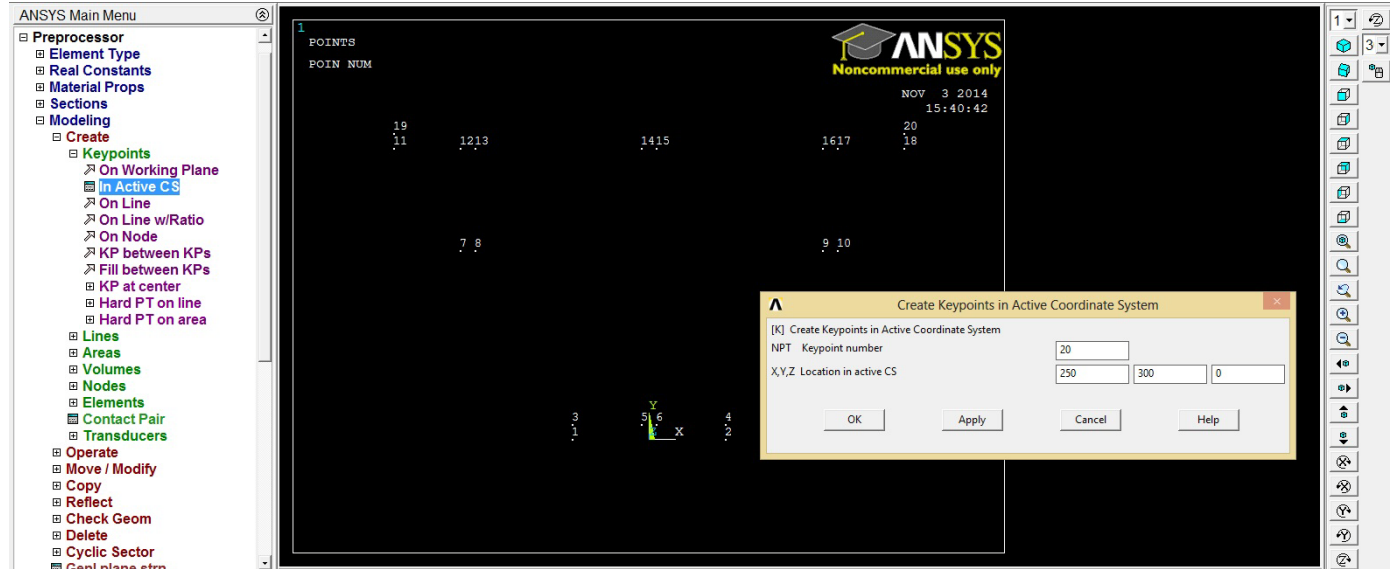


Figure-5.47: Creating Keypoints.

- Creating Lines & Areas

Keypoints are used to generate the lines as well as the areas. In our case the areas have been generated through the keypoints directly. the associated lines are formed automatically. Following figure shows the area created through the keypoints generated from earlier figure.

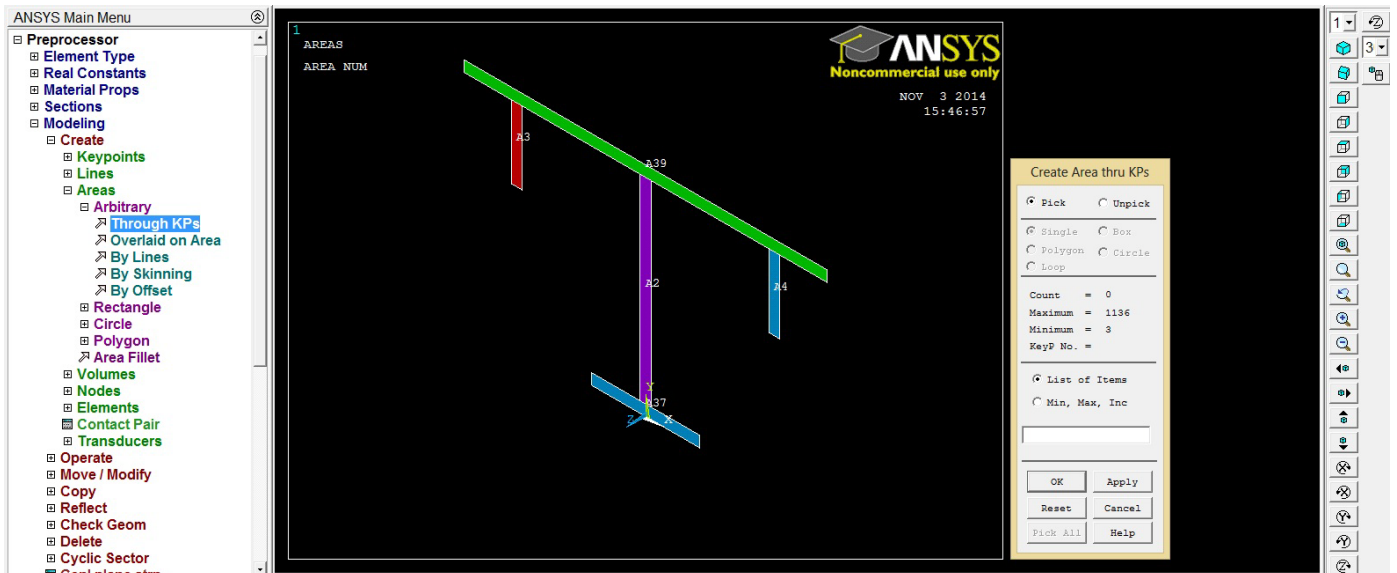


Figure-5.48: Creating Areas

- Creating Volumes

Volumes has been generated through the extrude operations of areas being formed through keypoints. ANSYS allows to extrude the areas into volumes in the active co-ordinate system along Z axis. As described above, local co-ordinate systems have also been made to extrude areas in direction other than global Z direction.

- Operating and Modifying the Created Volumes

Ansyp provides the boolean operations to add, subtract, glue, divide , overlap, intersect and other options to modify the created volume. And the move, copy, delete etc are available directly under the modeling substep.

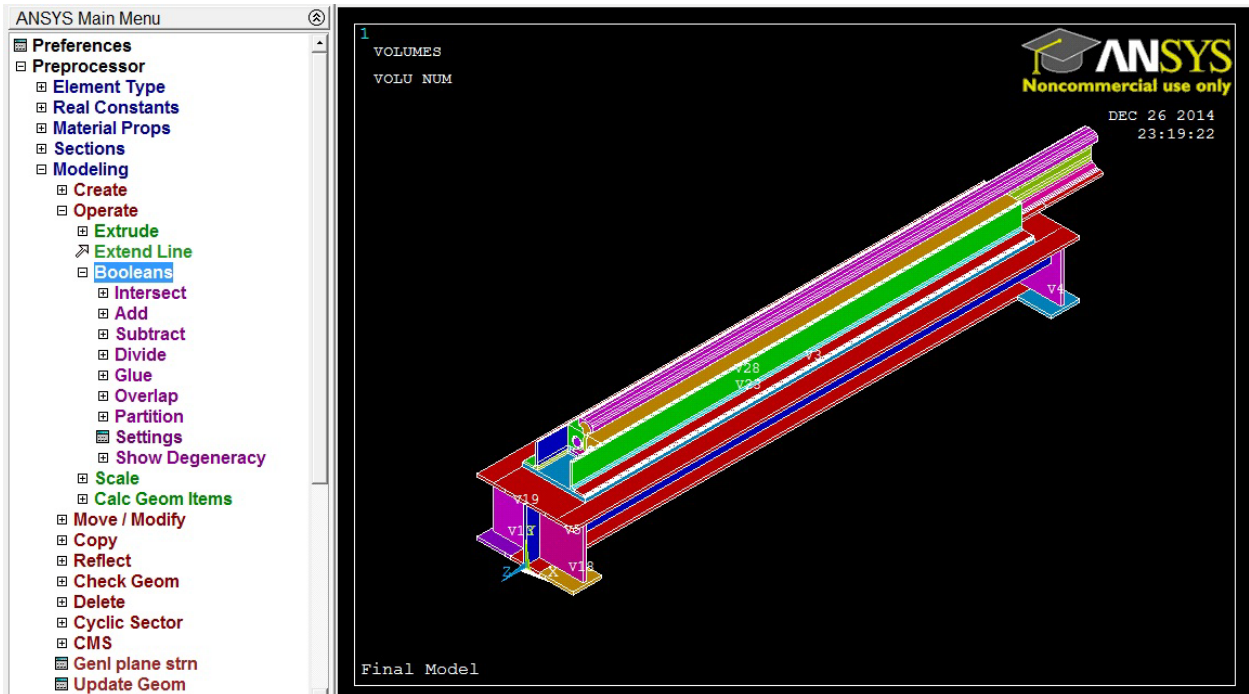


Figure-5.49: Creating and modifying Volumes

- Joining Different parts

There are three different ways to connect the different parts of the volumes in ANSYS. They are sub named under preprocessor tab as glue, add and merge, overlap etc. All of them

have different purpose. Glue is employed when interface between the two materials is considered perfect without any thickness. Glue is intended to use for unmeshed areas, volumes and lines. Merge is for nodes in the mesh. Merge and Glue makes the two materials bonded perfectly, no slippage, no interfacial pressure, nothing in between but continuity. Addition is simply adding more than one physical part with continuity but the difference in that case is the resulting volume crates complex topology of one single volume.

In addition to that direct processes of connecting physical parts of the model there is another way by using contact elements which is employed to study the interface or friction at the interface. Contact elements also bring nonlinearity in the analysis. Convergence is major issue with contact elements.

So, during simulation if it is required to keep the surfaces connected for all unforeseen forces acting on the bodies , glue is better but if it is required to monitor for how long or in what condition these bodies needs to be in connection use of contact elements are ideal.

However, during the simulation in the thesis, contact elements have not been used. The adhesive materials used for contact between the embedding material and steel angle as well as the base plate has high adhesive strength (greater than 10 MPa and 35 MPa for steel angle and base plate respectively) that has been suggested enough to restrict any slippage between them by Edilon)(Sedra and the test observation also reveals so. However, the response from the laboratory test has been recorded and separation of physical parts of the arrangement has been found only in two cases;

1. Between the PVC pipe and the Embedding material at the beginning and end.
2. Between elastomer and the underlying steel girder at the end.

These two separation has been modeled manually and the model has been analyzed both for the glued and partially unglued at the above stated regions taking into consideration different length of separation. The main reason of such consideration is to identify the possible influence of such separation on the results. Again, there were lack of data for contact parameters between PVC pipe and Embedding material. Moreover, convergence of contact element also makes the solution complex and increases the computational time significantly.

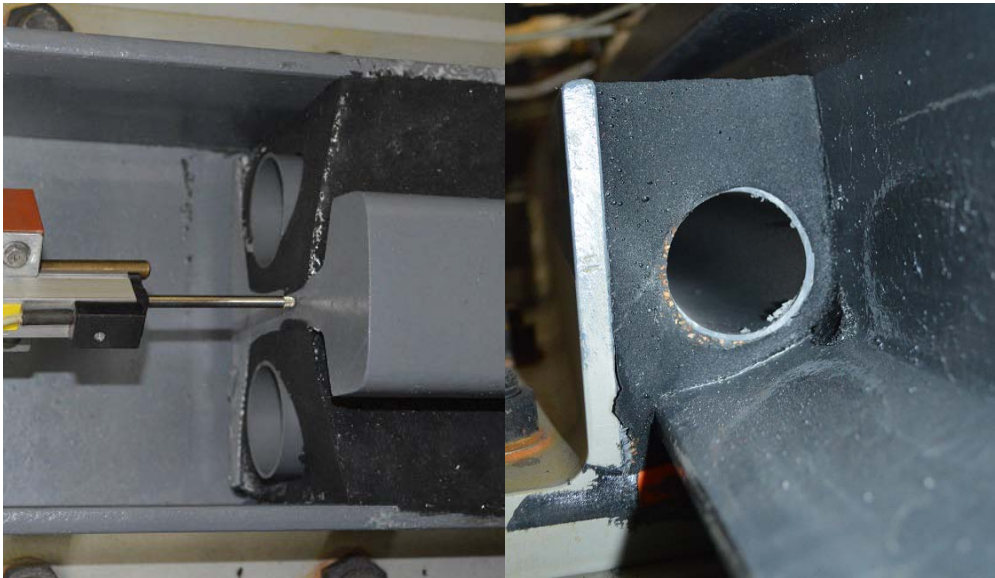


Figure-5.50: Separation of PVC pipe from embedding (Front and rear end)



Figure-5.51: Separation of Elastomer Strip from Steel Girder (Rear end)

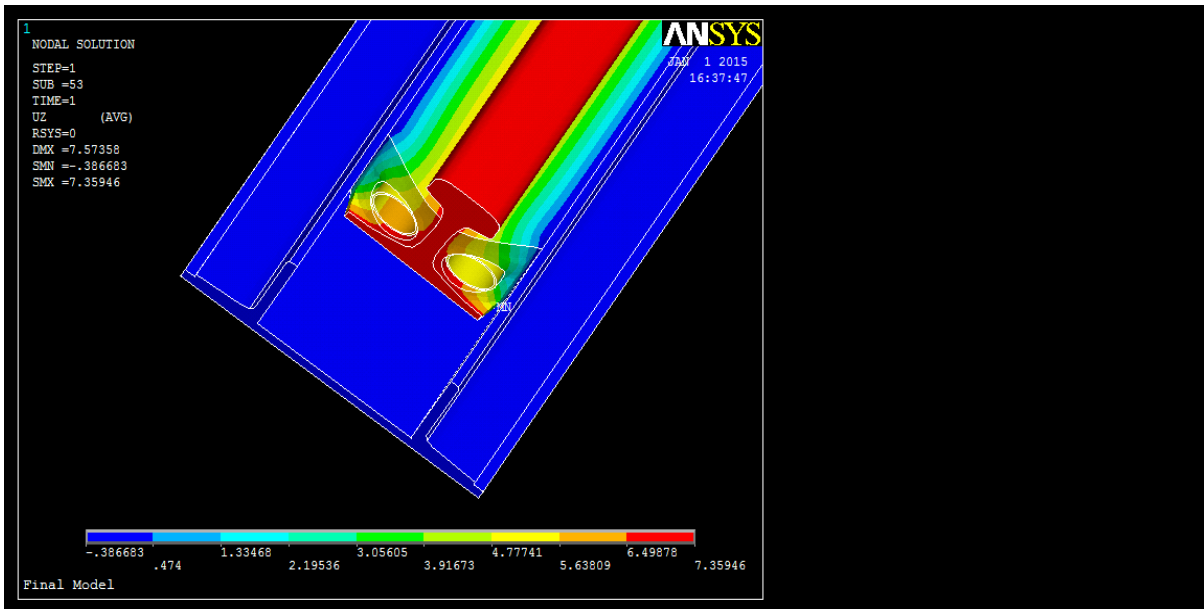


Figure-5.52: Simulation for Separation of PVC Pipes

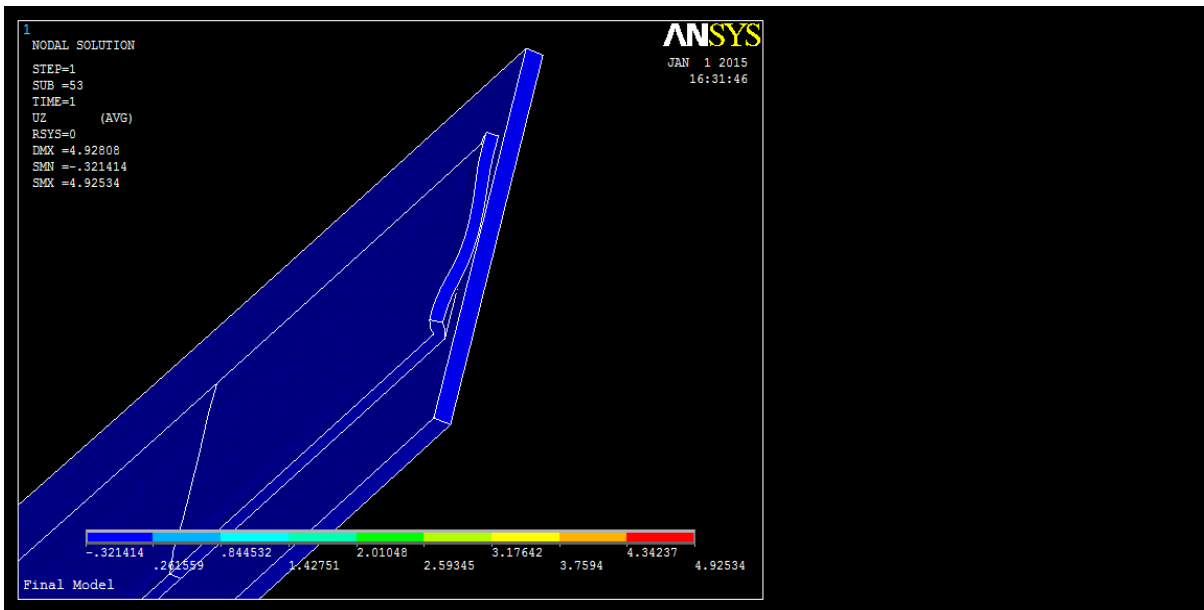


Figure-5.53: Simulation for Separation of Elastomer

5.6. Defining Elements and Material Properties

Elements:

As described earlier, two types of Solid elements, SOLID185 and SOLID186 has been used for the modeling. SOLID185 has been defined twice; one for pure displacement characteristics for the most of the physical parts and one with mixed u/p for compatibility with incompressible materials like elastomer.

Materials

- Linear material properties of steel has been defined with the following parameters,
Modulus of Elasticity, $E = 2 \times 10^5$ MPa
Poison's Ratio, $\nu = 0.3$
- With support of the supplied material data by Edilon)(Sedra, as stated at chapter 4, the material properties of embedding and elastomer is linear in tension whether non-linear in compression. Linear elastomer property of elastomer in tension has been defined with (Edilon)(Sedra supplied test result (Appendix-I).

Modulus of Elasticity, $E = 1.8$ MPa

Poison's Ratio, $\nu = 0.49$

- Linear Embedding material property in tension has been defined with,
Modulus of Elasticity, $E = 3.5$ MPa
Poison's Ratio, $\nu = 0.35$

The Poisson's ratio of uncompressed polyurethane is nearly 0.5 [20] and the material Edilon)(Sedra Crokela material is a mixture of polyurethane resins with cork granulate and mineral fillers. No test data has been provided for the actual Poisson's ratio. Hence, an approximate value of 0.35 has been used.

- For PVC pipe, the following linear material properties has been used,
Modulus of Elasticity, $E = 2896.6$ MPa (ASTM D638)
Poison's Ratio, $\nu = 0.33$ (Ref. www.professionalplastics.com)

• ANSYS provides numbers of model to define the hyperelastic material property of elastomer in compression. There are two types of model mainly, physical and phenomenological models. Uniaxial test data along with biaxial, shear test, simple shear test and volumetric test data are required to model the hyperelasticity through those models. In our case, test data for single mood that is uniaxial compression test data was available. Hence, limited test data was available for filling in the model parameters. Moreover, the phenomenological model follows the test behavior until the provided test data and fails to relate beyond if it requires during analysis. Hence, Arruda Boyce model physical model has been used which extrapolates the stress-strain behavior as required. ANSYS curve fitting tool provides the way to calculate the parameters related to uniaxial test data. But in all the cases, volumetric test data is required to find the last parameter d. Parameter d is related to the bulk modulus and defined as,

$$d = 2/k, \text{ where, } k = \text{Bulk modulus}$$

However, data for the Bulk modulus of elastomer material has been considered as 2 GPA. Hence d has been calculated as, $d = 2/2000 = 0.001$.

Filling in the uniaxial compression data the following result has been found in ANSYS,

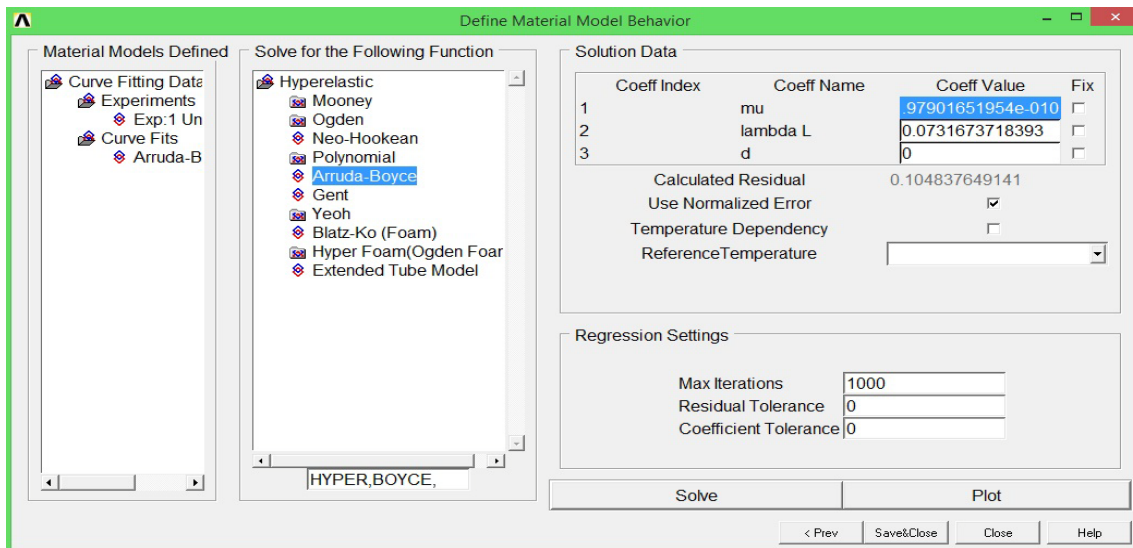


Figure-5.54: Arruda Boyce model parameter

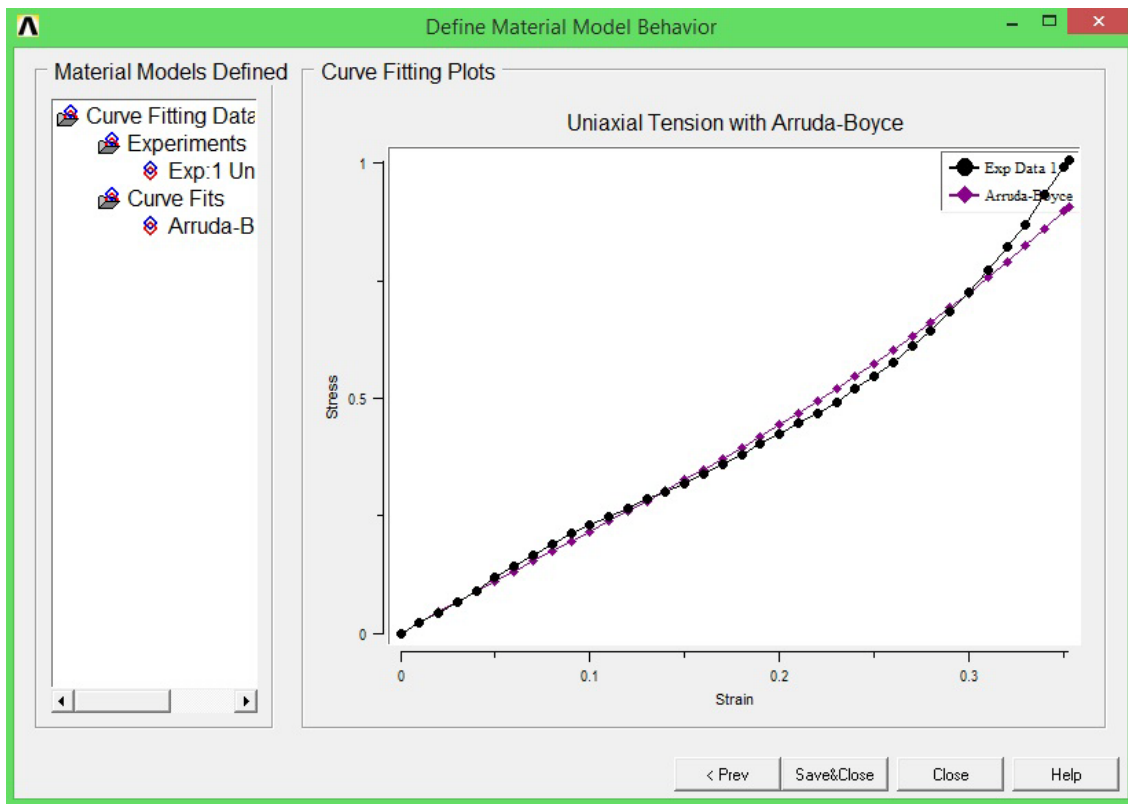


Figure-5.55: Arruda Boyce curve vs. curve from Experimental data.

- The material property of embedding material in compression is also nonlinear. But the compressive stress vs. compressive strain curve shows a fairly constant gradient. And merely varies from 5.9 to 6.9 (Table-5.4). Moreover, there was limitation of volumetric test data and it is not a common material to find out reference bulk modulus value to simulate the nonlinear behavior in ANSYS. Hence, the static compressive modulus suggested by Edilon)(Sedra has been used. The material property of Embedding in compression has been defined with,

Modulus of Elasticity, $E = 5.9\text{MPa}$

Poison's Ratio, $\nu = 0.35$

Table-5.4: Compressive stress-strain data and Modulus of elasticity of embedding material in compression

Strain	Stress	Slope
0	0	
1	0.037	0.059
2	0.096	0.061
3	0.157	0.063
4	0.22	0.059
5	0.279	0.061
6	0.34	0.059
7	0.399	0.063
8	0.462	0.06
9	0.522	0.063
10	0.585	0.065
11	0.65	0.066
12	0.716	0.067
13	0.783	0.068
14	0.851	0.067
15	0.918	0.07
16	0.988	0.0677419
16.31	1.009	0.0618639

It is worthy to mention that, for a low amount of stress below 0.037 the compressive modulus can be considered also as low as in tension. This has been also considered while separating the tension and compression zone of embedding material in the FEM.

5.7. Assigning Attributes and Meshing

The process of generating the mesh for nodes and elements requires three main steps.

1. Setting the element attributes,
2. Setting the automatic mesh control options or manually mesh the lines/areas and,
3. Generating the mesh.

- Setting the element attributes requires to specify the following parameters,
 - Selection of element type from the defined element list
 - Selection of Real Constant defining the geometric properties if required such as thickness or cross sectional area.
 - Selection of material properties from the defined material list
 - Element co-ordinate system if there is more than one co-ordinate systems defined and,
 - Section ID (for beam elements)

However, model has been created in Global Cartesian co-ordinate system only and no beam element has been used. Different element and material properties has been assigned to

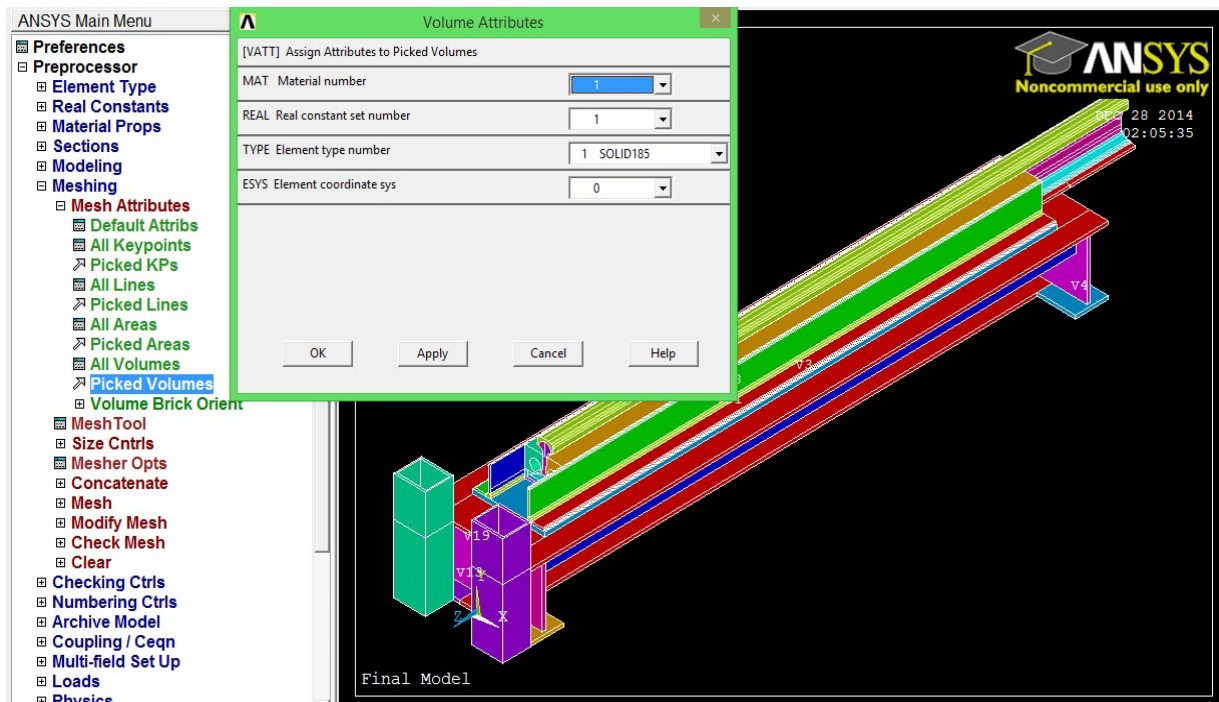


Figure-5.56: Assigning attributes for element generation

pertinent components of the model before meshing to create the elements. ANSYS always asks for element and material properties prior creating the elements. As an example, 8 node Solid185 element and material property of steel defined under material number 1 (Modulus of Elasticity, $E = 2 \times 10^5$ MPa, Poisson's Ratio, $\nu = 0.3$) has been assigned for all the steel sections of the girder.

□ There are several options for meshing in ANSYS. ANSYS Mesh Tool provides flexible control over meshing options. As described earlier, hexahedral mesh has been used in overall model. There are three mainstream types of meshing i.e., free, mapped and sweep methods of meshing. Free meshing option is not available for hexahedral meshing. And as the model itself is of high geometric complexity and all parts are connected to each other, mapped meshing was not possible to execute for all the parts. For map meshing a complex volume it is required to be sliced several times along with some area and line concatenation.

□ However, volume sweeping has been used. Volume sweeping is a process of meshing an existing volume by sweeping an area mesh. This is the most suitable option for complex geometry, where the only critical requirement is to identify the valid source and target areas (which needs to be identical) for sweeping. And the size of mesh has been manually controlled by setting the line and area meshing using Mesh Tool.

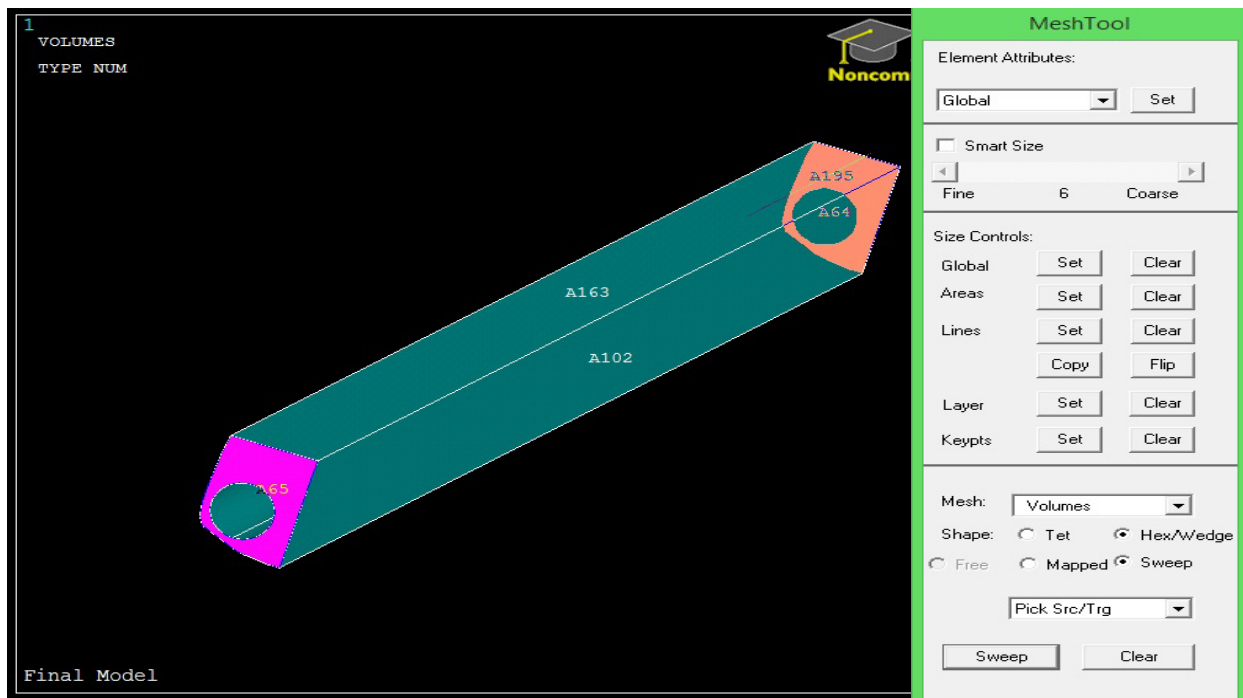


Figure-5.57: Volume Sweeping options for Mesh Generation

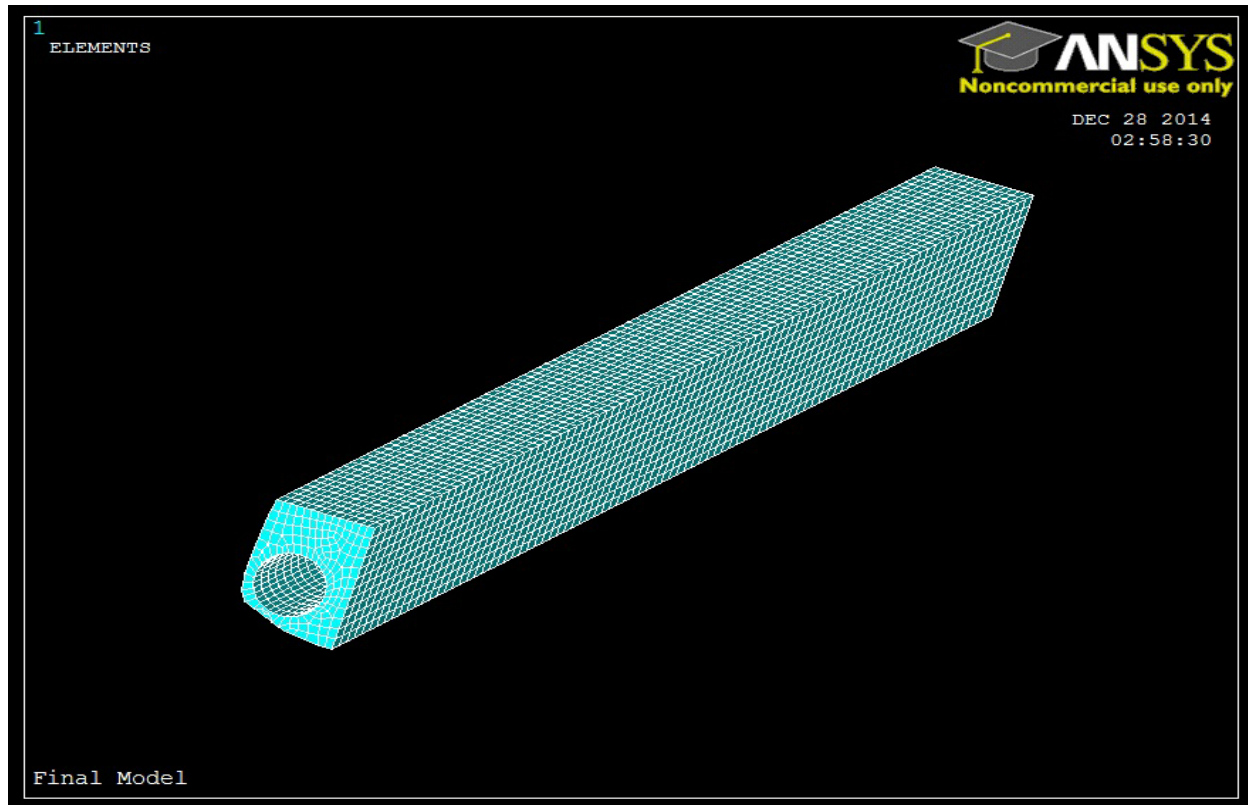


Figure-5.58: Meshed Volume

5.8. Assigning Loads and Constraints

□ Loads have been applied according the data available from the test. Longitudinal load has been applied from both sides. Load from longitudinal load cell has been applied as pressure load on the surface of the rail end that was in contact during loading operation. However, ANSYS defines the Centroid of the pressure load itself according to the arrangement of the element. In that case, a small amount of eccentricity is expected due to the geometric difference in load cell circular surface and irregular contact surface of the rail.

Counter action from M30 bars has been applied on the steel box sections connected on the other side of the girder. Concentrated nodal force has been applied on the required height (175mm above girder top). The box sections used here are of equivalent area and section

modulus of two UPN140 used in the laboratory test. This has been used only for simplicity of modeling and mesh generation.

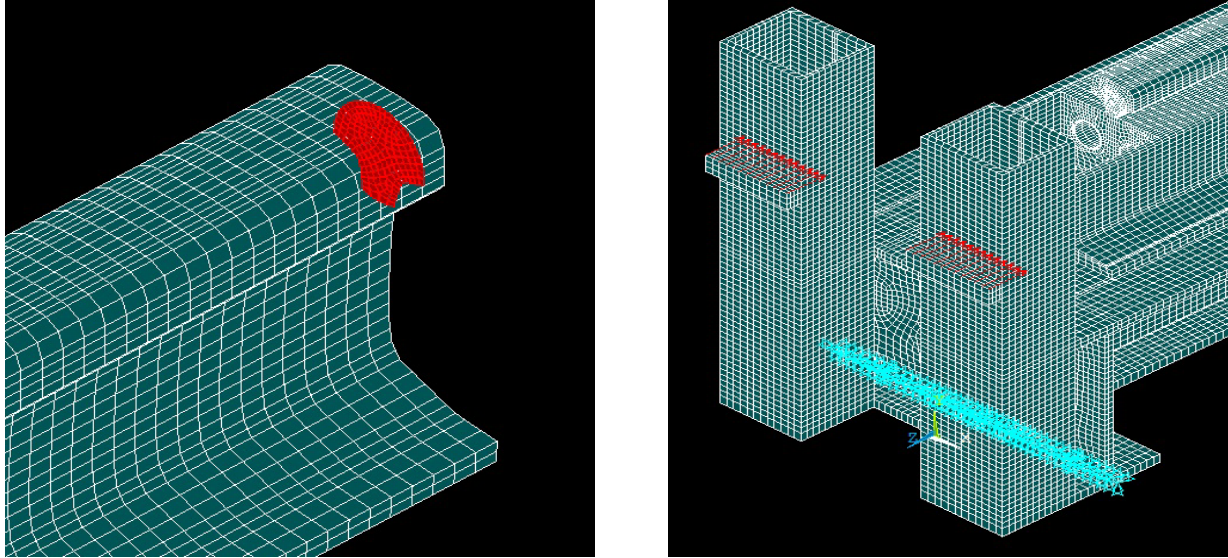


Figure-5.59: Longitudinal surface Load from load cell and concentrated counter load from M30 bars

Vertical load from vertical load cell has also been applied as concentrated nodal load because of the irregular surface of top of the rail.

□ Boundary conditions have been applied as for simply supported beam. DoF UX, UY and UZ were chosen for the further end from the longitudinal load cell and DoF UX and UY have been chosen for the near end. But for the validation of the static scheme it was required to provide the vertical support only. But for FEM analysis a slight unbalance of load in Z direction (longitudinal) would produce infinite displacement and provide error for an unconstrained model. However, after each solution nodal reaction solution has been checked whether the sum of UZ component is found nearly zero to satisfy the static scheme. Solution has been accepted for a nearly zero value of the summation.

5.9. Final Model

The final model along with generated elements and all boundary conditions can be figured out as figure-

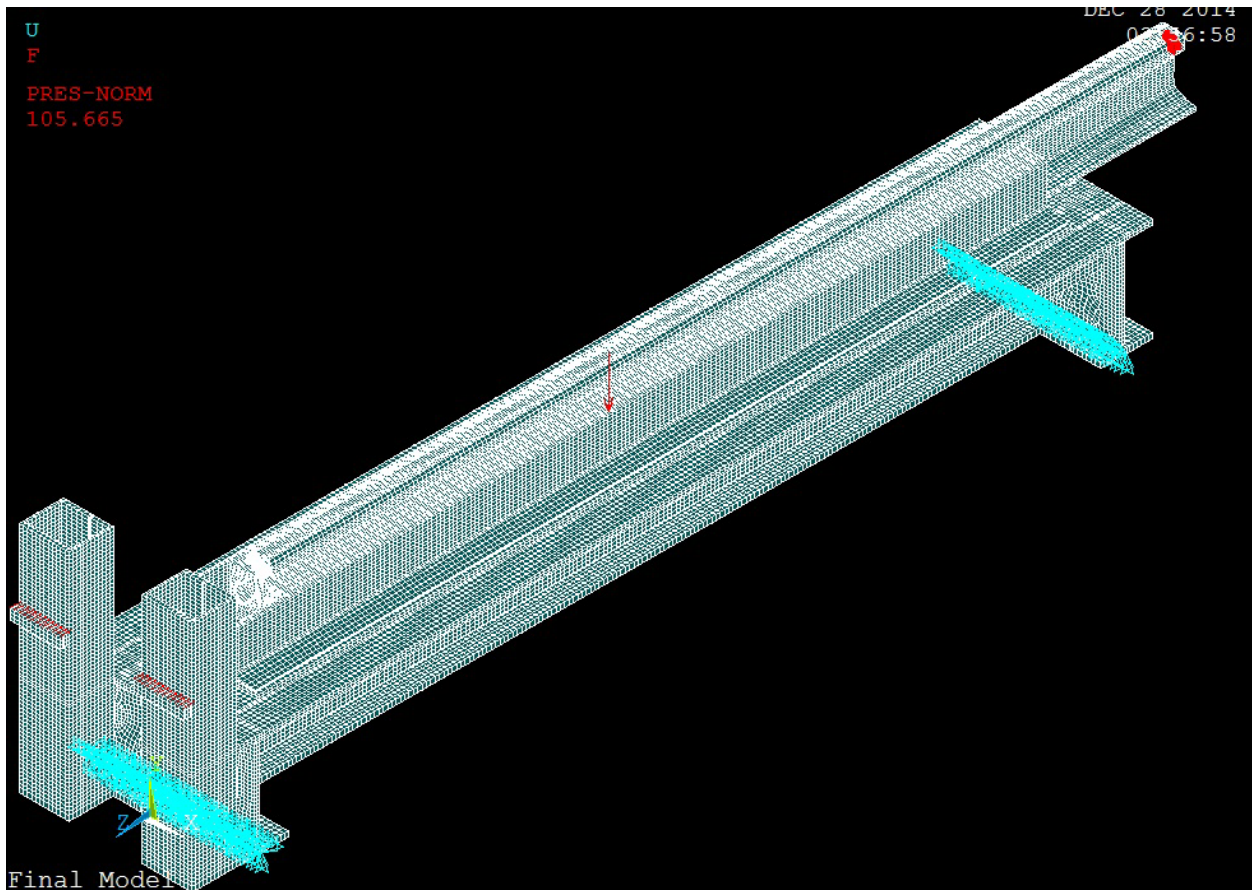


Figure-5.60: The Final Model

5.10. Analysis Option

Nonlinear static analysis has been performed for the generated model. A static analysis can be either linear or nonlinear and ANSYS involves all types of nonlinearities like, large deformation, plasticity, hyperelasticity and so on. When the strain in the elements change more than few percent the changing of geometry due to this deformation can no longer be neglected. Both hyperelastic material and large deformation is involved in the analysis. Specially, the

elastomer material was expected to show large deformation. The large volumetric deformation of hyperelastic material has been recognized with using mixed u-p elements.

Hence, the following solution control options has been used for nonlinear analysis in ANSYS,

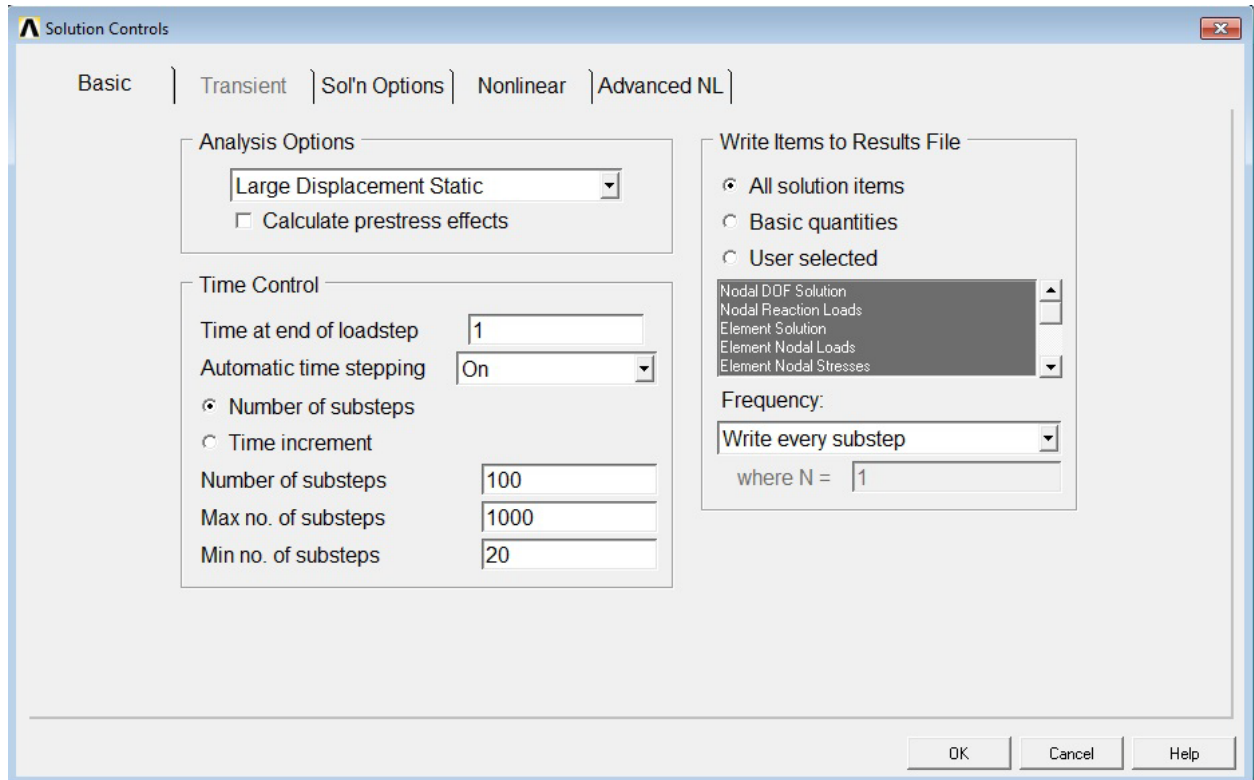


Figure-5.61: Analysis options

6. Verification of the Model

Verification and validation (V&V) are the primary processes for quantifying and building confidence (or credibility) in numerical models. Adopted from the 1998 AIAA Guide, Ref. [21], verification is the process of determining that a model implementation accurately represents the developer's conceptual description of the model and the solution to the model. It is concerned with identifying and removing errors in the model by comparing numerical solutions to analytical or accurate benchmark solutions. In performing verification, it is useful to divide the verification activity into two distinct parts. One is recognizing the different function of software developers producing a code that is error free, robust, and reliable, and the other is whether the use of that software obtains solutions to engineering problems with sufficient accuracy.

6.1. Verification of the software

The ANSYS program has been in commercial use since 1970 and has been extensively used in the field of aerospace, automotive, construction, electronic, manufacturing services, nuclear, plastics, oil and steel industries. In addition, many consulting firms and hundreds of international universities use ANSYS for analysis, research and educational use. It is recognized worldwide as the most widely used and capable software of its type. Verification Manual for Mechanical APDL Application [22] demonstrates the use of wide range of ANSYS elements for classical and readily obtainable theoretical solutions in an attempt to justify its solution capabilities and to provide users confidence towards ANSYS solution. Therefore, the verification for ANSYS has been recognized from its wide range use in structural engineering already and the use of the solution processes and codes here has been readily considered credible with confidence.

6.2. Verification of the solution accuracy

The purpose of verification for solution accuracy is to quantify the error of a numerical simulation by demonstration of convergence for the particular model under consideration and, if possible, to provide an estimation of the numerical errors induced by the use of the model. In an

attempt to this verification several steps have been followed while simulation and the result found has also been verified for accuracy in different ways.

6.2.1. Proper use of Element Characteristics

□ Use of Current-technology Elements

As technology has advanced, ANSYS has continued to develop robust new element types and now it suggests using current-element technology elements or new generation elements other than the older/legacy element (ANSYS Element References). Several attentions have been given while choosing the elements along with its internal formulation characteristics. SOLID185 and SOLID186 are the current-technology elements in place of older SOLID45 and SOLID95. There are several benefits that has been obtained for the thesis from these current technology elements like, the use of curve-fitting tool for calibrating material parameters through experimental data which supports hyperelasticity (for the case of elastomer material), ANSYS Variational Technology(VT) for optimal analysis and flexible control of element technologies while element formulating.

Legacy Element Type [1]	Suggested Current Element Type [2]	Suggested Setting(s) to Approximate Legacy Element Behavior [3]	
		Element KEY-OPT	Comments
PLANE25	SOLID272	KEYOPT(6) = 0	---
PLANE42	PLANE182	KEYOPT(1) = 3	---
PLANE53	PLANE233	See Legacy vs. Current-Technology 2-D Magnetic Elements in the <i>Low-Frequency Electromagnetic Analysis Guide</i> .	
PLANE82	PLANE183	---	---
PLANE83	SOLID273	KEYOPT(6) = 0	---
SHELL41	SHELL181	KEYOPT(1) = 1, KEYOPT(3) = 2	---
SHELL63		KEYOPT(3) = 2	May require a finer mesh.
SHELL57	SHELL131	KEYOPT(3) = 2	Issue SECTYPE „SHELL
SOLID5	SOLID226	---	---
SOLID69		KEYOPT(1) = 110	---
SOLID45	SOLID185	KEYOPT(2) = 3	---
SOLID92	SOLID187	---	---
SOLID95	SOLID186	KEYOPT(2) = 1 KEYOPT(2) = 0 for nonlinear analysis	---
SOLID98	SOLID227	---	---
SOLID117	SOLID236	See Legacy vs. Current-Technology Edge-Based Elements in the <i>Low-Frequency Electromagnetic Analysis Guide</i> .	

Figure-6.62: ANSYS current technology element recommendations

□ Problems of shear and volumetric locking

There remain few problems regarding the use of low order solid elements (SOLID185) in ANSYS. We encounter 2 main 'locking' type of problems with lower-order continuum elements: shear locking and volumetric locking.

Shear locking is a function of the geometry, and it occurs because lower-order bricks cannot 'bend' since they have linear sides. Hence, parasitic shear strains develop, and the traditional formulation is too stiff in bending.

Volumetric locking is a function of the material, and it occurs when the effective Poisson's ratio approaches 0.5 (nearly-incompressible). Since, hydrostatic pressure = volumetric strain * bulk modulus, if volumetric strain ≈ 0 , then bulk modulus tends to infinity. This is a problem for higher- and lower-order elements when dealing with nearly-incompressible materials (e.g., hyper elasticity or plasticity when plastic strains \gg elastic strains).

To alleviate these 2 problems, SOLID185 have different formulations which either reduce the integration points (hence relaxing the internal constraints) or add extra degrees of freedom.

SOLID185 has 4 options two deal with these two locking problems.

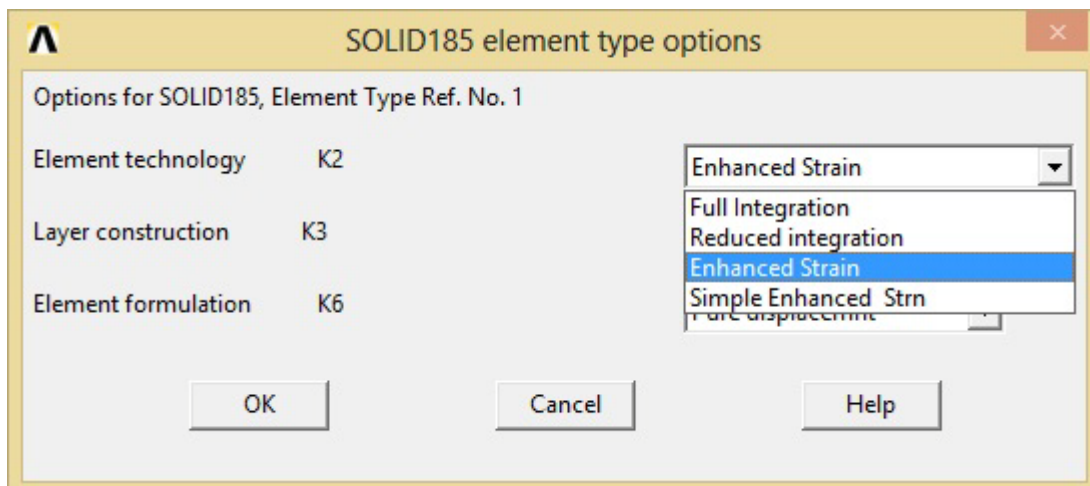


Figure-6.63: Use of flexible element control options

With KEYOPT(2)=2 i.e., enhanced strain the idea here is the addition of internal 'bending' type of DOF to make the element more flexible in bending to alleviate shear locking. But in addition to extra internal 'bending' DOF, it also adds some internal DOF to alleviate volumetric locking. Thus SOLID185 can work for a wide range of nonlinear constitutive models, including hyperelasticity, visco-elasticity, in addition to plasticity and visco-plasticity.

The above formulations assume use of hexahedral elements, so the formulations such as Enhanced Strain are not applicable when elements are in tetrahedral form. In the model we used hexahedral mesh for element generation. Hence it was the appropriate choice to deal with enhanced strain in SOLID185.

□ Mixed u-p Formulation in Nonlinear analysis

Classical pure displacement formulation is the widely used formulation for handling most of the non-linear deformation problems. It takes only the displacement as the primary unknown variable. All other quantities such as stress, strain etc are calculated from the displacement. However the accuracy of any displacement formulation is dependent on the Poisson's ratio or bulk modulus. Under nearly incompressible condition of materials (elastomer in our case) with Poisson's ratio nearly 0.5 or bulk modulus approaches infinity, volumetric displacements derived from displacements may not be as accurately predicted as the original displacements. . The physical meaning of incompressible material is that the deformation does not change the volume of the material. This makes decomposing the model into distortional and volumetric components (U/P) necessary to solve, as the state of deformation is not unique to a state of stress. So any small error in predicted volumetric strain may appear as a large error in hydrostatic pressure and subsequently in the stress. So it has been one of the disadvantages of pure displacement formulation that cannot handle the fully incompressible material deformation such as the incompressible hyperelastic materials.

To overcome the problem, mixed u-p formulation has been developed by ANSYS and incorporated in the current technology elements. Here the hydrostatic pressure P or the volume change rate is interpolated on element level and solved on the global level independently in the same way as displacements. The final stiffness matrix has the form of,

$$\begin{bmatrix} K_{uu} & K_{uP} \\ K_{Pu} & K_{pp} \end{bmatrix} \begin{Bmatrix} \Delta u \\ \Delta P \end{Bmatrix} = \begin{Bmatrix} F \\ 0 \end{Bmatrix}$$

Where, Δu = displacement increment

ΔP = Hydrostatic pressure increment

Since, the hydrostatic pressure is obtained from global level instead of being calculated from volumetric strain, the calculation is independent of Poisson's ratio or bulk modulus. Hence, it is more robust for nearly incompressible material. That is why the mixed u-p formulation has been used for defining the element for hyperelastic elastomer used in the model.

6.2.2. Mesh quality

The objective of finite element analysis of real life models is to simulate the original testing using minimum amount of computer memory, computation time and modeling time. But, once the prototype has been designed, it must be tested to ensure that, it will perform according to specifications rather than go through the expensive and time-consuming process. Mesh quality plays an important role on achieving those objectives, i.e., in getting the solution convergence as well as the result quality of any FEM. Several concerns have been taken into consideration while meshing and generating the elements in the thesis model.

1. Mesh type
2. Mesh Density
3. Mesh Quality Parameters

6.2.2.1. Mesh Type

There are several topology of mesh shape for 3D solid modeling like, tetrahedron, pyramid, prisms and hexahedron (Figure). The mixing of the types or hybrid meshing is also possible. The most common uses are the tetrahedron and hexahedrons in most finite element analysis. However, in this thesis, linear and quadratic (low and high order) hexahedral mesh has been used only. No tetrahedral mesh has been used.

In Practice, there are no general rules which can be applied to decide which element shape should be preferred. The underlying phenomenon is depended highly on the complexity and type of specific case of the model itself. The consideration in that case were,

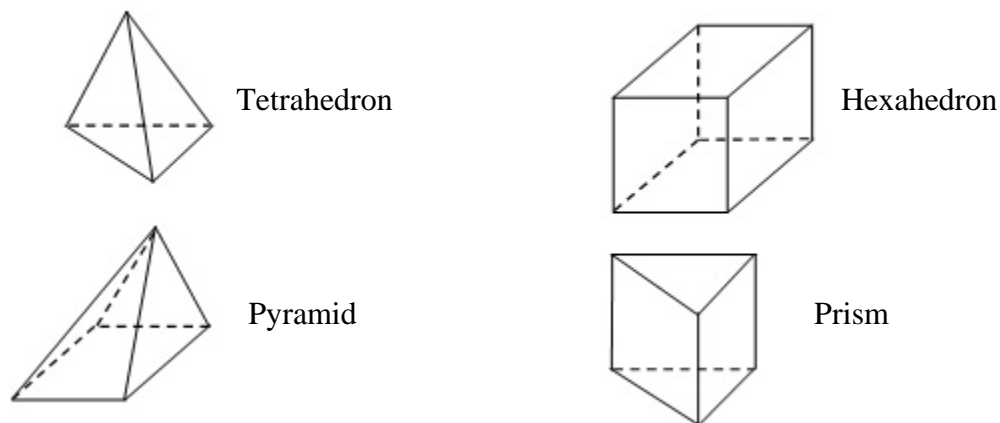


Figure-6.64: Topologies of Solid Elements

Set up time

In this thesis the model is a complex one as a whole but in most of the cases it is composed of regular shapes which have been easily meshed into structural grids, specially, the parts of steel girder, base plate and the channels. But the other parts i.e., the rail and the embedding were of complex shape. However, though the time required for setting up the whole model was time consuming, the other requirements like accuracy of result and the computational time were given the higher priority.

Computational expense

For the same volume of meshing, hexahedral mesh will generate lesser cells or element than tetrahedral mesh. It is evident that the computational effort is highly depended on the number of nodes, not the elements, i.e., the it is highly depended on the use of higher and lower order element as the higher order elements give rise to creation more than double folded number of nodes than the lower order elements. Higher order element in the thesis model was used only at the irregular shape of the rail to ensure proper connection along the boundary of different segments. Hence, most of the model was comprised of lower order elements. Therefore, the computational effort was expected to be much less than the lower order tetrahedron elements and it has been considered justified to use the hexahedron elements all through.

Result accuracy

For the same cell amount, the accuracy of solutions in hexahedral meshes is the highest. There are many reasons why the eight-node hexahedral element produces more accurate results than other elements in the finite element analysis of real world models.

The eight-node hexahedral element is linear, with a linear strain variation displacement mode. Tetrahedral elements are also linear, but can have more discretization error because they have a constant strain. Hexahedral element has the capacity to overcome shear and volume locking also. Though higher order tetrahedron can overcome these problems but will lead to huge number of node creation.

Hexahedrons permit a much larger aspect ratio than triangular/tetrahedral cells. A large aspect ratio in a triangular/tetrahedral cell will invariably affect the skewness of the cell, which is undesirable as it may impede accuracy and convergence. The result is a coarser mesh though; convergence will generally be faster, possibly saving you some computational expense.

Besides being more accurate, the hexahedral element presents other advantages in FEA model building. Meshes comprised of hexahedrons are easier to visualize than meshes comprised of tetrahedrons. In addition, the reaction of hexahedral elements to the application of body loads more precisely corresponds to loads under real world conditions.

6.2.2.2. Mesh Density

Mesh density has substantial influence until the optimum density is attained. The model has been checked with relatively high (length= 25mm in Z direction and nearly 10x10 in cross section) and low (length= 12.5mm in Z direction and nearly 10x10 in cross section) mesh density and the result was found more or less similar. However, it could be made denser but it would give rise to huge amount of computational effort.

6.2.2.3. Mesh Quality Parameters

There are mainly three parameters to control the quality of mesh, these are,

- i. Aspect Ratio of element
- ii. Smoothness in transition areas
- iii. Element shape and skewness

Aspect ratio

It is the ratio of longest to the shortest side in a cell. For hexahedral mesh, it refers to the ratio HxLxD of cubical finite elements (shape of a cube or a box). Ideally it should be equal to 1 to ensure best results. That is for hexahedral elements, one have to ensure that ratio between height/length/depth of the element is near 1. It has been experimentally found that; Solid finite element 1x5x5 mm is heavily distorted and introduces error. One has to use solid elements 1x2x2 which are error-free (but that need thousands of elements for same analysis result). However, as described under Mesh Density subhead, high concern was also given on building an aspect ratio of nearly one throughout the model. But due to complexity of nature and as the elements were glued to each other in most of the cases, aspect ratio of 1 in one end gave rise to aspect ratio more than 2 to other end.

Smoothness

The change in size should also be smooth. There should not be sudden jumps in the size of the cell because this may cause erroneous results at nearby nodes. The local variations in cell size should be minimal, i.e. adjacent cell sizes should not vary by more than 20%. Though the

shapes were irregular, they were same in longitudinal direction. the variation was mainly in cross section. And the size were found varying gradually

Skewness

The skewness of a grid is also an indicator of the mesh quality and suitability. Large skewness compromises the accuracy of the interpolated regions. There are three methods of determining the skewness of a grid. Common measure of quality is based on equiangle skew. Definition of equiangle skew is given by,

$$\max \left[\frac{\theta_{\max} - \theta_e}{180 - \theta_e}, \frac{\theta_e - \theta_{\min}}{\theta_e} \right]$$

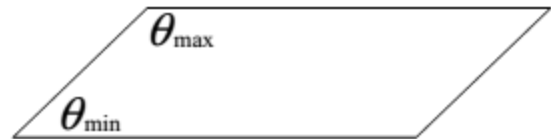


Figure-6.65: Skewness Measurement of Quadrilaterals

Where,

θ_{\max} = largest angle in face or cell.

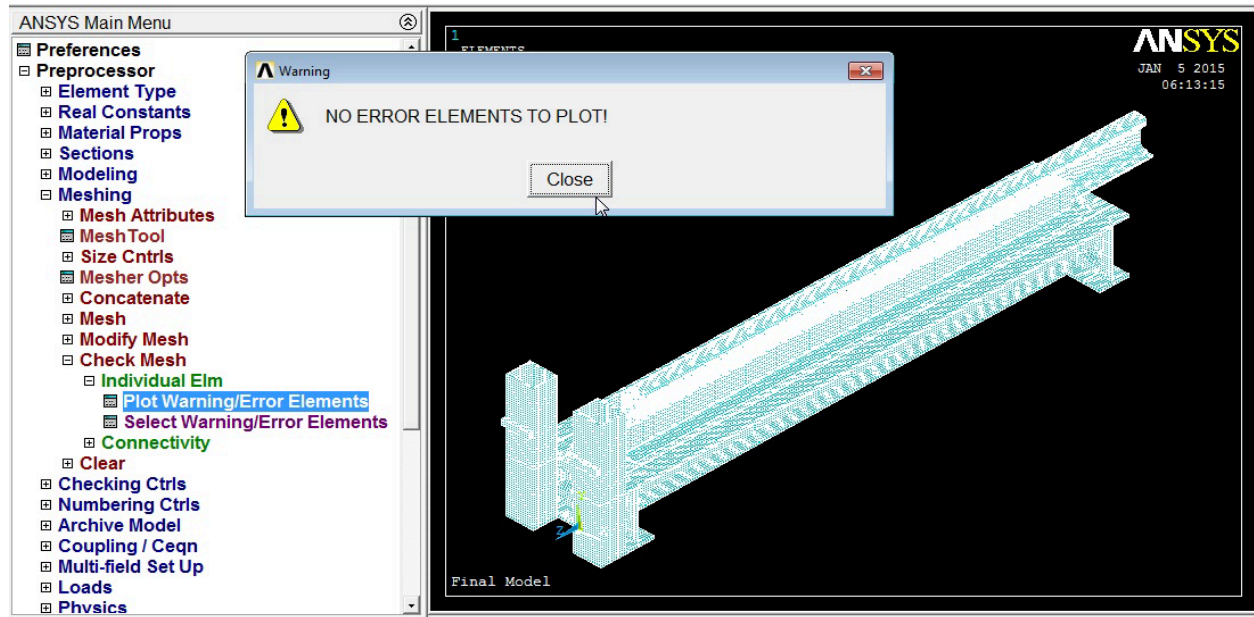
θ_{\min} = smallest angle in face or cell.

θ_e = angle for equiangular face or cell. (e.g., 60 for triangle, 90 for square)

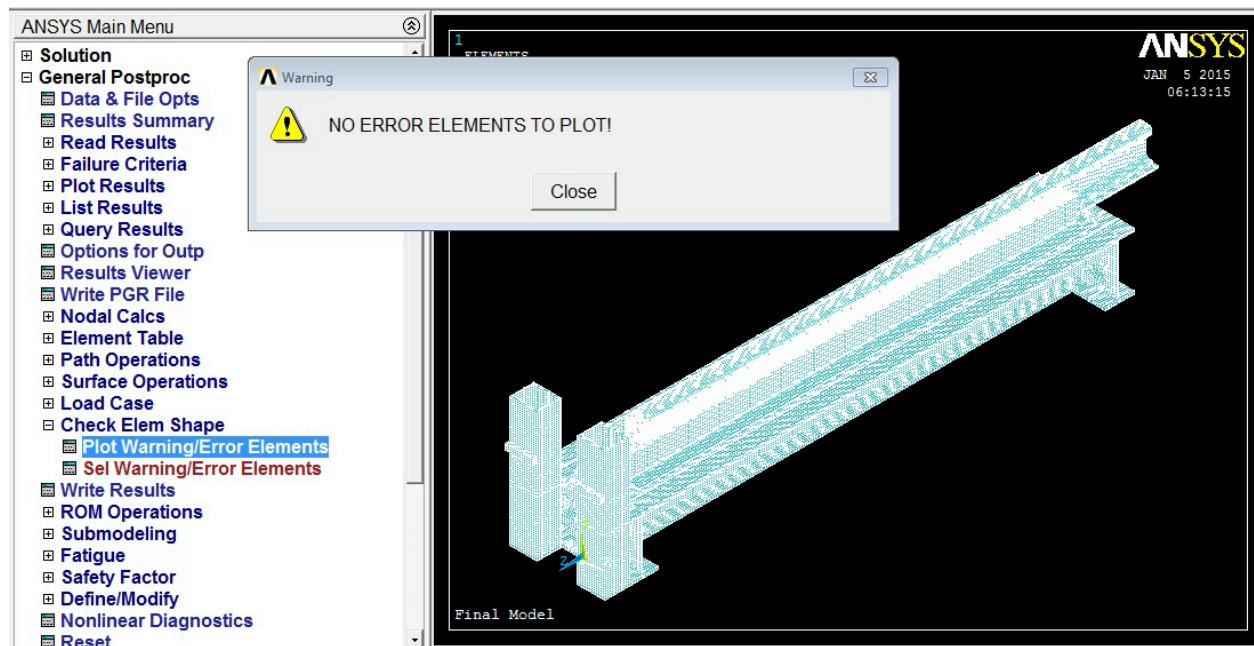
And the range varies from 0 to 1, 0 being the best and 1 being the worst case. Skewness was not a big concern for the structured mesh part. Best quality have been achieved for that parts in the model. However, it was very difficult to control the skewness in the irregular part of the model. But consideration has been given to smaller mesh size on that part to reduce the skewness as low as possible.

6.2.3. Check for unloaded model in ANSYS

Giving all the quality parameters, the set up model has been checked for shape warning in ANSYS and no shape warning has been found for the unloaded and analyzed model. (Figure-6.66)



Element shape check before analysis



Element shape check after analysis

Figure-6.66: Shape error check in ANSY

7. Validation of the Model

Validation is the process of determining the degree to which a model is an accurate representation of the real test specimen or the real world subject matter under consideration from the perspective of the intended uses of the model. It is concerned with quantifying the accuracy of the model by comparing numerical solutions to experimental data [21].

7.1 Validating dimensions and locations of result points

First attempt to generate the actual prototype was to measure the dimensions of the individual component of the test specimen and to model it with the actual dimensions. The dimensions as well as the positions of the displacement transducers, strain gauges were recorded prior to the execution of the test. The model has also been checked with the final report of the test provided by the **Klokner Institute (KI)**, Czech technical University and also with the data provided by producer and supplier of the ERS i.e., **Edilon)(Sedra**. However, there were several strain gauges placed inside the embedding material for which the vertical positions could not be physically checked during the test. It was assumed that the strain gauges have been placed at the centroid of the rail section. The longitudinal positions of them have only been verified. The Final report from the Klokner Institute and data from Edilon)(Sedra has been annexed to Appendix-I & IV.

7.2. Validating FEA results with Experimental results

There are numerous uncertainty involved which can lead to the deviation of the FEA data from the experimental data. The particular ones in this thesis can be identified as,

1. As discussed earlier, separation of layers have been visible during the test between elastomer and girder as well as in between PVC pipes and the embedding material. There can be other internal zones which have locally separated and were not visible.
2. The eccentricity of both the vertical and horizontal loading may deviate from the assumed positions and may lead to variation with FEA result as it considers the ideal situation.

3. Uncertainty was also involved with the material properties. There have been lacks of some material property data which have been discussed in 5.6.

Other than these uncertainties there were some limitations in the FEM itself which could not be resolved instantaneously (or required more time) and were operated with some assumptions. Such assumptions may be listed as;

1. Both the embedding and the elastomer material show bimodular material properties in tension and compression. ANSYS does not have the capacity to or there have been no element found which can alter the assigned material properties of the meshed elements according to tension and compression. Therefore, beforehand picking result from an analysis a trial run was given to find out the tension and compression zone of these materials. Then the corresponding volumes have been cut into parts to assign different material properties prior to the final run. It was approximate in that sense that the distribution of tension and compression is not of regular pattern to match the segmentations made in the model (Figure-7.67 & 7.68).
2. Discrete amount of separation have been assumed prior the analysis in PVC pipes and embedding, also in elastomer to girder at the loading end. But certainly, these separations have increased gradually and had some resistance until that point. The amount of separation has been assumed as table below.

Table-7.5: Bonding conditions

Bonding Case no	Load combination kN	PVC pipe debonding (Both ends) mm	Elastomer debonding (loading end) mm
1	V=0	0	0
2	V=0	25	25
3	V=40	25	25
4	V=80	50	50
5	V=125	50	50

For both the bimodular materials i.e., embedding and elastomer the ANSYS element table has been used to find out the elements in compression and tension. It has been found that the embedding portion on both sides of the rail web contains significantly low amount of compression elements and simple regular segmentation is not possible for those irregular distribution of elements. Therefore, the embedding materials on both sides of the rail web have been defined as tension material. Elements of embedding on both sides of rail foot changes to compression element from tension element significantly during $V=80\text{kN}$ vertical load case. Therefore, the same has been followed in defining the material of those portions. For the elements of embedding beneath the rail foot, segmentation has been made as figure below.

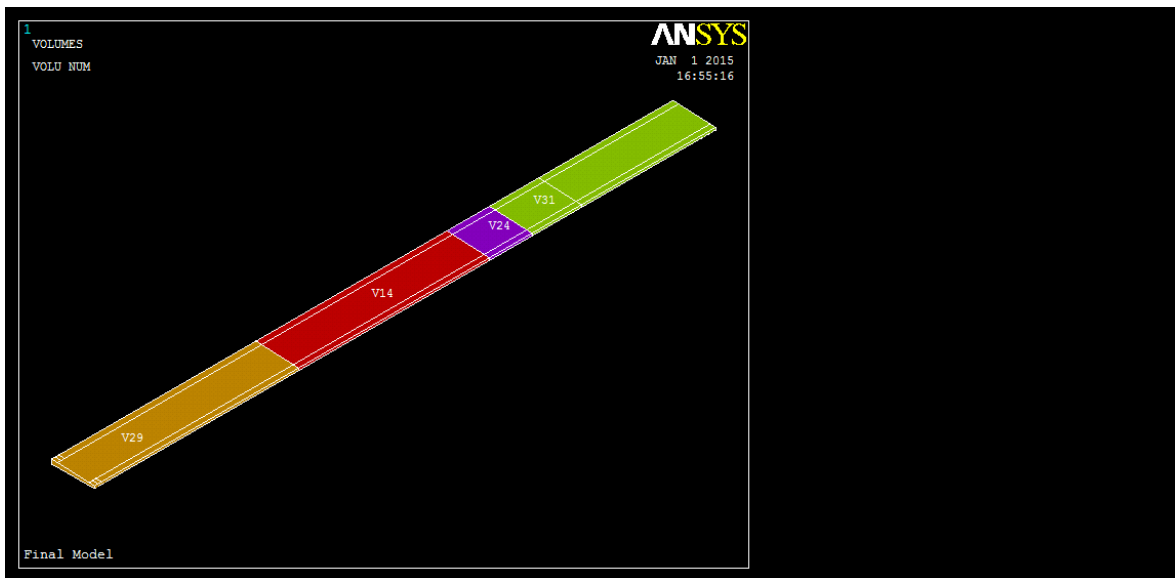


Figure-7.67: Segmentation of embedding below rail foot for assigning different tension and compression properties.

Compression element has been found for initial volume shown in figure on left side for $V=0\text{kN}$ load case. And for the subsequent load cases, compression has been found underneath the vertical load zone and it increases as the load increases.

The change of compression –tension elements for elastomer strip has been found of similar pattern like the embedding material under the rail foot and has been segmented as shown in figure below.

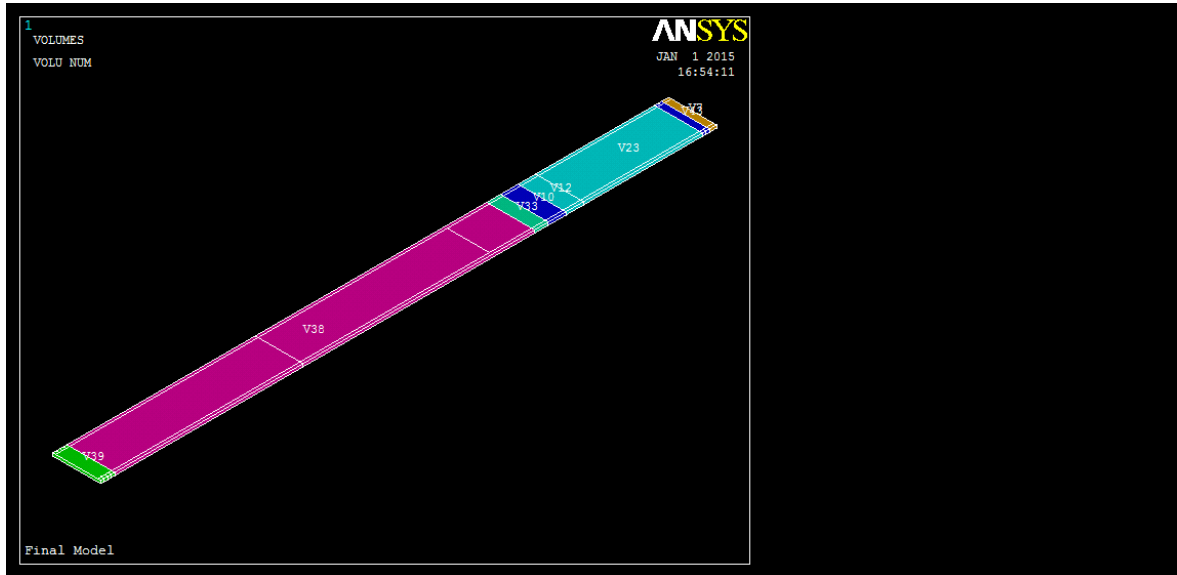


Figure- 7.68: Segmentation of elastomer strip for assigning different tension and compression properties.

7.2.1. Loading case-1 and 2 (Zero Vertical Load)

However, for the first load combination i.e., with zero vertical load, the FEM run has been made for fully bonded case and some small amount of deboning case (Bonding case no 1 and 2 respectively in table-7.5). Following table 7.6 & 7.7 shows the result found from FEA for these two cases.

Table- 7.6: FEA Results for fully bonded case with zero vertical load (Bonding case-1)

Longitudinal Displacement (mm)					
Location (mm)	310	710	1295	1945	2580
FEA result	8.28	7.82	7.92	8.11	8.34
Vertical Displacement (mm)					
Location (mm)	535	985	1595	2210	
FEA result	-0.871	-0.583	0.00192	1.262	
Longitudinal stress on Rail (MPa)					
Location (mm)	680	1310	1930	2610	
FEA result	-9.02	-18.44	-22.14	-31.153	
Longitudinal stress on Girder (MPa)					
Top Flange					
Location (mm)	1325				
FEA result	-7.175				
Bottom Flange					
Location (mm)	1325				
FEA result	17.294				

Table- 7.7: FEA Results for partially debonded case with zero vertical load (Bonding case-2)

Longitudinal Displacement (mm)					
Location (mm)	310	710	1295	1945	2580
FEA result	8.34	7.88	7.99	8.2	8.41

Vertical Displacement (mm)				
Location (mm)	535	985	1595	2210
FEA result	-0.872	-0.575	0.0212	1.293

Longitudinal stress on Rail (MPa)				
Location (mm)	680	1310	1930	2610
FEA result	-9.03	-18.44	-22.15	-31.167

Longitudinal stress on Girder (MPa)	
Top Flange	
Location (mm)	1325
FEA result	-7.174

Bottom Flange	
Location (mm)	1325
FEA result	17.28

One of the finding from these two sets of result is that, effect of bonding has not been found prominent for debonding. But the effects have been found logical as debonding has incurred, longitudinal displacement and stress values has been found slightly increasing in the rail. Debonding in PVC pipes are releasing the embedding material at the ends and giving rise to higher displacements. However average of these two results has been considered for validation.

Table- 7.8: Comparison of FEA and Experimental Data for V=0 kN load case

Longitudinal Displacement (mm)					
Location (mm)	310	710	1295	1945	2580
FEA result-1	8.28	7.82	7.92	8.11	8.34
FEA result-2	8.34	7.88	7.99	8.2	8.41
Average	8.31	7.85	7.955	8.155	8.37
Experimental result	7.06	6.84	6.77	6.81	6.69
Deviation	15.05%	12.85%	14.90%	16.49%	20.07%
Vertical Displacement (mm)					
Location (mm)	535	985	1595	2210	
FEA result-1	-0.871	-0.583	0.00192	1.262	
FEA result-2	-0.872	-0.575	0.0212	1.293	
Average	-0.8715	-0.579	0.01156	1.2775	
Experimental result	-0.471	-0.19	-0.149	-0.147	
Deviation	-0.401	-0.389	0.161	1.425	
Longitudinal stress on Rail (MPa)					
Location (mm)	680	1310	1930	2610	
FEA result-1	-9.02	-18.44	-22.14	-31.15	
FEA result-2	-9.03	-18.44	-22.15	-31.17	
Average	-9.025	-18.44	-22.145	-31.16	
Experimental result	-5.41	-13.83	-18.46	-27.41	
Deviation					
Longitudinal stress on Girder (MPa)					
Top Flange					
Location (mm)	1325				
FEA result-1	-7.175				
FEA result-2	-7.174				
Average	-7.1745				
Experimental result	-6.78				
Deviation	5.51%				
Bottom Flange					
Location (mm)	1325				
FEA result-1	17.294				
FEA result-2	17.28				
Average	17.287				
Experimental result	19.02				
Deviation	-10.02%				

Longitudinal stress in Rail

For the longitudinal stress case, the percentage deviation has not been taken into consideration. The longitudinal stress in the rail is varying linearly from maximum value to minimum in every case and the deviation of results is more or less of same span. So percentage of deviation will lead to a significantly higher value for the lower base value and significantly low for higher base values. Hence, as the deviation has been found similar, and being the values are limited to 3.5-4 MPa in all cases, it has been considered that they meet the nature of developing longitudinal stress similarly as of the experiment. Only exceptional case of stress at 1310mm has been discussed later in chapter 8.

The comparison of longitudinal stress between FEA result and Experiment result has been shown in figure- 7.69.

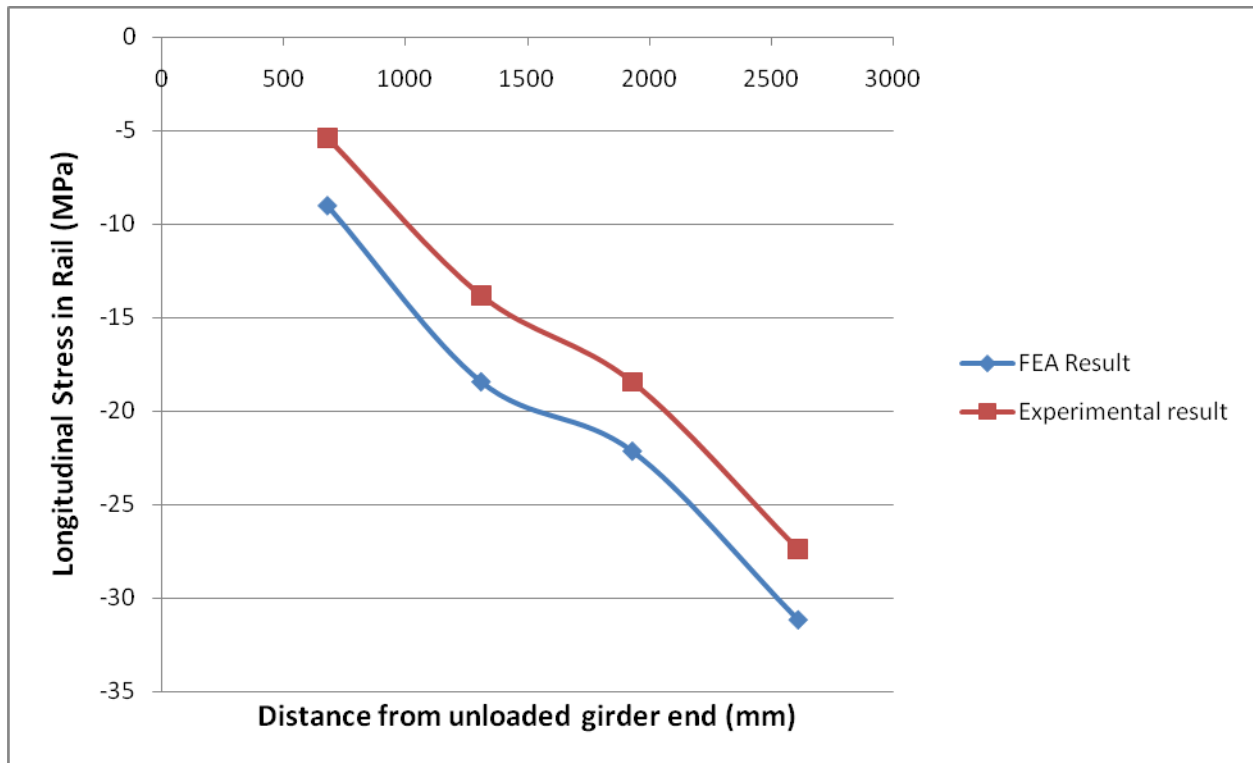


Figure-7.69: Comparison of FEA and Experimental results for longitudinal stress in rail ($V=0$ kN).

Longitudinal Displacement in Rail

The longitudinal stress development is also related to the displacement incurred in the rail. Higher the displacement, higher the stress would carry from loading end to the free end. The displacement values have been found higher than the experiment and it also resembles with the higher value of stress development in longitudinal stress at the end of the rail. Percentage of deviation has been taken into consideration as the base values are similar in that case. In fact, the values of displacements in longitudinal direction are supposed to be same and it has been found so. The fractional deviations from a constant value can be characterized by the location, arrangement and displacement of the displacement gauges themselves and effect of poisson's ratio of the steel. However, the deviation can be considered satisfactory with respect to the percentage values.

Stress on Girder

The stress value computed by FEA has been found relatively close to the experiment result as shown in table- 7.8.

Vertical Displacement of Rail

The result values found for vertical displacement case has been found exceptional from the experiment result. The displacement values are too small and therefore, other than the deviation, the nature of displacement has been taken into consideration. The comparison of vertical displacements between FEA result and Experiment result has been shown in figure- 7.70.

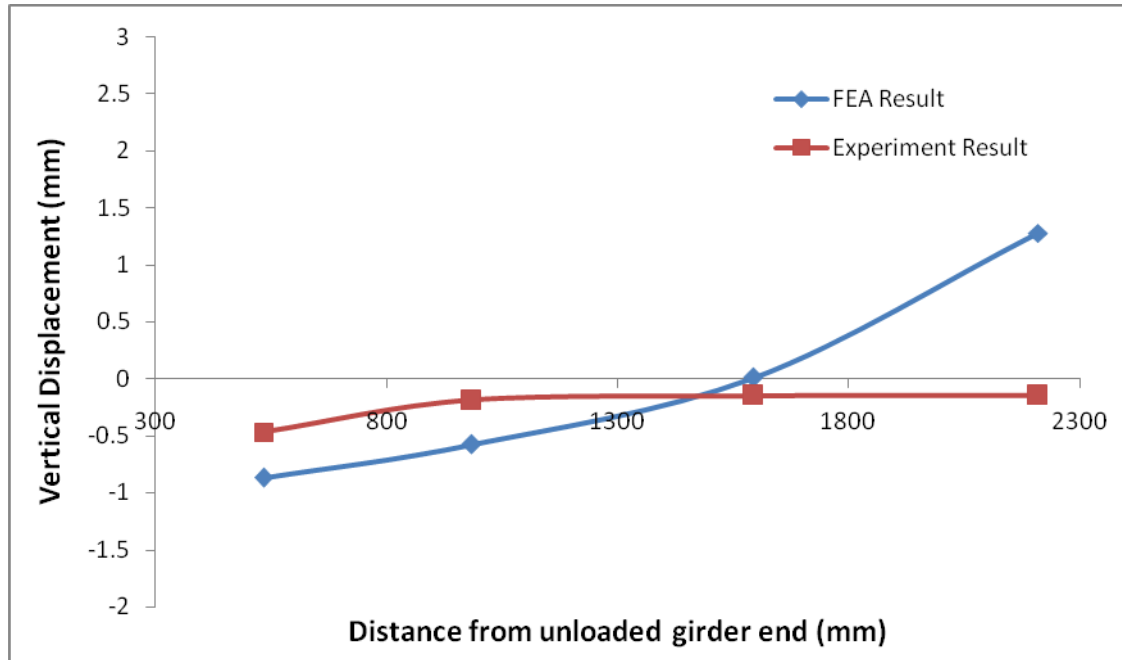


Figure-7.70: Comparison of FEA and Experimental results for vertical displacement of rail ($V=0$ kN).

The nature of displacement has not also been found similar. The experiment result shows an upward movement at the mid rail section and downward at the rear end, while it is showing downward at the rear end and upward at the loading end for FEA. The reason behind this has been fairly considered as the eccentricity of pressure load in FEA which is slightly higher than the actual case. The load cell pressure center is at the center of the circular contact area, but in case of FEM the contact pressure area is the irregular area of the rail itself. Hence, the upward deflection is explained by the loading center at higher position than the actual (Described in 5.8). Moreover, the actual values are differing in fractions of millimeter. Hence it can be considered meeting the ideal situation in conjunction with all other FEA data has shown comparable results to the experimental data.

7.2.2. Validation for static scheme

The static scheme has been described in chapter 4. Referring to that, though the arrangement was made for a simply supported beam in FEA, result has been taken as correct when the $\sum F_x = 0$ criteria has been met. The reaction solution data from ANSYS provides the following information (Z axis being the simulated X axis in FEA),

Table-7.9: Reaction solution from FEA for V=0kN load case

NODE	FZ		NODE	FZ
937514	-5835.6		938028	-2815.4
937566	1115		938029	-4583.6
937579	-194.42		938030	-5569
937592	-1559.4		938031	-6910.8
937605	-2894		938032	-8379.6
937618	-3539.3		938033	-9872.6
937631	-3776.4		938124	-5829.5
937644	-2652.4		942687	3634.4
937657	-1482.5		942902	4885.3
937670	-2814.2		943117	6114.3
937683	-4568		943332	7375
937696	-5561.6		943547	8761.1
937709	-6915.8		943762	10301
937722	-8370.9		943977	10388
937735	-9875.1		944192	9550.5
937748	2433.2		944407	10392
937923	2418.1		944622	10309
938020	1099.9		944837	8771.8
938021	-207.59		945052	7387
938022	-1569.1		945267	6126.9
938023	-2907.7		945482	4898.6
938024	-3551.5		945697	3649.6
938025	-3785.8			
938026	-2646.4		TOTAL	LUES
938027	-1460		VALUE	-516.77

Therefore, it shows an imbalance of 516.77N out of 258075N longitudinal load of first load combination. This is only 0.2% of total load. Moreover, there is some moment imbalance involved due to the eccentricity of mass of different sections as described in 4.2.1.

7.2.3. Comparison of FEA and Experimental data for the Higher Vertical load cases

Bonding case-3 (Vertical Load = 40 kN)

Debonding has already occurred after the first test (V=0kN). Therefore, for the case of V=40kN, 25mm debonding of PVC as well as Elastomer has been considered as shown in table-7.5. Following table shows the result found from FEA and Experiment for this load case,

Table- 7.10: Result comparison for V=40kN load case (Bonding case-3)

Longitudinal Displacement (mm)					
Location (mm)	310	710	1295	1945	2580
FEA result	6.73	6.12	6.25	6.473	6.664
Experimental result	5.90	5.58	5.59	5.68	5.34
Deviation	12.41%	8.81%	10.59%	12.24%	19.88%
Vertical Displacement (mm)					
Location (mm)	535	985	1595	2210	
FEA result	-1.10768	-1.4095	-1.43212	-0.37738	
Experimental result	-1.258	-1.342	-1.229	-0.633	
Deviation	13.6%	-4.8%	-14.2%	67.7%	
Longitudinal stress on Rail (MPa)					
Location (mm)	680	1310	1930	2610	
FEA result	-7.52	-10.19	-17.06	-25.31	
Experimental result	-3.58	-1.74	-14.38	-22.34	
Deviation	-3.94	-8.45	-2.68	-2.97	
Longitudinal stress on Girder (MPa)					
Top Flange					
Location (mm)	1325				
FEA result	-7.321				
Experimental result	-9.20				
Deviation	20.42%				
Bottom Flange					
Location (mm)	1325				
FEA result	25.628				
Experimental result	37.47				
Deviation	31.60%				

The comparison of longitudinal stress between FEA result and Experiment result has been shown in figure- 7.71.

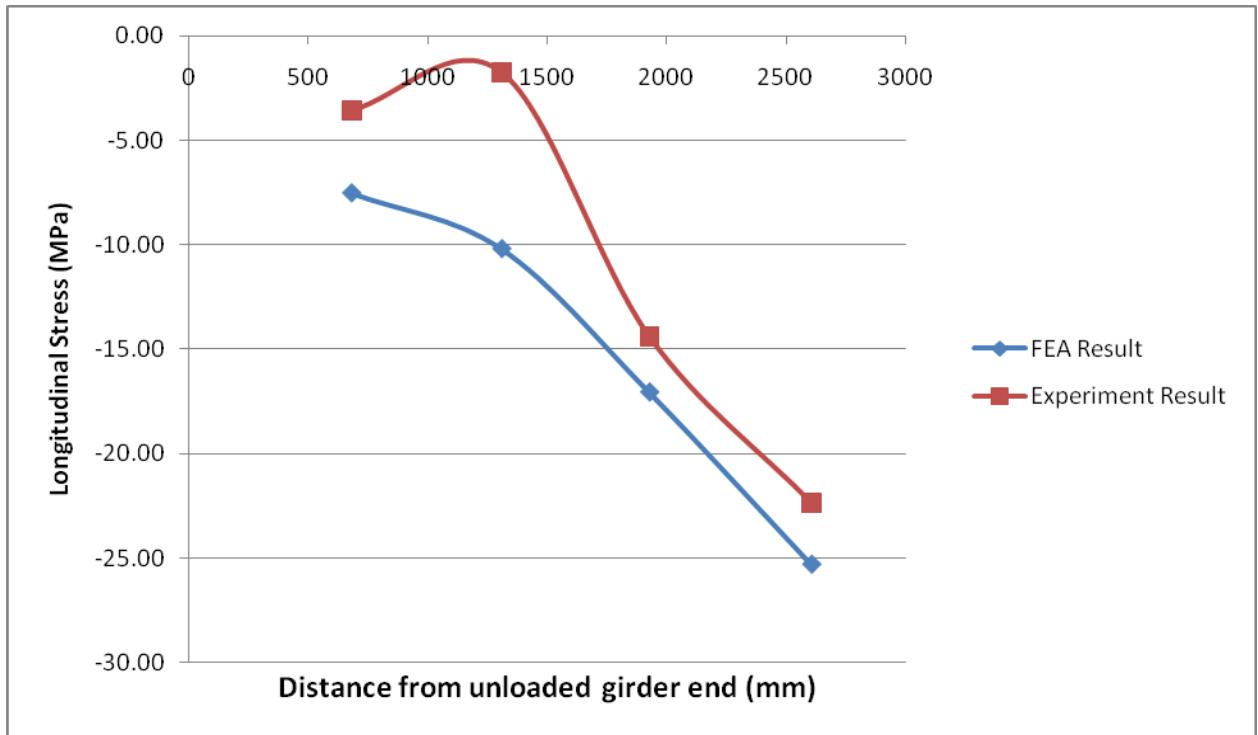


Figure-7.71: Comparison of FEA and Experimental results for longitudinal stress in rail ($V=40$ kN)

Effect of vertical load is visible from figure-7.71 but the stress at 1310mm is not even closer to the experimental value. A parametric study has been done to identify the underlying reasons behind this and shown on that chapter 8.

The comparison of longitudinal displacements between FEA result and Experiment result from the table shows that it is getting closer to the value of experimental results as compared to the case of unloaded condition.

The comparison of vertical displacements between FEA result and Experiment result has been shown in figure- 7.72.

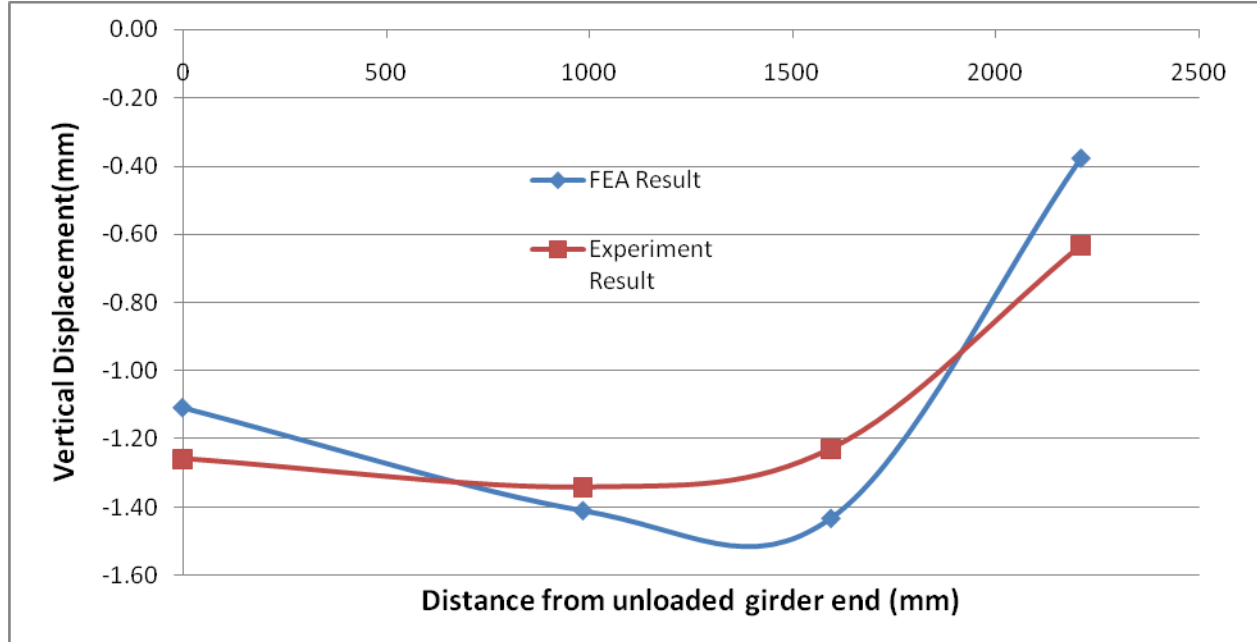


Figure-7.72: Comparison of FEA and Experimental results for vertical displacement of rail ($V=40$ kN).

The vertical displacement values are showing the similar nature of vertical deflection of the rail. But the higher value at the middle and lower values at the end clearly indicates softer material in FEA than in the test. For simplicity, the embedding elements on two sides of the rail have been modeled with tension element only which is of tension modulus 3.5 MPa, where the compression modulus for the same material is 5.9-6.9 MPa. The bimodular characteristics of embedding has been approximated beneath the rail and on two sides of the rail foot but more complex form and scattered distribution of compression elements on other parts could not be approximated. However, the amount of compression elements has not been found much on those sections and the result thus found is not varying in greater percentage.

Bonding case-4 (Vertical Load = 80 kN)

It has been observed from the experiment that, debonding has increased as the vertical load was increased. Therefore, for the case of V=80kN, 50mm debonding of PVC pipe as well as elastomer has been considered as shown in table- 7.5. Following table shows the result found from FEA and experiment for this load case,

Table- 7.11: Result comparison for V=80kN load case (Bonding case-4)

Longitudinal Displacement (mm)					
Location (mm)	310	710	1295	1945	2580
FEA result	5.6115	4.933	4.98	5.25	5.42
Experimental result	5.19	4.94	4.95	4.95	4.83
Deviation	7.44%	-0.04%	0.56%	5.75%	10.98%
Vertical Displacement (mm)					
Location (mm)	535	985	1595	2210	
FEA result	-1.246	-1.988	-2.454	-1.42	
Experimental result	-1.854	-2.183	-2.049	-0.956	
Deviation	48.8%	9.8%	-16.5%	-32.7%	
Longitudinal stress on Rail (MPa)					
Location (mm)	680	1310	1930	2610	
FEA result	-6.91	-3.95	-13.99	-21.94	
Experimental result	-2.42	5.7	-14.09	-19.70	
Deviation	-4.49	-9.65	0.10	-2.24	
Longitudinal stress on Girder (MPa)					
Top Flange					
Location (mm)	1325				
FEA result	-8.8363				
Experimental result	-11.05				
Deviation	20.03%				
Bottom Flange					
Location (mm)	1325				
FEA result	36.403				
Experimental result	50.99				
Deviation	28.61%				

The comparison of longitudinal stress between FEA result and Experiment result has been shown in figure- 7.73.

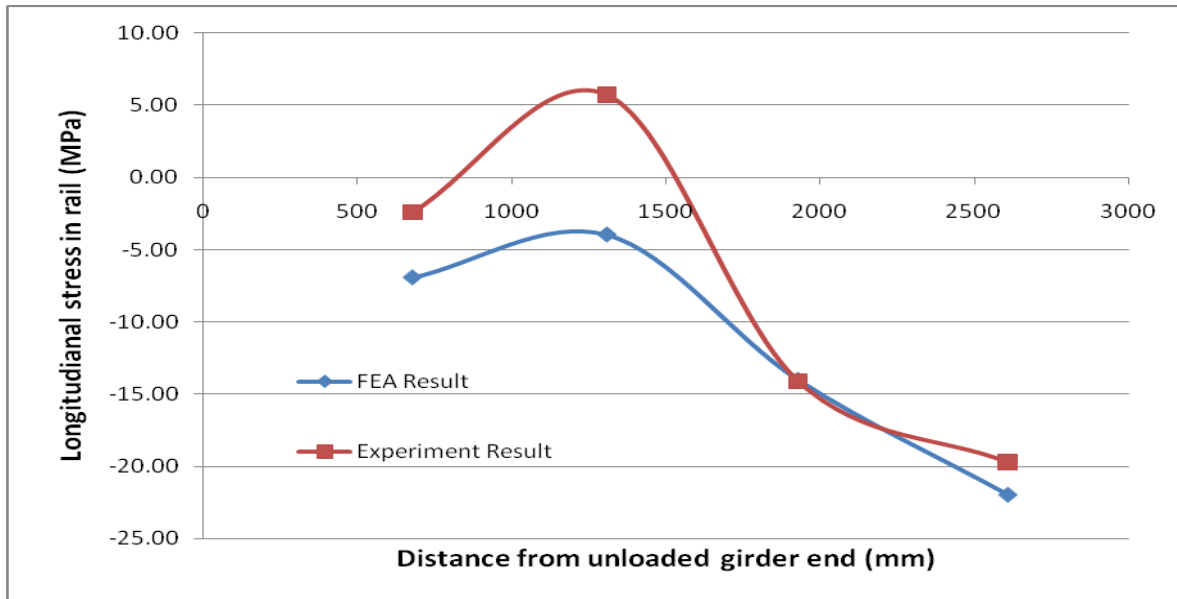


Figure-7.73: Comparison of FEA and Experimental results for longitudinal stress in rail ($V=80$ kN)

The comparison of vertical displacements between FEA result and Experiment result has been shown in figure- 7.68.

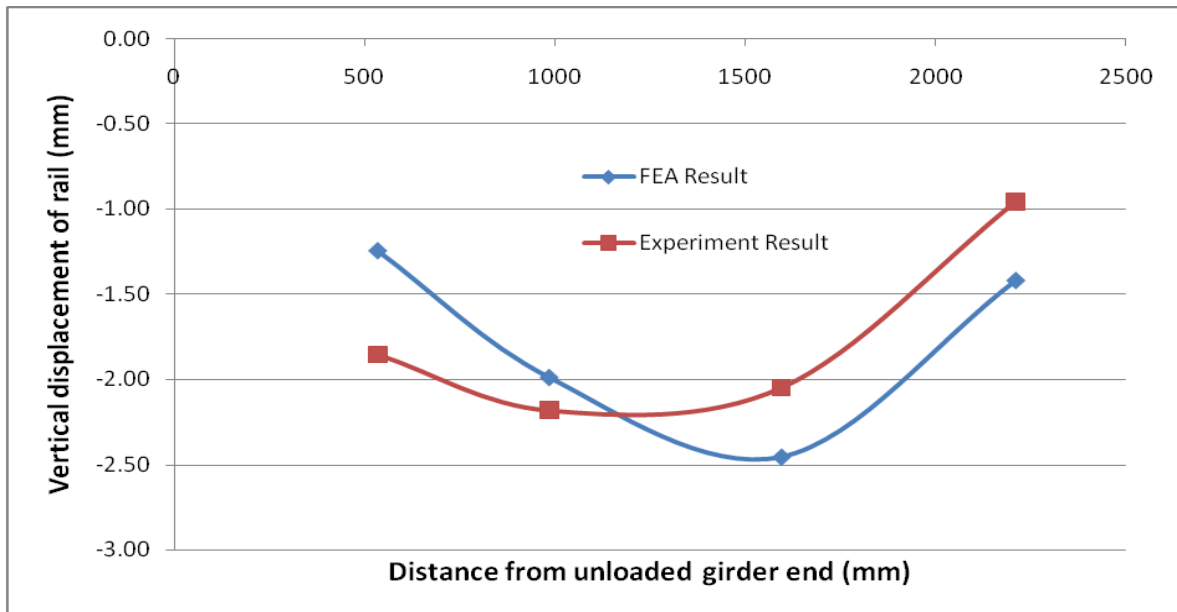


Figure-7.74: Comparison of FEA and Experimental results for vertical displacement of rail ($V=80$ kN).

Bonding case-5 (Vertical Load = 125 kN)

For the case of V=125kN, similar 50mm debonding of PVC as well as Elastomer has been kept as no significant effect has been found due to debonding and the visible debonding in the test has not been found in a larger scale. Following table shows the result found from FEA and Experiment for this load case,

Table-7.12: Result comparison for V=125kN load case (Bonding case-5)

Longitudinal Displacement (mm)					
Location (mm)	310	710	1295	1945	2580
FEA result	7.02	5.88	6.12	6.52	6.75
Experimental result	7.447	-7.01	-6.983	-6.976	-6.83
Deviation	6.1%	-219.2%	-214.1%	-207.0%	-201.2%
Vertical Displacement (mm)					
Location (mm)	535	985	1595	2210	
FEA result	-2.092	-3.353	-4.15	-2.74	
Experimental result	-2.748	-3.144	-2.926	-1.528	
Deviation	31.4%	-6.2%	-29.5%	-44.2%	
Longitudinal stress on Rail (MPa)					
Location (mm)	680	1310	1930	2610	
FEA result	-9.18	-2.67	-18.34	-29.26	
Experimental result	-3	8.5	-18.17	-25.69	
Deviation	-6.18	-11.17	-0.18	-3.57	
Longitudinal stress on Girder (MPa)					
Top Flange					
Location (mm)	1325				
FEA result	-12.707				
Experimental result	-14.82				
Deviation	14.26%				
Bottom Flange					
Location (mm)	1325				
FEA result	53.594				
Experimental result	70.40				
Deviation	23.87%				

The comparison of longitudinal stress between FEA result and Experiment result has been shown in figure- 7.75.

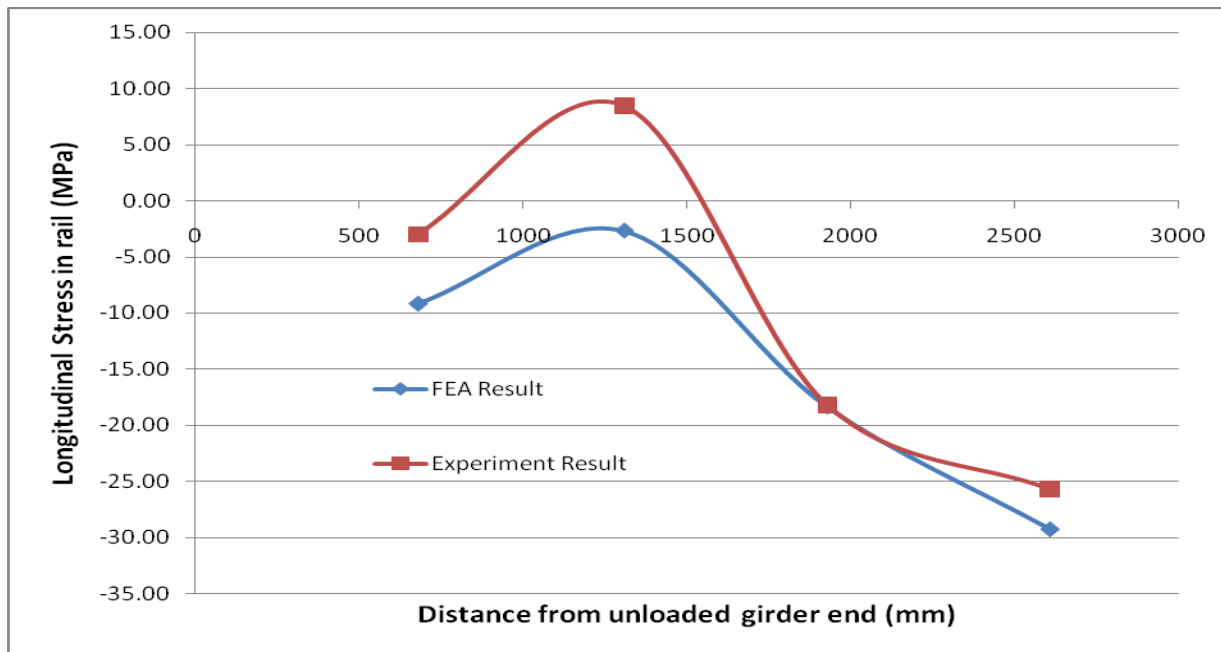


Figure-7.75: Comparison of FEA and Experimental results for longitudinal stress in rail ($V=125$ kN)

The comparison of vertical displacements between FEA result and Experiment result has been shown in figure- 7.76.

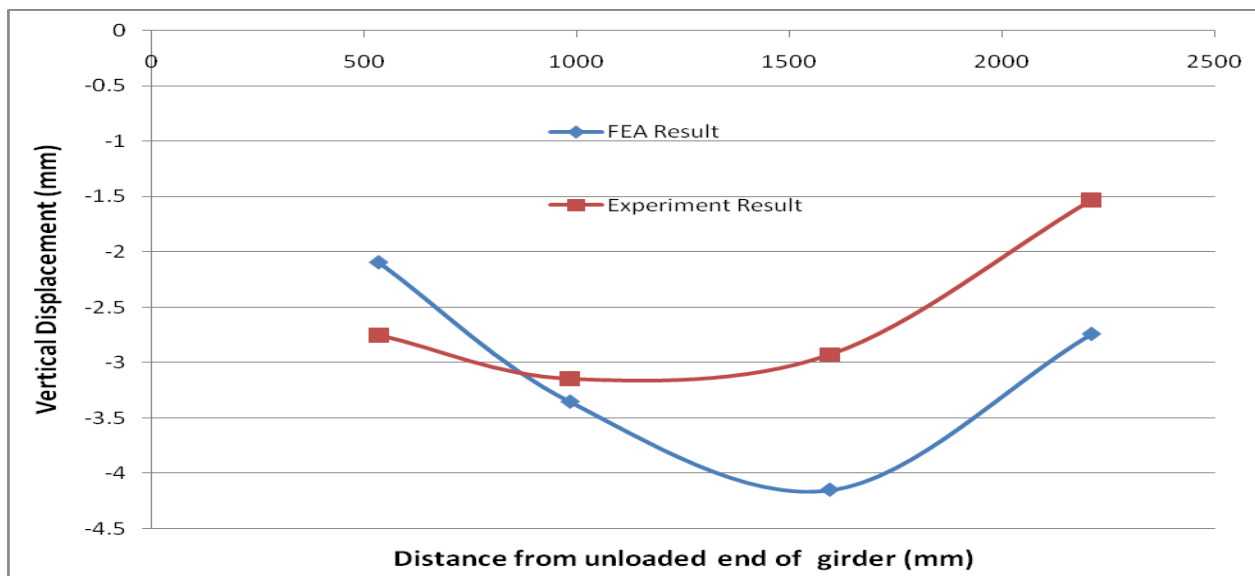


Figure-7.76: Comparison of FEA and Experimental results for vertical displacement of rail ($V=125$ kN).

7.3. Reason behind the deviation of FEA results from Experimental results

Reasonably close results has been found for $V=0\text{kN}$ and $V=40\text{ kN}$ load cases. The possible causes for particular deviations have been explained under the respective results of these two load cases. But the deviation of FEA results started to vary with the combination of vertical load cases.

For both the later load cases, it has been observed that the longitudinal displacement values are gradually becoming closer to the experimental results or in other ways the longitudinal displacements are decreasing for the higher load cases. It is quite understandable from the static scheme that higher vertical load will restrict the horizontal displacement. But from the experimental results, the similar displacements have been found for decreasing longitudinal load with the increment of vertical load. The subsequent results are related to the longitudinal displacement of the rail. Hence, finding the reason behind such behavior would best describe the result deviations for later load cases.

The debonding of PVC pipe or the elastomer has been simulated but it has not shown much influence to match the results for such behavior.

As described earlier in this chapter, the elements turning into compression elements could have been a cause for lower longitudinal displacement value as the embedding material possesses higher modulus of elasticity in compression. But, it has been found that with the increment of vertical load the compression elements tend to decrease in bulk portion of the embedding material (Figure- 7.77). Therefore, the assignment of only tension properties in the embedding material on both sides of the rail web becomes a valid assumption. Moreover, in all other portions of embedding material as well as the elastomer material, the segmentation has been done and compressive modulus has been assigned accordingly. As such the effect of bimodular behavior can be ignored or can be considered having insignificant influence on lowering the longitudinal displacement capacity of the rail. It is to mention here that the compression elements have been found only at both ends (Figure-7.77) of the embedding material beside the rail web. Therefore, assignment of higher elasticity at the ends will more simulate the vertical displacement values at the ends also.

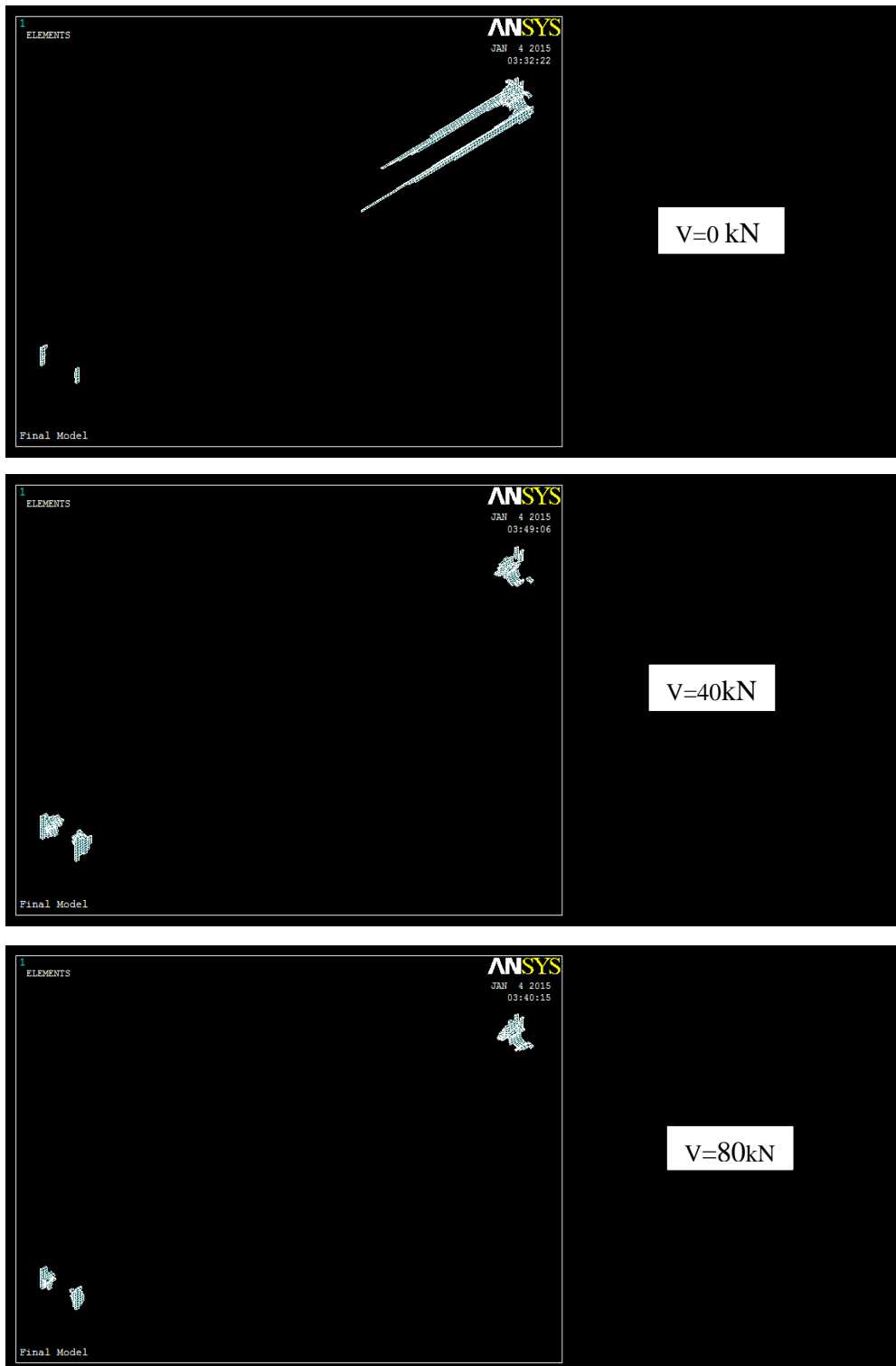


Figure-7.77: Compression element generation at the end section of embedding material besides rail web

The elastic softening characteristics of the embedding material could be a better explanation in that situation for which separate tests has to be done and extensive material data will be required to incorporate in the simulation. All the tests in the experiment have been performed in quick succession and the repetitive load action was there on the embedding material. Gradual softening of the material elasticity will lead to higher displacement under same load and will influence the subsequent behavior of the other parts adjoin to that material. The lower the stiffness of the embedding will be the higher will be the stress in girder also. Also the vertical displacement values have been found higher on later load cases; especially at the loading end. This also describes the possibility of elastic softening of material under several rounds of loading.

8. Parametric Study

Two parameters have been checked in the model to find out the significant effect of those parameters on the results and whether they can fit the FEA results better to the experimental results. These are,

1. The Poisson's ratio of the embedding material for which separate experiment is required to find the exact value. (both in tension and compression)
2. The eccentricity of vertical load along transverse direction of the rail to find out the reason behind much higher stress value underneath the vertical load.

8.1. Effect of Poisson's Ratio of embedding material

The parametric study for poisson's ratio has been carried out for the first two load cases i.e., $V=0$ kN and $V= 40$ kN with two different poisson's ratio. As explained in Model Generation chapter, the polyurethane resin has poisson's ratio of nearly 0.5 (incompressible) [20]. But the embedding material is a mixture of polyurethane resin, cork granulate and mineral filler. Cork material possesses the poisson's ratio nearly zero. Therefore, two different poisson's ratio has been chosen between poisson's ratio of steel and rubber tentatively, i.e., 0.35 and 0.45.

Table- 8.13: Result comparison for different poisson's ratio for (V=0 kN load case)

Longitudinal Displacement (mm)					
Location (mm)	310	710	1295	1945	2580
Poisson's ratio=0.35	8.31	7.85	7.955	8.155	8.37
Poisson's ratio=0.45	8.8	8.32	8.43	8.62	8.855
Experimental result	7.06	6.84	6.77	6.81	6.69
Vertical Displacement (mm)					
Location (mm)	535	985	1595	2210	
Poisson's ratio=0.35	-0.8715	-0.579	0.01156	1.2775	
Poisson's ratio=0.45	-0.742	-0.575	-0.1032	1.062	
Experimental result	-0.471	-0.19	-0.149	-0.147	
Longitudinal stress on Rail (MPa)					
Location (mm)	680	1310	1930	2610	
Poisson's ratio=0.35	-9.03	-18.44	-22.15	-31.16	
Poisson's ratio=0.45	-9.07	-18.38	-22.20	-31.16	
Experimental result	-5.41	-13.83	-18.46	-27.41	
Longitudinal stress on Girder (MPa)					
Top Flange					
Location (mm)	1325				
Poisson's ratio=0.35	-7.1745				
Poisson's ratio=0.45	-6.92				
Experimental result	-6.78				
Bottom Flange					
Location (mm)	1325				
Poisson's ratio=0.35	17.287				
Poisson's ratio=0.45	16.577				
Experimental result	19.02				

The effect of higher poisson's ratio of the embedding material increases the longitudinal displacement values and decreases the vertical displacement values which are identical to the property of incompressible material property. It is causing more displacement with the longitudinal load as it is retaining its volume in the longitudinal direction more than before and the changes in the vertical displacement values are the reciprocal effect of same behavior. Other values are more or less similar.

Table- 8.14: Result comparison for different poisson's ratio for (V=40 kN load case)

Longitudinal Displacement (mm)					
Location (mm)	310	710	1295	1945	2580
Poisson's ratio=0.35	6.73	6.12	6.25	6.473	6.664
Poisson's ratio=0.45	7.13	6.52	6.68	6.87	7.06
Experimental result	5.90	5.58	5.59	5.68	5.34
Vertical Displacement (mm)					
Location (mm)	535	985	1595	2210	
Poisson's ratio=0.35	-1.10768	-1.4095	-1.43212	0.37738	
Poisson's ratio=0.45	-0.9371	-1.257	-1.327	-0.3305	
Experimental result	-1.258	-1.342	-1.229	-0.633	
Longitudinal stress on Rail (MPa)					
Location (mm)	680	1310	1930	2610	
Poisson's ratio=0.35	-7.52	-10.19	-17.06	-25.31	
Poisson's ratio=0.45	-7.67	-8.30	-17.16	-25.31	
Experimental result	-3.58	-1.74	-14.38	-22.34	
Longitudinal stress on Girder (MPa)					
Top Flange					
Location (mm)	1325				
Poisson's ratio=0.35	-7.321				
Poisson's ratio=0.45	-7.5327				
Experimental result	-9.20				
Bottom Flange					
Location (mm)	1325				
Poisson's ratio=0.35	25.628				
Poisson's ratio=0.45	25.734				
Experimental result	37.47				

Same explanation goes for the V=40 kN load case. But the difference in longitudinal stress under the vertical load point near 1310mm is significant.

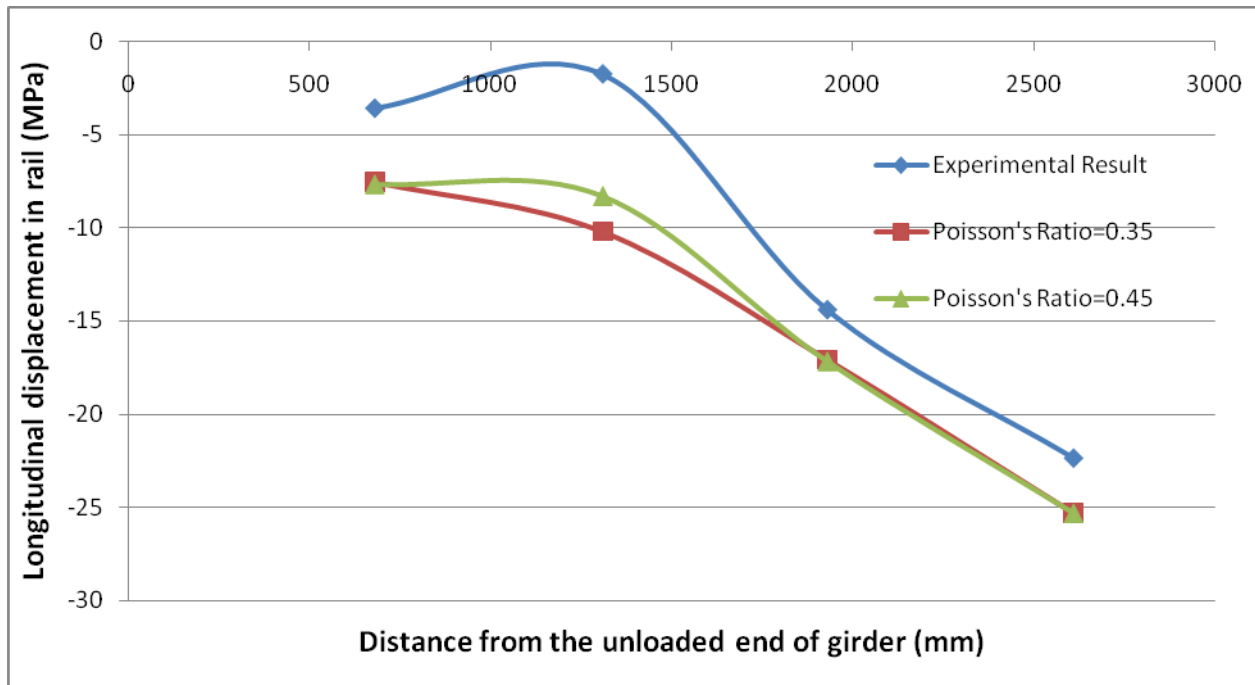


Figure-8.78: Effect of Poisson's ratio on longitudinal stress on rail

But this can not only define the high amount of deviation found in the validation data. Moreover, already conservative results have been found for longitudinal displacement and other longitudinal stress values. Hence, Poisson's ratio might have its effect but definitely in conjunction with other reasons that needs to identify.

8.2. Effect of eccentricity of vertical load

The eccentricity of vertical load has been studied for the last load combination case i.e., V=125 kN load case.

Table- 8.15: Result comparison for eccentricity of vertical loading (V=125 kN load case)

Longitudinal stress on Rail (MPa)				
Location (mm)	680	1310	1930	2610
FEA result (load eccentric)	-9.48	4.36	-17.75	-28.82
FEA result (load at center)	-9.17	3.68	-18.16	-28.84
Experimental result	-3	8.5	-18.17	-25.69

The stress value tends to decrease due to bending in transverse direction. It is quite understandable that for transverse bending, stress value will decrease on one side and increase on other side of the rail web. Therefore, data has been recorded at the face that shows the higher decrement of stress. From the figure it can be observed that, the influence of eccentricity is there on the longitudinal stress under the location of vertical load.

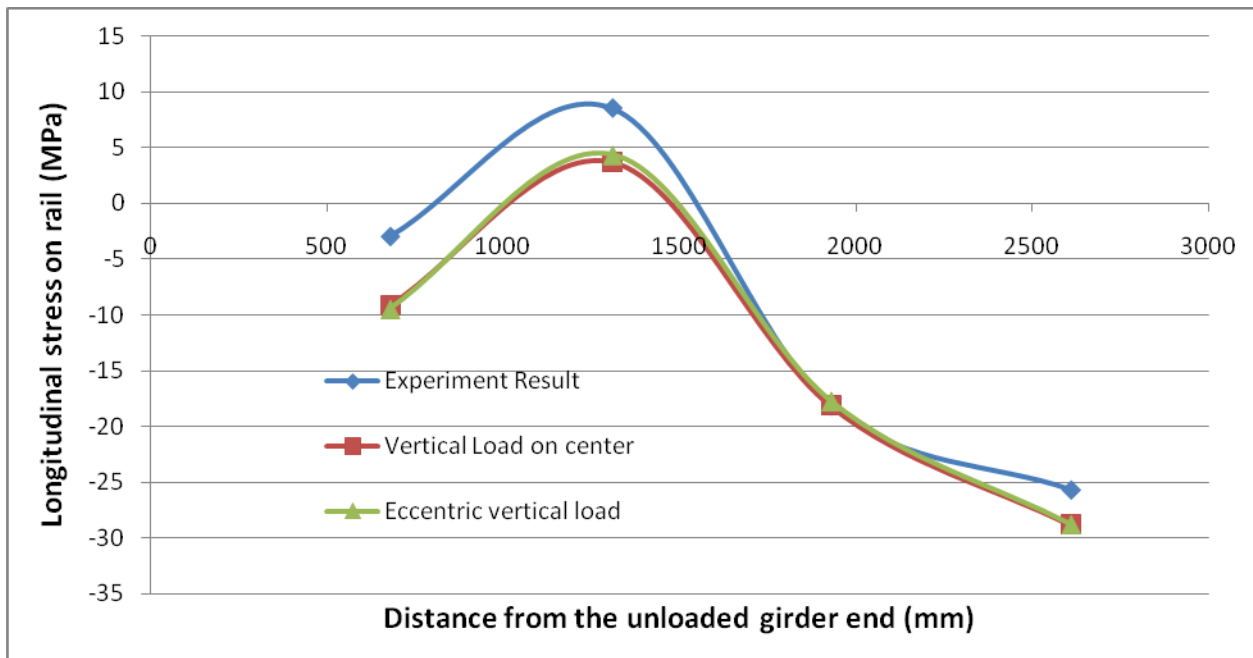


Figure-8.79: Effect of eccentric vertical loading on longitudinal stress on rail.

Hence, there might be possibility of positioning the strain gauge close to one side of the web where more tension has developed. The further finding is that the stress gradient is high in the vertical direction of the rail web. It may be also possible that it has been positioned a bit lower than the centroid and gave rise to high decrement of longitudinal stress at that point.

9. Findings

9.1. Coupling relationship of the ERS rail track

Several runs has been made in FEM for intermediate values of longitudinal loads in combination with $V=0\text{kN}$ (unloaded track) and $V=125\text{ kN}$ (Loaded track) vertical load condition to develop the relationship between longitudinal resistance and longitudinal displacement of rail track.

Unloaded track

The comparison of coupling relationship for 2190mm of embedding on a single rail has been found as figure below,

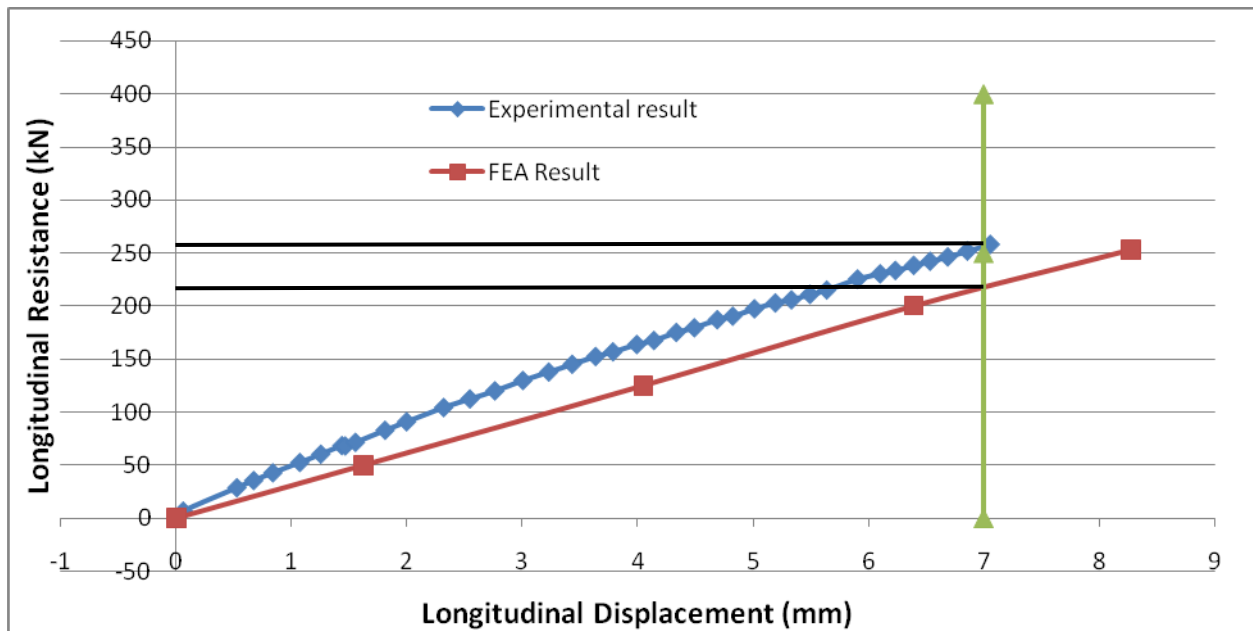


Figure-9.80: Comparison of longitudinal resistance found from FEA and Experiment (for 2.19m ERS on single rail)

Converting the relationship for a 1 m track assembled with ERS system can be suggested as figure-9.81. Here, the conversion has been made by dividing the resistance force by total length of embedding used in the experiment (or FEA) and multiplying it by 2 (for two lines of

rail in the track). The result found in FEA is conservative than the experimental result for unloaded track. Therefore, the following can be suggested as the longitudinal resistance as a function of longitudinal displacement for 1 meter length of rail track assembled with ERS for unloaded condition (FEA result).

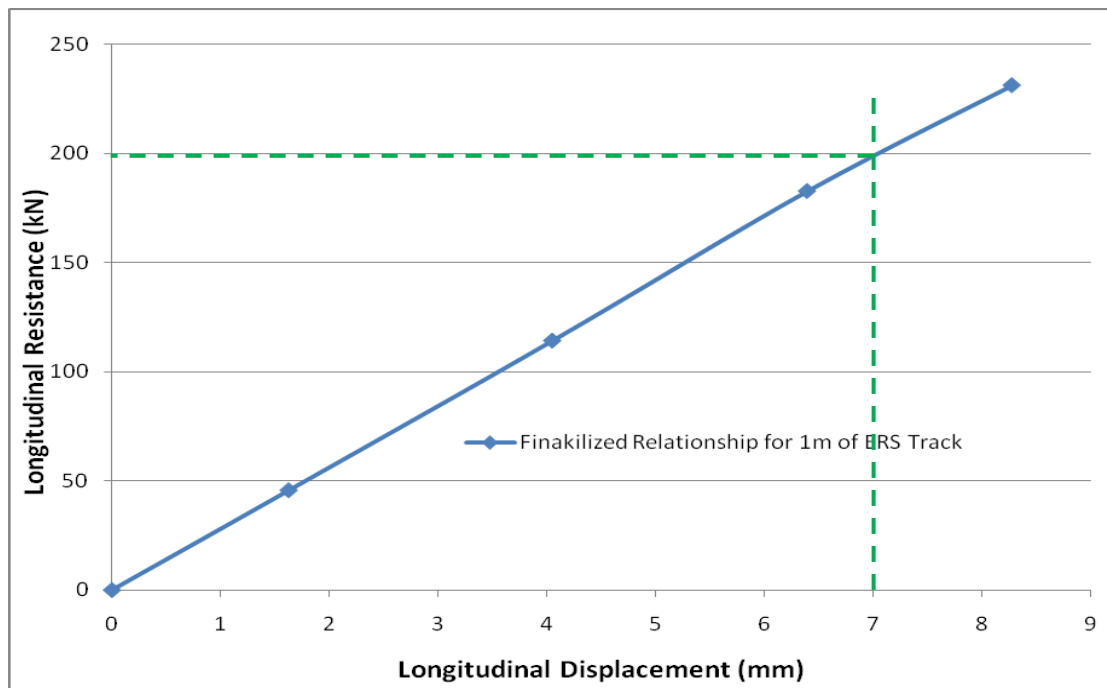


Figure-9.81: Longitudinal resistance as a function of longitudinal displacement of 1 m ERS track (unloaded)

Given the maximum allowable longitudinal displacement of 7mm in UIC-774-3R for embedded rail, maximum longitudinal resistance have been found 200 kN for unloaded track in FEA.

During the experiment, the sample has been further tested to identify maximum longitudinal resistance of ERS. After the sample has been tested for the desired combined loads, it has been loaded longitudinally until it reaches the maximum longitudinal displacement/longitudinal resistance and starts to lose resistance with subsequent increment of displacement

(Appendix-III). It has been observed that the displacement at maximum longitudinal resistance (303.2 kN) is 14.36 mm and data has been recorded until the displacement reaches to 18.62 mm. Resistance recorded at that point was 178.82 kN. Hence, it can be concluded that under the impact of moving locomotive (traction, braking and associated bridge deformation force) the short term behavior of ERS will be as shown as the firm line in figure- 9.81. And for the temperature variation, the long term displacement behavior for which ERS will suffer less rapid deformation and can be approximated as the dotted line shown in the same figure. Therefore, a long term and short term response of the ERS for a 1m track of ERS (Experimental Result) can be depicted as below.

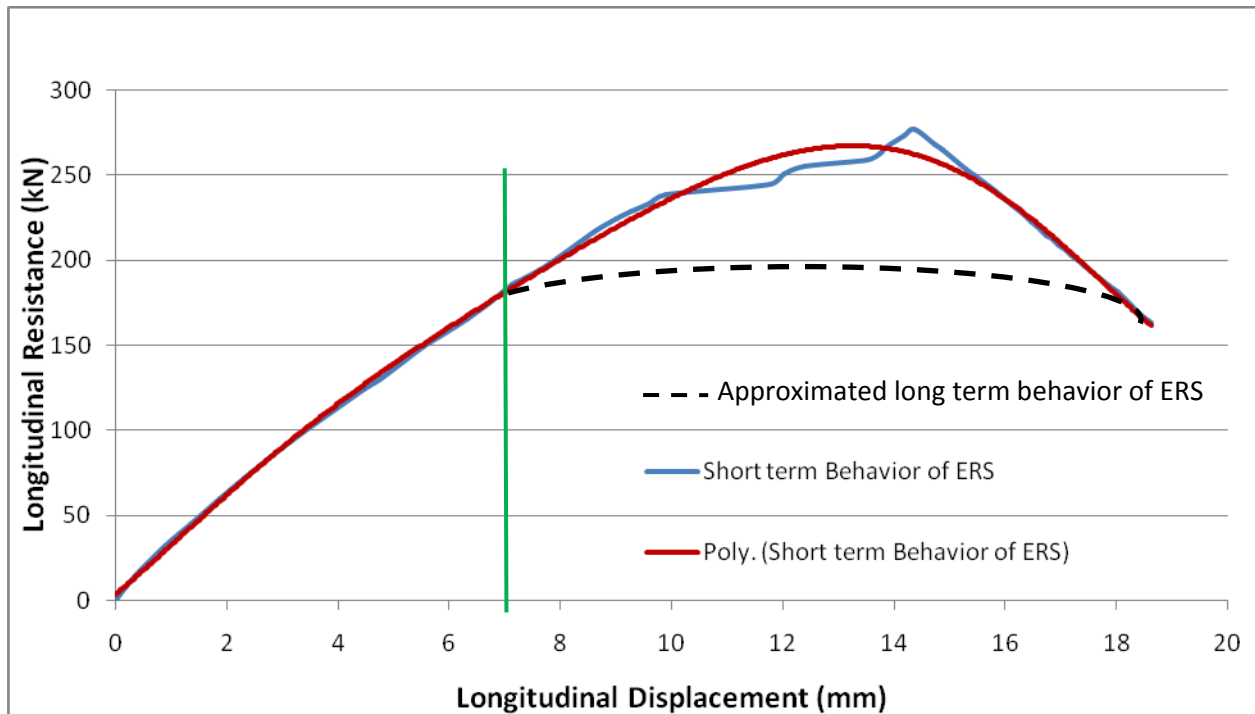


Figure-9.82: Short & long term response of ERS (unloaded track).

Here, it should be included that the resistance at 7 mm has been taken as maximum displacement criteria from UIC-774-3R. Also to mention that, the above figure shows less resistance value than the first test under unloaded ($V=0\text{kN}$) condition, which again suggests the elastic softening characteristics of the embedding material under repetitive load as explained in 7.3.

Loaded track

The result found in FEA is not conservative than the experimental result for loaded track. The possible reason for that has been explained in 7.3. The resistance value found for loaded embedded track in FEA is higher than the unloaded condition and which also matches with the recommendation given by UIC-774-3R (Table below). But the resistance for loaded track found in the experiment is lower than the unloaded track. The findings have been furnished below for further verification with the reasons for deviation explained and can be justified with future studies.

Table-9.16: Comparison of resistance k value of track (UIC vs FEA & Experimental result)

Categories	Unloaded track (kN/mm)	Loaded track(kN/mm)
UIC Recommendation	13	19
FEA	28.57	31.42
Experiment Result	33.01	30.66

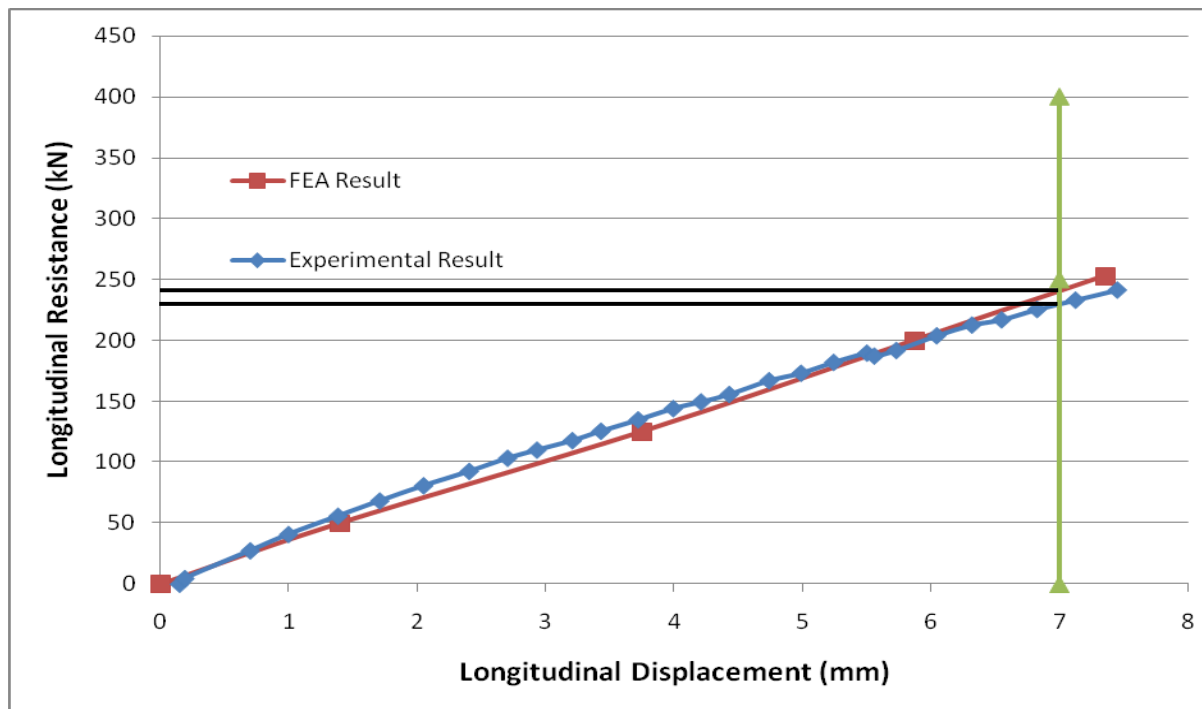


Figure-9.83: Comparison of longitudinal resistance found from FEA and Experiment (for 2.19m ERS on single rail)

Therefore, converting the resistance again for 1 m of ERS track, the following can be approximated as the longitudinal resistance as a function of longitudinal displacement for 1 meter length of rail track assembled with ERS for loaded condition (FEA result).

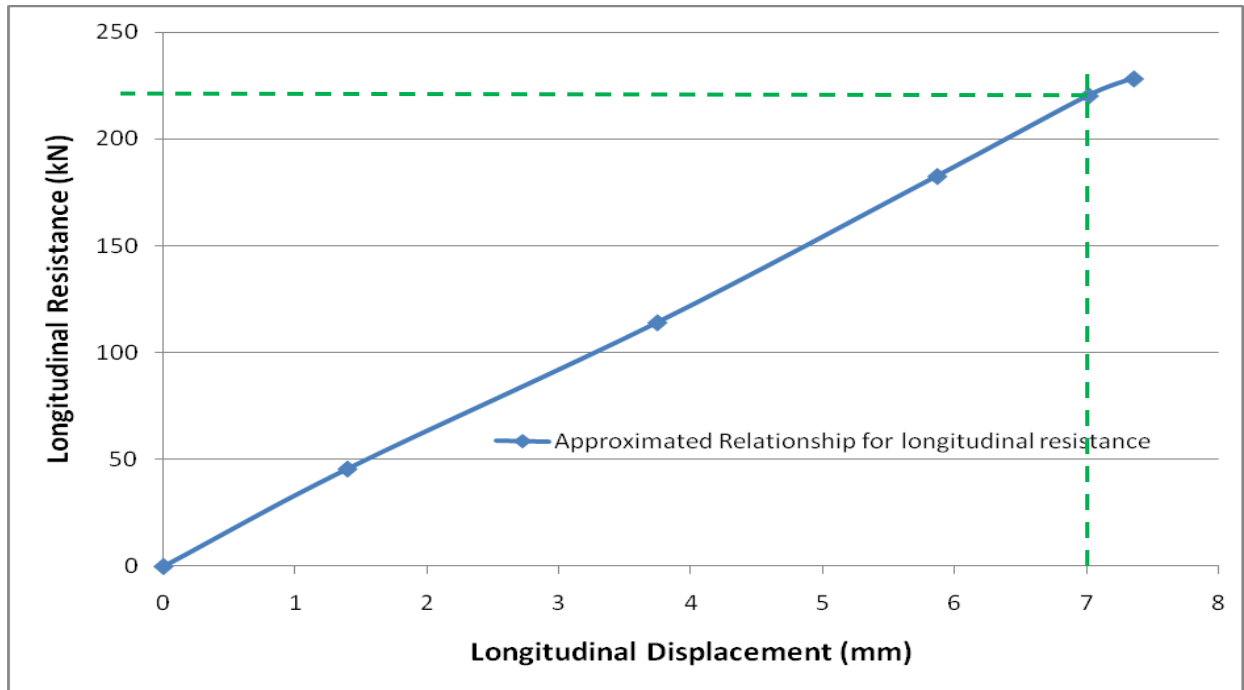


Figure-9.84: Longitudinal resistance as a function of longitudinal displacement of 1 m ERS track (loaded)

Given the maximum allowable longitudinal displacement of 7mm in UIC-774-3R for embedded rail, maximum longitudinal resistance have been found 220 kN for loaded track in FEA.

However, one of the most significant findings about the longitudinal resistance of both loaded and unloaded track is that, whether it reduces or increases for experiment and FEA respectively, the resistance value do not vary in a large scale and the resistance value found for Edilon)(Sedra ERS is much higher than the earlier recommendation of UIC-774-3R.

9.2. Design stress for Bridge Deck with ERS

Distribution of vertical pressure along length of ERS

To find out the vertical pressure distribution beneath the ERS, FEA has been done for vertical load 125 kN only and the following pressure distribution has been found along the central line of the steel base plate top i.e., just below the elastomer strip,

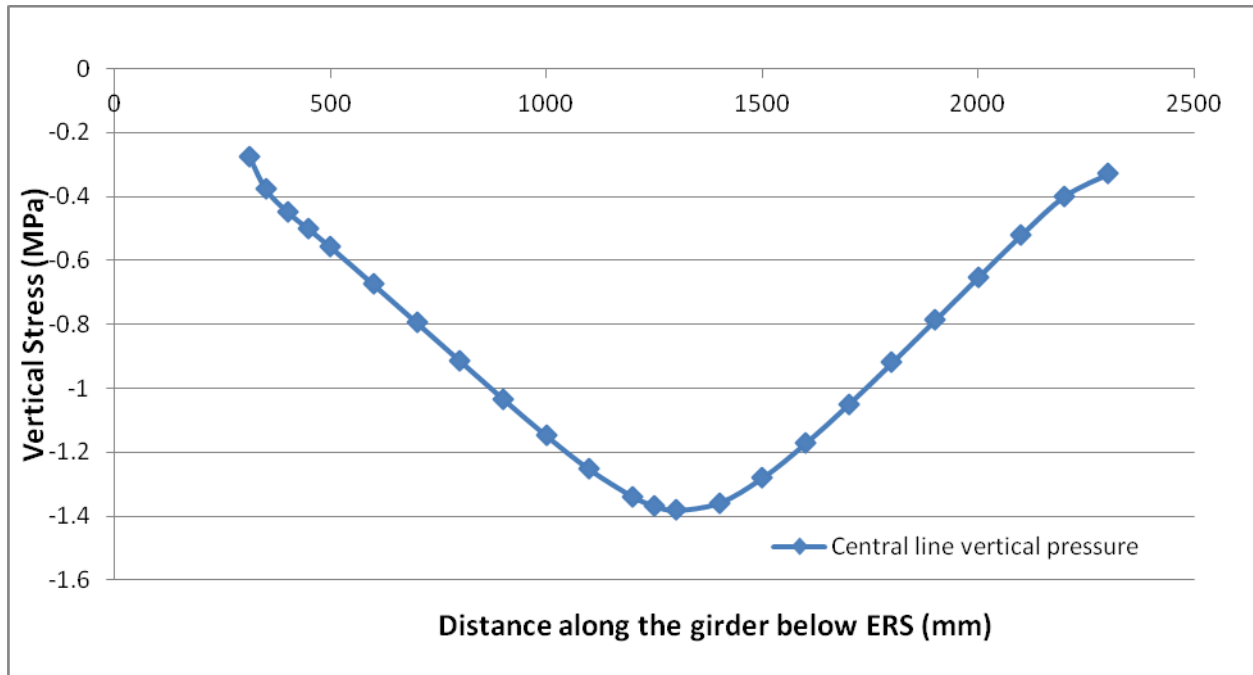


Figure-9.85: Vertical Stress distribution along the central line of base plate top (below elastomer)

From the idea of effective width of stress distribution, an attempt has been made to find out a general shape of this distribution. The peak pressure found was recorded as 1.3803 MPa. The area under the pressure curve has been calculated as 1792.4465 N/mm.

Here the effective width for the load has been calculated from,

$$b_{\text{eff}} = \frac{\text{Total area under the stress}}{\text{Peak Stress from stress curve}}$$

$$= 1792.4465/1.3803$$

$$= 1298.69 \text{ (say 1300mm)}$$

Therefore, distributing the peak stress along the effective length the general distribution for vertical pressure can be given as figure-9.86.

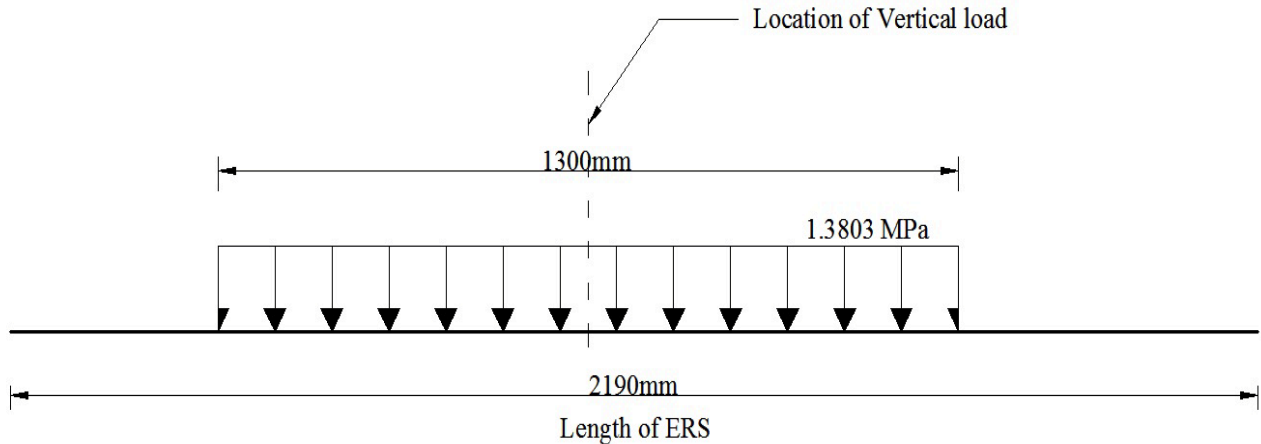


Figure-9.86: Vertical Stress distribution along the length of ERS (generalized pressure distribution on effective width)

Transverse distribution of vertical pressure along length of ERS

The distribution of the vertical pressure in transverse direction has been checked along the plane of peak stress as well as along two other intermediate planes (figure-9.87, 9.88, 9.89). The vertical pressure in transverse direction can be also be idealized as distributed over an effective length calculating like above. The stress has diminished within closer band of width as it can be seen from the figures below.

Table-9.17: Effective width calculation of vertical pressure distribution in transverse direction

Location of Transverse plane (mm)	Peak stress in transverse direction (MPa)	Area under the stress curve (N/mm)	Effective width of stress distribution (mm)
Z=800	0.91362	54.6673	59.83
Z=1300	1.3803	82.8718	60.03
Z=1800	0.91966	48.420	52.64

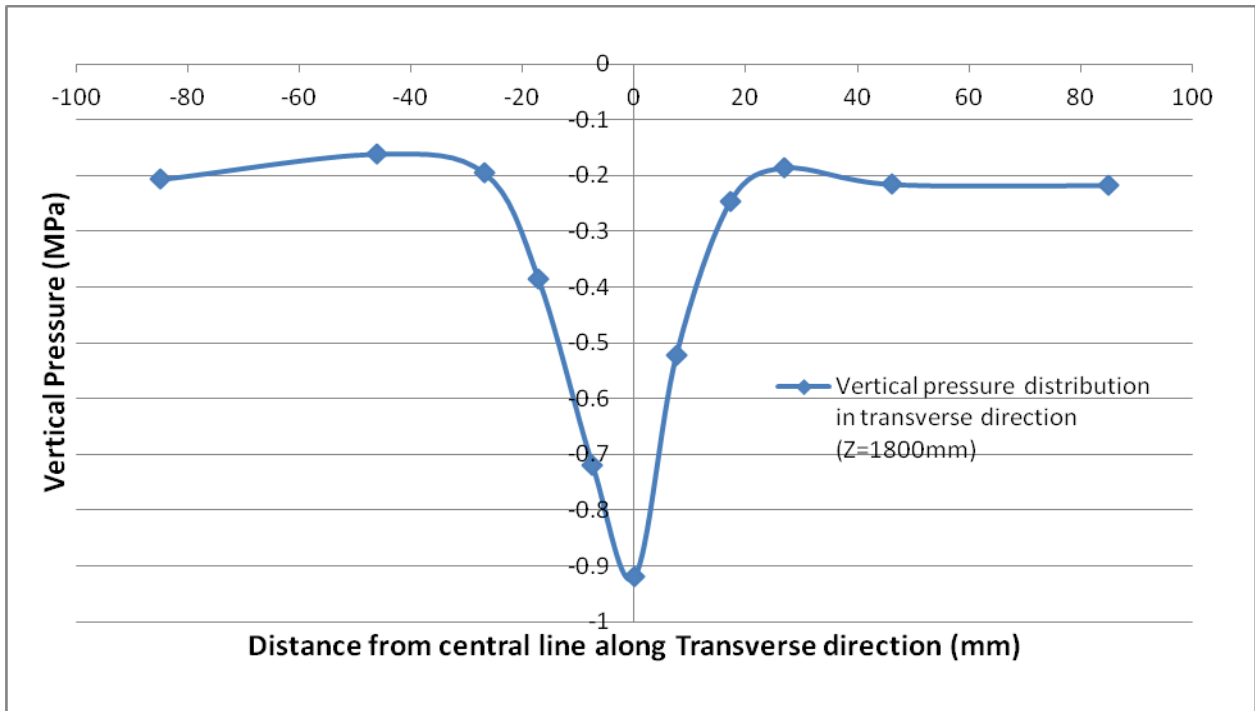


Figure-9.87: Vertical Stress distribution along transverse direction (Z=1800mm)

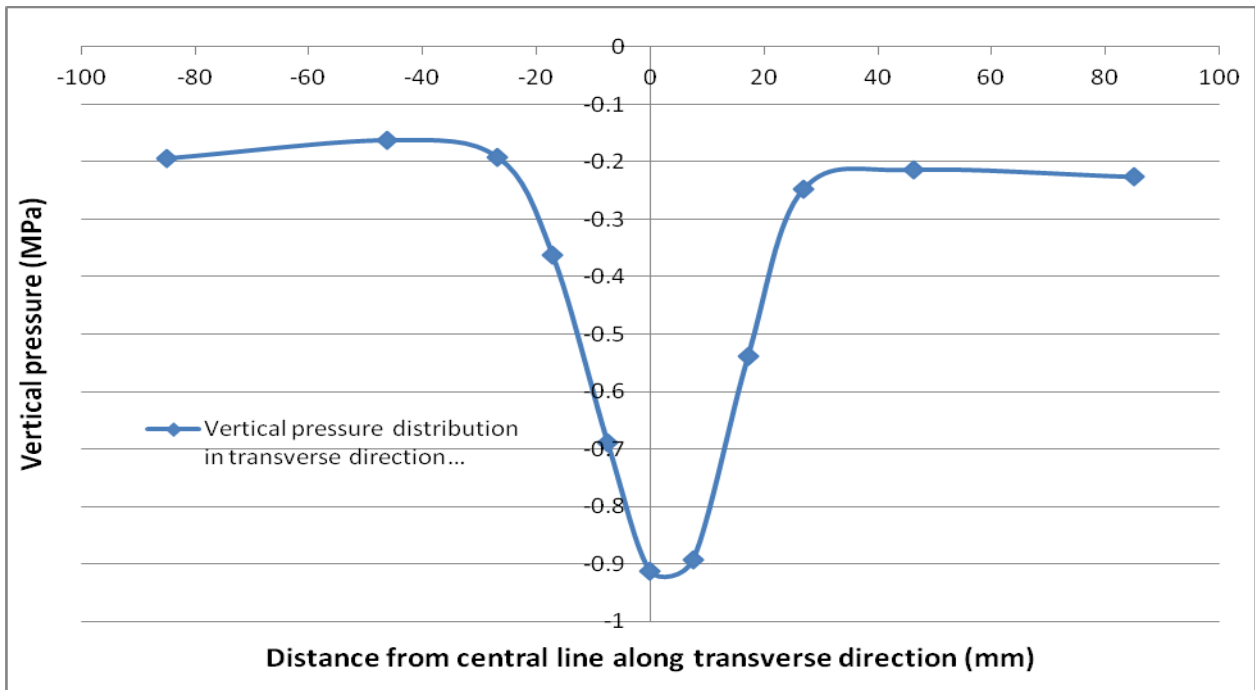


Figure-9.88: Vertical Stress distribution along transverse direction (Z=800mm)

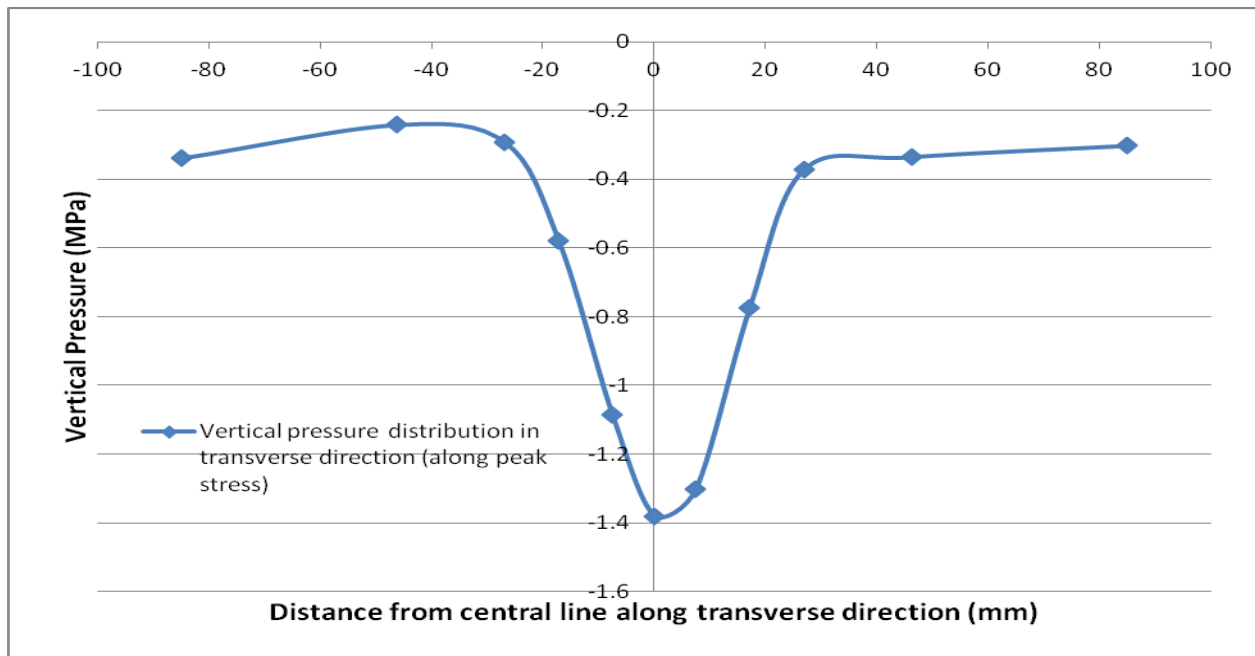


Figure-9.89: Vertical Stress distribution along transverse direction ($Z=1300\text{mm}$)

In all three cases it has been found that the vertical stress is diminishing with in 30mm on either side from central line of the base plate. Therefore, from the above figures and table 9.17, the vertical pressure distribution along transverse direction can be suggested over a width as long as 30mm on both sides of the central line of the girder or base plate and as the maximum width has been found under peak pressure it can be considered for the design pressure.

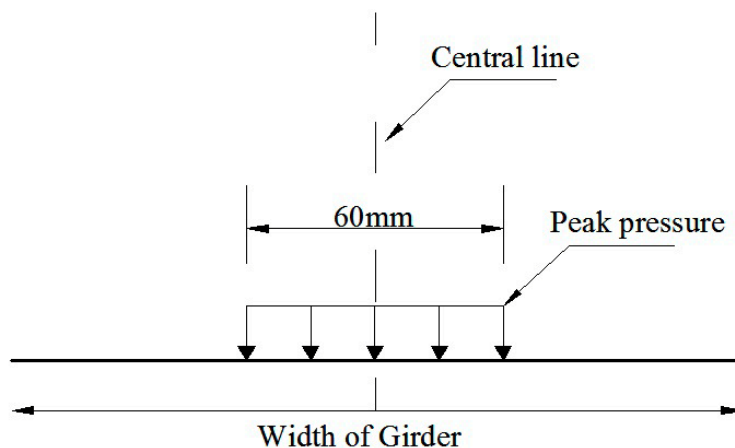


Figure-9.90: Idealized vertical pressure distribution in transverse direction

9.3. Effect of ERS in Stress development in Rail and Girder

For the loaded track condition, further analysis has been performed with and without the ERS assembly and the following comparison can be drawn for top and bottom fiber stress of the girder.

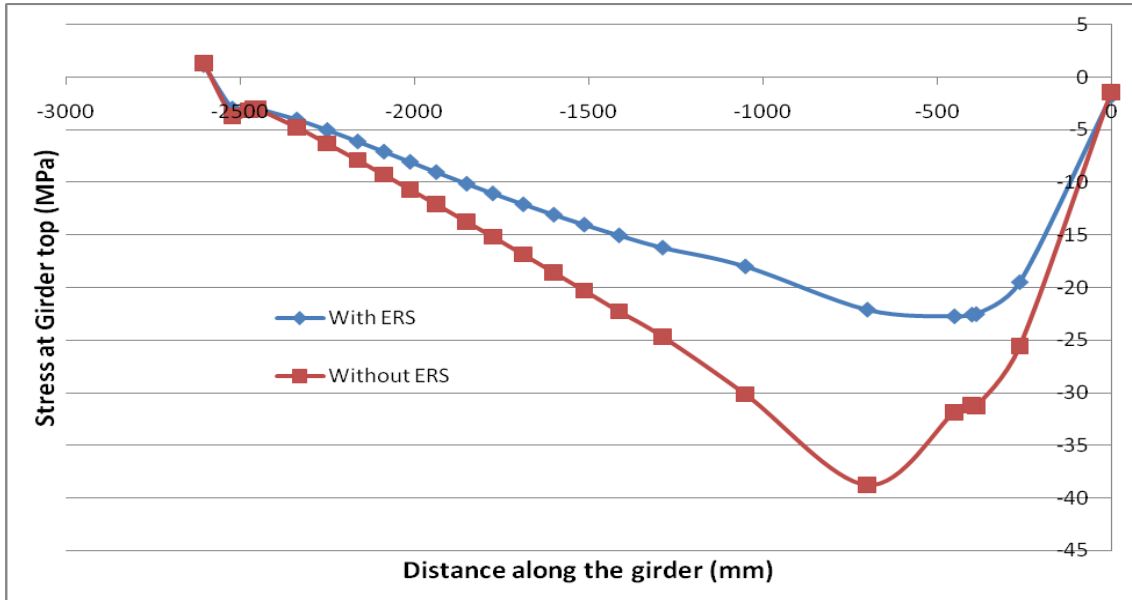


Figure-9.91: Stress comparison for top fiber stress of girder (With & without ERS assembly)

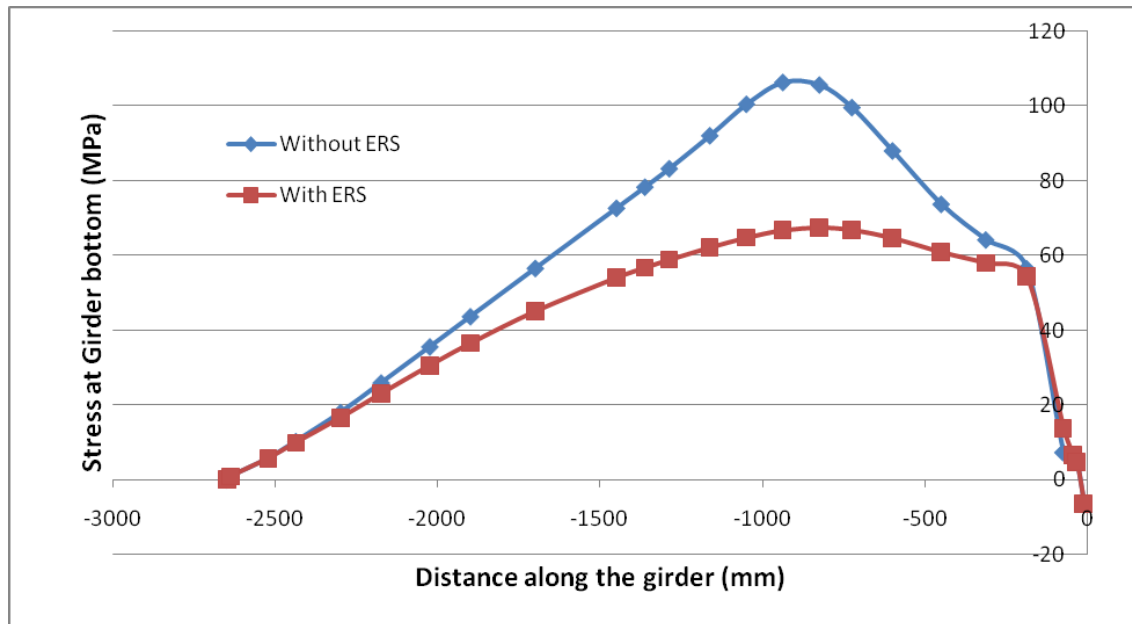


Figure-9.92: Stress comparison for bottom fiber stress of girder (With & without ERS assembly)

The stress values due to the use of ERS have shown that the peak stress improves as much as shown in following table-9.18. This idea can be well exploited for the old bridges where the use of ERS for rail track may significantly improve the condition of stress development and provide longevity to the structures.

Table-9.18: Improvement of girder stress due to use of ERS

Categories	Bottom fiber peak stress (MPa)	Top fiber peak stress (MPa)
With ERS	67.576	-22.735
Without ERS	106.32	-31.856
Improvement with ERS	36.45%	28.63%

9.4. The FEM and areas of possible refinement

With the explanation given in verification and validation part, it can be proposed that the physical model in ANSYS has been built with precision and can be used as a prototype for similar experiment with more necessary material data.

Besides, the possible areas of further refinement can be identified as,

1. Creating a Macro in ANSYS to assign bimodular material properties with respect to tension and compression elements that are generated during different loading condition.
2. Assigning multi-linear material property data for embedding material along with its poisson's ratio/bulk modulus both in tension and compression. Also the hyper-elastic material property data for elastomer in tension would give more refinement to the results.
3. Finding the response of embedding material under repetitive load and incorporating the necessary changes in material properties in the FEM as required.
4. Good care has been given to keep a good aspect ratio of the elements formed in FEM. Nearly half a million elements has been generated keeping the aspect ratio less than 2.5. A better aspect ratio can be tried with (close to 1) to check for further refinement of the result.

10. Future Study

There is considerable scope to continue extended study regarding ERS and find out more precise response results. The laboratory test has been performed on a single specimen. The response can be made more universal performing more tests on several samples of similar prototype. Moreover, the response under repetitive load can be more interesting and can resemble the experiment data more closely. There was lack of some specific material data also for embedding material. Therefore, future continuation for the current study can be proposed as-

1. Study on the interaction of Embedded Rail System (ERS) on bridges for viscoelastic and bimodular embedding material behavior.
2. Study on the interaction of Embedded Rail System (ERS) on bridges under repetitive/dynamic load.

11. Summary and Conclusion

The study has been conducted with a view to find out the response of Embedded Rail System (ERS) on bridges under different combination of vertical and longitudinal load. Initially, a small scale laboratory test has been performed on an ERS mounted over an asymmetric steel girder in Klokner Institute, Czech Technical University to collect the response data. The assembly of the ERS has been fabricated and supplied by Edilon)(SedraTM, an international supplier and manufacturer of rail track systems since 1970. Therefore, the material data has also been collected from Edilon)(SedraTM and used for detail analysis.

The test has been performed for four load combinations. The longitudinal load has been controlled on the basis of maximum allowable displacement (7mm) recommended for embedded rail system by UIC-774-3R. The maximum vertical point load from rail axle is 250 kN for loaded track as recommended by load model 71 in EN 1991-2. As the test has been performed on a single rail, maximum vertical load has been considered until 125 kN. Therefore, the four load combinations considered are displacement controlled longitudinal load along with 0, 40, 80 and 125 kN vertical load respectively.

With a view to continue with the detail analysis, a Finite Element Model (FEM) has been developed first to simulate the test specimen along with the gathered material properties and loading combinations. Globally recognized and verified finite element tool ANSYS (APDL version 14.0) has been used to build the model. Due concern has been given to build the model to precisely simulate the test prototype and to find correct solution result. After the FEM being developed and verified, nonlinear static analysis of the whole assembly has been performed for all the load combinations used in the test.

There has been some uncertainty involved regarding extensive material property data, loading eccentricity and separation of the material layers while building the representative FEM. Moreover, there have been few assumptions considered during the analysis. Assigning the bimodular property of embedding and elastomer material has been done by discrete segmentation at the required zone. Poisson's ratio of embedding has been assumed 0.35. And also the

separation of PVC pipe-Embedding material and Elastomer-Girder observed during the test has been modeled manually.

However, the result found from the FEA has shown closer and conservative results for the case of unloaded track or zero vertical load case. The particular deviation of result for this combination in one location has been verified by parametric study. The results found for the higher vertical load combinations has been found gradually varying. It has been found that for the experimental results, the resistance of the rail track is decreasing with the increment of vertical load while the same has been found increasing in FEA. The stress development in the steel girder has been found increasing in both cases but with lower rate in FEA than the experiment.

The longitudinal resistance value as a function of longitudinal displacement of the ERS has been compared with the UIC-774-3R and found much higher than the recommended values. Though the resistance values found are behaving in opposite manner in FEA, it has been found that the resistance is not varying significantly for loaded and unloaded case. The value of resistance in FEA has been found 28.57 kN/mm and 31.42 kN/mm for unloaded and loaded condition respectively. While it has been found 33.01kN/mm and 30.66 kN/mm for unloaded and loaded condition respectively from the experiment. The influence of the ERS on girder stress has also been identified and found improving the stress generation magnitude as large as 28.63% and 36.45% for top and bottom fiber respectively as compared to a fastening system with and without ERS.

The limitation to assigning bimodular material properties of embedding and elastomer material precisely (for highly irregular distribution of compression and tension elements) has been verified in the analysis and the little impact of the assumptions has been identified to describe the deviation of the FEA result for higher vertical load cases. Moreover, debonding of adjoining layers that has been observed in the experiment was adopted during the analysis. It is evident that gradual elastic softening of the material elasticity will lead to higher displacement under same load and will influence the subsequent behavior of the other parts adjoin to that material. The lower the stiffness of the embedding will be, the higher will be the stress in girder;

resembling the test results more precisely. All the tests in the experiment have been performed in quick succession and the repetitive load action was there on the embedding material. Therefore, the elastic softening characteristics of the embedding material under repetitive load has been assumed to play the significant role behind the deviation of the result for higher vertical load conditions.

Further refinement of the FEM has been suggested with the incorporation of extensive material property data and building separate macro for automatic assigning of bimodular material behavior of elastomer and embedding material during FEA solution. And it has been also recommended to continue further study on ERS under cyclic load with the appropriate material data identified from separate testing of concerned materials.

References

1. Esveld, C. (1999), Recent developments in slab track application, Rail Tech Europe.
2. Eszter, L. (2002), Elastic behavior of continuously embedded rail system, Periodica Politechnica, Cer. Civ. Eng. Vol. 46, No.1.PP 103-114, Department of Highway and Railway Engineering, Budapest University of Technology and Economics.
3. Edilon)(sedra Embedded Rail System (ERS-HR) Rail Fastening System for High-Speed and Heavy Rail (www.edilonsedra.com)
4. Union Internationale des Chemins de fer (UIC), (2001), 774-3R. Track/bridge interaction, Recommendations for calculations, Paris.
5. Technical Document (2011), Continuous welded railway bridge analysis (in accordance with UIC774-3).
6. J C Chaurasia Sr DEN/Co/SEE/ECR, Ganesh Kumar XEN/Br/II/CR, LWR on Bridges-IR Vs UIC Approach.
7. Kormos, G.Y. (2002), The longitudinal behavior of the rail embedded in flexible material, Periodica Polytechnica Ser. Civ. Eng. Vol. 46, No. 1, PP. 115–124, Department of Highway and Railway Engineering, Budapest University of Technology and Economics.
8. European Committee for Standardization (CEN) (2003), Brussels, Eurocode1, Part 2 (EN 1991-2). Actions on Structures: Traffic loads on bridges.
9. Widarda, D. R. (2009), Longitudinal forces in continuously welded rails due to nonlinear track-bridge interaction for loading sequences, Dissertation Paper, Technical University of Dresden.
10. Michas, G. (2012), Slab track systems for high-speed railways, Master Thesis Paper, Division of Highway and Railway Engineering, Department of Transport Science, Royal Institute of Technology, Stockholm, Sweden.
11. Esveld, C. (2001), INNOVATIONS IN RAILWAY TRACK, TU Delft, Germany.
12. Markine, A. P. de Man, S. Jovanovic, C. Esveld,C., Optimum design of embedded rail structure for high -speed lines, Section of Road and Railway Engineering, Faculty of Civil Engineering, Delft University of Technology.
13. Ruge, P., Birk, C. (2006), Longitudinal forces in continuously welded rails on bridge decks due to nonlinear track–bridge interaction, Faculty of Civil Engineering, Technical University of Dresden, D-01062 Dresden, Germany.

14. Zand, J. V. and Moraal, J. (1997), Ballast resistance under three dimensional loading, Report 7-97-103-4, Roads and Railways Research Laboratory, TU Delft.
15. Bin, Y., Gong-lian, D. and Hua-ping, Z. (2012), Beam-track interaction of high-speed railway bridge with ballast track, Department of Civil Engineering, Central South University, Changsha 410075, China, J. Cent. South University, 19: 1447–1453, Central South University Press and Springer-Verlag Berlin Heidelberg.
16. Esveld, C. (1989), ‘Modern Railway Track’, MRT-Productions, ISBN 90-800324-1-7.
17. Lou, P. (2007), Finite element analysis for train–track–bridge interaction system, Arch Appl Mech 77: 707–728, Springer-Verlag Berlin Heidelberg.
18. Wen-shuo, L. , Gong-lian D. and Xu-hui, H. (2013), Sensitive factors research for track-bridge interaction of Long-span X-style steel-box arch bridge on high-speed railway, School of Civil Engineering, Central South University, Changsha 410075, China, 20: 3314–3323, Springer-Verlag Berlin Heidelberg.
19. ANSYS Inc (2009), Chapter-4, Element Library, Element Reference, Release 12.1.
20. Tsukinovsky, D., Zaretsky, E. and Rutkevich, I. (1997), Material behaviour in plane Polyurethane - Polyurethane impact with velocities from 10 to 400 m/sec, J. Phys. IV France 07, C3-335-C3-339.
21. American Institute of Aeronautics and Astronautics (1998), Guide for the Verification and Validation of Computational Fluid Dynamics Simulations, AIAA-G-077, Reston, VA.
22. Jones, R. M. (1977), Stress-strain relations for materials with different moduli in tension and compression, AIAA Journal, Vol.15, No. 1ef cf, pp. 16-23.doi: 10.2514/3.7297